INVESTIGATION OF THE SUITABILITY OF PERIPHERAL LYMPHOCYTE MITOCHONDRIA AS AN INTRINSIC BIOLOGICAL DOSIMETER

A Thesis

Submitted to the Graduate Faculty of the
Louisiana State University and
Agricultural and Mechanical College
in partial fulfillment of the
requirements for the degree of
Master of Science

in

The Department of Nuclear Engineering

by
Charles E. Willis
B.S., Louisiana State University, 1975
December, 1980

DEDICATION

This thesis is appropriately dedicated to my wife, Diana, who has always been committed to it. Her technical assistance in the isolation of the peripheral lymphocytes was as essential to the successful completion of this project, as was her continuous faith and encouragement. When I consider her contribution, I remember a young woman, several months pregnant, asleep on a pallet of lab coats, enjoying a brief respite from her long day of academics, her evening of work-study dishwashing, and her night of laboratory work on this project. The project is complete, but the memory lingers on.

ACKNOWLEDGEMENTS

This thesis would never have been completed without the support of a long list of collaborators. The financial aid of my Mother, and the support of the rest of my family, was appreciated especially considering the duration of this project. The inspiration for this project, the mitochondrial isolation and swelling procedures, and the biological laboratory facilities were the contribution of Dr. W. L. French. If not for Dr. R. C. McIlhenny, the thesis might never have been written, or at best it would be of the unsophisticated style of Appendix B. Dr. McIlhenny was also instrumental in forcing me to carry out the calculations far enough for me to realize the applicability of target theory. Professor A. J. McPhate was kind enough to donate a computer program, and then teach me enough FORTRAN and numerical methods to use it. Dr. J. C. Courtney and Dr. R. M. Knaus offered helpful discussions and encouragement. Thanks are also in order for Dr. H. B. Gray, Jr., who allowed me to complete this thesis while pursuing a Ph.D at the University of Houston. Also at the University of Houston is Dr. George Fox, who encouraged me to finish the Master's degree, and helped with the analytical solution to the swelling rate equation. This research was supported, in part, by the LSU Chapter Society of Sigma Xi Grant-in-Aid.

TABLE OF CONTENTS

TABLE OF CONTENTS (cont'd)

LIST OF TABLES

LIST OF FIGURES

LIST OF FIGURES (cont'd)

ABSTRACT

Using the human body as its own radiation dosimeter has attracted attention because the problem of questionable crossover functions is avoided. The possibility of using peripheral lymphocyte mitochondria as an indicator of radiation dose has not been examined previously, but has merit based on the chemiosmotic hypothesis of mitochondrial function. Swelling-response differences between damaged and undamaged mitochondria in irradiated specimens can be detected by a spectrophotometric method, which relates theoretically to the volume dependence of light scattering. Cobalt-60 gamma irradiated samples of isolated bovine peripheral lymphocyte mitochondria, exposed to doses from 2 to 275 rads, and control samples swelled under identical conditions yielded analytical data to test two theoretical models. The results do not allow unambiguous distinction between single-hit and multi-hit/multi-site hypotheses, but estimated target volumes by either hypothesis are near mitochondrial membrane volume. Probit analysis and empirical curve fitting lead to D_{37} of approximately 170 rads. If it were possible to apply the results to human lymphocytes isolated post irradiation, the method would yield useful dosimetry between 2 and 250 rems.

CHAPTER 1

INTRODUCTION

In order to better utilize nuclear technology, scientists and engineers must be able to measure radiation exposures accurately. Accurate measurements are of primary importance before it will be possible to assess both the short and long term physiological impact of radiation exposures.

There are three major shortcomings in the state-of-the-art for evaluation of personnel exposures. Exposures must be measured by some device; the device must be interpreted; and the interpreted measurement must be correlated to an expected biological effect.

First, our present system requires that the subject of radiation exposure wear on his person, or have in his proximity an appropriate radiation dosimetry device. More often than not, the subject is either not wearing his dosimeter or does not have easy assess to one. Dosage in this case is usually estimated by field measurements or calculations before or after the exposure event.

Second, the matter of interpretation of the properly worn dosimeter is a matter of some ambiguity because of the physical characteristics of the particular device, the spatial distribution of the radiation dose, location of the dosimeter, and temporal distribution of dose.

Third, the response of a given dosimeter may or may not be correlated to any real biological response to radiation exposure. For example, the Relative Biological Effectiveness (RBE) is a correction factor introduced into the dose calculation to adjust values obtained through physical dosimetry to approximate some particular observed biological response. There is still controversy over whether there is a threshold for radiation damage in humans, which is associated with statistical interpretation of largely non-existent data (Fremlin, 1980; Land, 1980). Some measurable doses of radiation cause no detectable biological effects, and some effects manifest themselves in the apparent absence of detectable radiation dose above background. The choice of the biological effect to be monitored is likewise no simple matter since there is still no consensus of opinion as to the specific primary site of radiation damage in living organisms.

With the ultimate aim of obviating the inherent deficiencies of physical dosimetry, the purpose of this thesis is to investigate the feasibility of the use of lymphocyte mitochondria as a limiting indicator of radiation dose to the whole organism.

CHAPTER 2

CRITERIA FOR SELECTION OF AN INTRINSIC BIOLOGICAL DOSIMETER

Theoretically, all three problems introduced in Chapter 1 can be circumvented by the use of an intrinsic biological dosimeter, that is, some organ or structure, common to all members of a species, which will manifest some detectable response to the absorption of energy from a radiation field. In the most idealistic case, this dosimeter would be easily extractable in its native state, with little or no concommittant harm to the donor organism; would be sensitive enough to radiation to measure small doses, especially prior to the onset of the acute physiological syndromes; and would lend itself to study in the extracted state. If the structure in question is not, itself, the primary site of radiation damage, it should at least share functional characteristics with other structures of the body, and be well enough dispersed to provide random sampling and a representative picture of the remainder of the organism. The selection of a candidate tissue for radiobiological dosimetry is not a simple matter, and requires some knowledge of the differential response of human tissues to radiation.

Selection of a Radiosensitive Tissue

The attribute of relative "radiosensitivity" has meaning for comparison of two tissues only when qualified by the criterion used to evaluate sensitivity. Based on the criterion of "early cell death", defined as death before a given number of mitotic cycles;

> Mature lymphocytes (one of the two major classes of circulating white blood cells), erythroblasts (red blood cell precursors), and certain of the spermatogonia (most primitive cell in the spermatogenic series) are undoubtedly the most radiosensitive mammalian cells. (Casarett, pp. 168-169)

Of these, both the erythroblasts and spermatogonia are localized, and although each has been proposed as a biological dosimeter (Segreto, et al., 1974; Ceraci, et al. 1974), neither are convenient because of the difficulties involved in sampling and the calculation of the spatial dose distribution. The mature lymphocytes are, on the other hand, freely circulating which would afford random sampling. Furthermore, lymphocytes are rather undifferentiated, as evidenced by their ability to survive and function in vitro, which implies that they should reflect the general characteristics of other cells. Casarett (p. 178) has reported that lymphocytes are sensitive to acute whole body exposures as low as 10 R. Earlier work with lymphocytes was restricted to cultured cells, by technical difficulties with quantitative isolation (Davis, 1967).

Lymphocytes have been studied extensively for the purpose of dosimetry with various damage indicators (Tamura and Sugiyama, 1974; Silberstein, et al., 1974; Madhvanath, 1976). These studies were done with cultured lymphocytes, which subjects the cells to a selection process, and can lead to misinterpretation of the results. The functional properties of cultured cells are notably different from those in the native state (Elkind and Whitmore, 1967; p. 154, Casarett). There are now a variety of techniques available for the extraction of pure, viable lymphocytes from relatively small samples of peripheral blood, and these methods were reviewed by Willis (unpublished, included in part as Appendix A).

Selection of the Manifestation of Radiation Damage

Regardless of which radiosensitive cells are selected, it is necessary to choose a particular physiological manifestation of radiation damage to be monitored. Historically, one of the first attempts to quantitate radiation exposure was the Skin Erythema Dose (SED), which was defined as that amount of radiation required to produce reddening of human skin within 1 to 2 weeks. The results of this method were not known until three weeks after the exposure, and the variability among subjects, was considerable. Skin reddening is not uniquely associated with radiation exposure, nor is it representative of the internal damage caused by the dose.

The occurrence and viability of lymphocytes has been used (Madhvanath, 1976) as an indicator of radiation damage, however the attenuation of the lymphocyte population in itself bears little information as to the generalized damage to other tissues. An intelligent choice of the biochemical indicator of radiation damage requires knowledge about the cellular response to radiation and understanding of theories about the primary site of radiation damage.

Theoretical Biological Lesions Caused By Radiation

Disturbances in metabolism are the most obvious effects of radiation at the physiological level. These disturbances are not confined to radiation effects, but also occur in natural pathological conditions. The first attempt to explain such physiological effects at the cellular level was the Enzyme Release Hypothesis (pp. 272-277, Bacq and Alexander), which proposed that the membranes of lysosomes were damaged by radiation, leading to the release of degradive enzymes and toxic substances that could cause the destruction of the cell. Later, when it was found that doses greater than 100 rads were necessary to produce detectable leakage of the lysosomal contents, this hypothesis was modified to suggest, instead, a physical disturbance of the spatial arrangement of the enzymes of the respiratory chain (v.i.). With aspersions

now cast on the Enzyme Release Hypothesis, the dominant theory became the Nuclear Damage Hypothesis (Coggle, 1971).

For many years it was known that ionizing radiation induced structural aberrations in chromosomes (Casarett, pp. 99-113) at doses of less than 10 rad (pp. 81-113, Coggle). In fact, H. J. Muller was awarded a Nobel Prize for demonstrating the induction of lethal mutations on Drosophilla chromosomes by the use of X-rays. Most of the work in the field of biological dosimetry has been directed toward determination of the dose-versus-chromosomal-aberration response function (Madhvanath, 1976). However, the usual cellular consequence of a chromosomal aberration is death during that particular mitotic cycle, or growth without cell division so that this gross manifestation is a poor rationale for the heritible changes produced by radiation. More subtle damage to chromosomal DNA is presumed to be the source of these mutations. Subtle damage should be reparable by one of several mechanisms now known to exist within the nucleus (Dugle, et al., 1976). Since it has been well established that a high percentage of random mutations are lethal (Rees, 1967), there is a statistical bias against residual damage being passed on to subsequent generations. If it is, heterozygosity often masks its expression in the adult. A contemporary version of the Nuclear Damage Hypothesis assumes damage to DNA repair mechanisms (Witkins, 1969).

From a chemical-physical perspective, the primary site of radiation damage is the cell's own water content. Radiation is known to generate free radicals in aquaeous solutions, and some degree of radiation protection is afforded by substances having free radical scavenging abilities. Free radicals are highly reactive chemical species and can propagate not only through water, but also through most biomolecules, and can directly interfere with some enzyme reactions (pp. 375-376, Bacq and Alexander). Free radical reactions in the cell result in additional production of toxic peroxides, which, however, can be removed by catalase.

The enzyme interference phenomenon is only observed during irradiation, which eliminates the possibility of direct dosimetry by this process because there is no stored information for post-irradiation recovery. Residual damage to a sensitive biological structure must still be identified to make use of this chemical information. Bacq and Alexander have identified two candidates with known sensitivity to free radicals: DNA; and sulfur-containing enzymes (Ibid, p. 328), most of which are located in the mitochondria.

There is general agreement that the mechanism of radiation damage in cells is not a discrete phenomenon, but a collection of effects on different cell structures.

However, there is a growing volume of evidence that the primary observed effects of radiation may be traced to multiple forms of damage to the cell's mitochondria (Coggle, 1971).

Mitochondria are small organelles with double membranes, occurring in all mammalian cells in numbers which vary from several to several thousands. Mitochondria contain their own DNA which replicates on a time schedule independent of the nuclear mitotic event. This attribute gives them interesting genetic significance (Fine, 1978; also p. 3, Appendix B). The mitochondrion's primary function is the production of high energy compounds (ATP) for utilization in most other cell processes. The production of ATP by oxidative phosphorylation depends on the integrity of the inner mitochondrial membrane, across which a proton (H^+) gradient (Mitchell, 1979) is developed and maintained by the mechanisms of an electron transport chain. This gradient provides the driving force for the production of ATP. One of the notable characteristics of radiation is that it uncouples the process of electron transport from the process of oxidative phosphorylation with exposures as little as 25-100 R (p. 331, Bacq and Alexander). The mode of action of other uncouplers is to cause the collapse of the proton gradient (p. 519, Lehninger). It is clear that a lesion (or hole) in the inner membrane caused by the action of radiation could

permit free passage of protons, which would result in the cessation of ATP production and an increase in ATP breakdown. The idea of a biochemical lesion to the inner mitochondrial membrane is a further modification of the Enzyme Release Hypothesis in that it incorporates aspects of both free radical chemical damage to biomolecules (Orlov, et al., 1976; Mustea, et al., 1978; Nohl and Hegner, 1978a, 1978b) and genetic consequences of radiation damage (von Wagenheim, 1976).

Selection of Damage Criteria

The application of mitochondria damage to radiation dosimetry requires quantitation of the damage, either by direct observation of separated cells, by observation of some change in cellular behavior, or by an altered property of the mitochondria themselves. Morphological changes in mitochondria are the earliest manifestations of radiation damage detectable by electron microscope (Goldfeder and Selig, 1969; Cottier, et al., 1963). Another direct microscopic observation of mitochondrial damage is "cloudy swelling," which is considered indicative of some disruptive cytological influence.

Mitochondria can be isolated and studied from several aspects. Activity of the enzyme malate dehydrogenase, normally retained inside the intact mitochondrion, is released if the organelle is damaged. The capacity of

isolated mitochondria to produce ATP can be measured by means of an oxygen polarigraph (Chance and Williams, 1955; Reed, 1972).

Two conformations of isolated mitochondria have been observed by both electron microscopy, and by isopycnic density gradient centrifugation (Beaufay, et al., 1964; Murfitt, et al., 1978; Holtzman, et al., 1978; Lemasters, 1978), as illustrated in Figure 1. The orthodox configuration is indicative of normal, energized, osmotically active mitochondria. The condensed configuration is associated with abnormal states, such as osmotic shock and myocardial infarction, and is deenergized and osmotically inactive.

Another interesting ability of the mitochondrion is to undergo large volume changes, called "mitochondrial swelling," which are observed both in vivo and in isolates. The presence, duration, and degree of mitochondrial swelling has been used as an indicator of damage in a variety of normal and pathological conditions (Mihai, et al., 1973; Chen and Chang, 1978; Fowler and Woods, 1977; Porter, et al., 1979). There is a significant difference between in vivo and in vitro swelling. As mentioned above, swelling observed in vivo is a phenomenon of nonspecific origin. In vitro swelling, on the other hand, is a demonstration of the mitochondrial response to its biochemical environment.

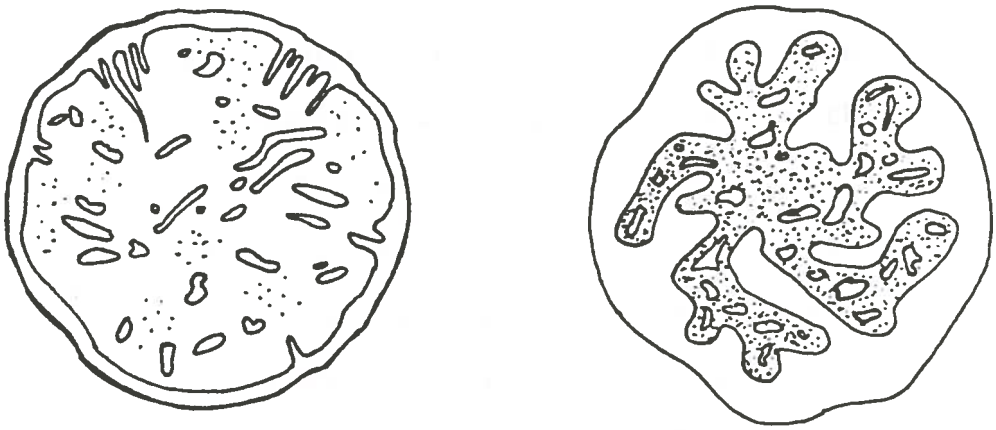

Configuration	ORTHODOX	CONDENSED
Associated metabolic state	Energized	Deenergized
Outer compartment oncotic pressure	High	Low
Osmotic pressure gradient	High	Low
Assumed structural state	Normal	Damaged

Figure 1. Two Conformations of Mitochondria (after Lemasters, 1978).

The three classes of *in vitro* swelling are: osmotic swelling; energy-linked swelling; and transport-related swelling (Harman and O'Hegarty, 1962; Lehninger, 1962; Packer, 1963). Osmotic swelling is caused by the uptake of water in order to satisfy a concentration gradient resulting from the rapid dilution of the mitochondria into a medium much lower in the concentrations of certain internal solutes, such as sucrose, which have a limited permeability. Energy-linked swelling is an increase in volume which accompanies the active process of oxidative phosphorylation. Volume changes are also associated with the active transport of metabolites across the membrane (Harris, 1972).

From a theoretical viewpoint, osmotic swelling is the simplest of the three swelling phenomena to describe. Swelling also offers direct observation of the dynamic behavior of isolated mitochondria, and therefore has the best possibility for success in the evaluation of mitochondria as an intrinsic biological dosimeter.

CHAPTER 3

THEORETICAL TREATMENT OF TURBIDOMETRIC MEASUREMENTS

On the basis of the foregoing development, lymphocyte mitochondria appear to be the best candidate for an intrinsic biological dosimeter, and osmotic swelling appears to be the most straightforward process to quantify damage. Theoretical details of the application of swelling measurements for dosimetric purposes are examined in the ensuing paragraphs.

Mitochondrial swelling was first observed *in vitro* in teased preparations by Koelliker (1888) using a light microscope. Since then, a variety of methods have been applied to the study of mitochondrial volume changes, including phase contrast microscopy (Pauly, *et al.*, 1960; Pauly and Packer, 1960), electron microscopy (Malamed, 1965), electronic particle sizing (Gebicki and Hunter, 1964), radioactive tracers (Tarr and Gamble, 1966), and light scattering/nephelometry (Latimer, 1979). By far the most commonly-used method is turbidometric measurement, by means of absorbance changes on a spectrophotometer. These absorbance changes are a result of light scatter caused by the difference in refractive index between the solution and the interior of the organelle (Wallach, *et al.*, 1966; Oster, 1948; Duniec and Thorne, 1977). An important

analytical treatment of osmotic changes in mitochondrial volume with respect to sucrose penetrability was conceived by Tedeshi (1965). The classical treatment of the relationship between absorbance and volume changes was by Koch (1961). In order to examine the osmotic response of mitochondria, it is necessary to describe the phenomena of swelling and light scatter changes more generally.

Simple First Order Approximation

By a purely thermodynamic argument for conditions of constant temperature, pressure, mass, etc., under which swelling occurs, one would expect the swelling process to exhibit first order kinetics. This presumes that once initiated, osmotic swelling depends on time as the only independent variable. Without detailed knowledge of the process, it is possible to suggest a simple diffusion-rate model, in which the rate of swelling, $d(V(t))/dt$, at any time, t, is proportional to the difference between the attainable volume, V_s. The maximum volume will be reached when the gradient driving forces are resolved. Mathematically,

$$\frac{d[V(t)]}{dt} = L[V_s - V(t)] \ , \qquad (3.1)$$

in which L is a constant of proportionality. An analytical solution of equation (3.1) for the function V(t) can be obtained as follows:

$$\frac{d[\,V(t)\,]}{dt} = y' = LV_s - Ly \ , \qquad (3.1a)$$

$$V_sL = y' + Ly \ ,$$

$$V_sLe^{Lt} = y'e^{Lt} + Le^{Lt}y \ . \qquad (3.2)$$

Using the Product Rule, when L is constant,

$$d[\,ye^{Lt}\,] = y'dt \cdot e^{Lt} + Le^{Lt}dt \cdot y \ ;$$

Or,

$$\frac{d[\,ye^{Lt}\,]}{dt} = y'e^{Lt} + Le^{Lt}y \ . \qquad (3.3)$$

Then, substituting equation (3.3) into equation (3.2):

$$V_sLe^{Lt} = \frac{d[ye^{Lt}]}{dt} \ ,$$

$$V_sLe^{Lt}dt = d[ye^{Lt}] \ . \qquad (3.4)$$

Integration of equation (3.4), with V_o as the constant of integration yields:

$$\int_o^t V_sLe^{Lt}dt = ye^{Lt} \ ,$$

$$ye^{Lt} = V_s e^{Lt}\Big|_o^t + V_o \ . \qquad (3.5)$$

But

$$y = V(t) \ ;$$

$$V(t)e^{Lt} = V_s(e^{Lt} - 1) + V_o \ ,$$

$$V(t) = V_s(1 - e^{-Lt}) + V_o e^{-Lt} \ ,$$

$$V(t) = V_s - V_s e^{-Lt} + V_o e^{-Lt} \ ,$$

$$V(t) = V_s - (V_s - V_o)e^{-Lt} \ . \qquad (3.6)$$

If a new parameter for the volume change, V_c, is defined such that

$$V_c = V_s - V_o \ ,$$

then equation (3.6) becomes

$$V(t) = V_s - V_c e^{-Lt} \ . \qquad (3.7)$$

The form of equation (3.7) is that of a typical saturation function. By this approximation, the volume of the mitochondrion increases rapidly at the onset of swelling, and assymptotically approaches a maximum value,

V_s. The rate of expansion is governed by a first order rate constant, L, and two constant coefficients, V_s and V_c.

Application of Fick's Law of Diffusion

Equation (3.7) is based on no knowledge of the mechanism of swelling. An alternate approach to the mathematical description utilizing Fick's Second Law of Diffusion has been proposed by Tedeshi (1965). This approach takes into account the fact that the rate of influx depends on the surface area available for diffusion, as well as time.

Tedeshi's statement of Fick's Law is as follows:

$$\frac{dC_i(t)}{dt} = k \frac{A(t)}{V(t)} [C_o - C_i(t)] \qquad (3.8)$$

in which $C_i(t)$ is the internal concentration of some solute, k is the permeability constant, A(t) is the surface area subject to diffusion of solute, V(t) is the volume, and C_o is the external concentration of solute. A special case for equation (3.8) is apparent when water is the permeable molecule and C_o is constant by virtue of an overwhelming concentration which changes little during the swelling process. For this case, when M is the mass of impermeable solute,

$$C(t) = M/V(t) \; . \qquad (3.9)$$

Use of this relationship in equation (3.8) yields

$$\frac{d[\frac{M_i}{V(t)}]}{dt} = k \frac{A(t)}{V(t)} \quad \frac{M_o}{V_o} - \frac{M_i}{V(t)} \quad , \tag{3.10}$$

in which the subscripts i and o refer, respectively, to internal and external quantities. For simplicity, equation (3.10) and all subsequent equations will be written without specific designation of time-dependent variables:

$$\frac{d(M_i/V)}{dt} = k(A/V) \ (\frac{M_o}{V_o} - \frac{M_i}{V}) \ . \tag{3.10a}$$

Because the impermeable solute mass remains constant,

$$M_i \frac{d(1/V)}{dt} = k \frac{A}{V} \ (\frac{M_o}{V_o} - \frac{M_i}{V}) \ ;$$

$$\frac{d(1/V)}{dt} = k \frac{A}{V} \ (\frac{M_o}{V_o M_i} - \frac{1}{V}) \ . \tag{3.11}$$

Rewriting,

$$d(1/V) = d(V)^{-1} = -(V)^{-2}dV = -dV/(V^2) \ ,$$

$$- \frac{1}{V^2} \ \frac{dV}{dt} = k \frac{A}{V} \ (\frac{M_o}{V_o M_i} - \frac{1}{V}) \ ,$$

$$- \frac{dV}{dt} = k \frac{A}{V} \ (\frac{M_o V}{V_o M_i} - 1) \ . \tag{3.12}$$

In a sucrose solution, mitochondria assume a nearly spherical shape (Pauly, et al., 1960); hence, the surface area and volume are functions of the time-dependent radius, r:

$$A = 4\pi r^2 \quad ; \tag{3.13a}$$

$$V = \frac{4}{3}\pi r^3 \quad . \tag{3.13b}$$

Substitution of these relations into equation (3.12), and rearranging, results in an expression for the swelling rate, as represented by the change of the radius with time:

$$- \frac{d(\frac{4}{3}\pi r^3)}{dt} = k \frac{4\pi r^2}{\frac{4}{3}\pi r^3} \left(\frac{M_o 4\pi r^3}{3\, V_o M_i} - 1\right) \quad . \tag{3.14}$$

Dividing $4\pi/3$ into both sides gives

$$- \frac{dr^3}{dt} = k \frac{3}{r} \left(\frac{M_o r^3}{V_o M_i} - \frac{3}{4\pi}\right) \quad ; \tag{3.15}$$

$$- \frac{dr^3}{dt} = k \frac{9}{4\pi r} \left(\frac{4\pi r^3 M_o}{3 V_o M_i} - 1\right) \quad . \tag{3.15a}$$

Recognition that $dr^3 = 3r^2 dr$, and substitution into equation (3.15a) results in:

$$- 3r^2 \frac{dr}{dt} = k \frac{9}{4\pi r} \left(\frac{4\pi r^3 M_o}{3 V_o M_i} - 1\right) \quad ,$$

which may be simplified to

$$\frac{dr}{dt} = -\frac{3k}{4\pi r^3}\left(\frac{4\pi r^3 M_o}{3V_o M_i} - 1\right)$$

Finally,

$$\frac{dr}{dt} = \frac{3k}{4\pi r^3} - \frac{kM_o}{V_o M_i} \quad . \tag{3.16}$$

Making use of the volume formula again and the definition of concentration (see equation 3.8):

$$\frac{dr}{dt} = \frac{k}{V} - \frac{kC_o}{M_i} \quad . \tag{3.17}$$

Definition of K_2 as an appropriate constant coefficient reveals the form of equation (3.17):

$$\frac{dr}{dt} = \frac{k}{V} - K_2 \quad . \tag{3.18}$$

At equilibrium dr/dt = 0; hence,

$$0 = \frac{K}{Veq} - K_2 \quad ,$$

$$K_2 = \frac{K}{Veq} \quad ,$$

$$Veq = \frac{K}{K^2} = \frac{K}{C_o/M_i} \quad , \tag{3.19}$$

or, simply,

$$Veq = \frac{M_i}{C_o} \quad . \tag{3.20}$$

The value of equation (3.19) is constant for the assumed conditions of C_o and M_i. Substitution of equation (3.19) back into equation (3.18) results in

$$\frac{dr}{dt} = \frac{k}{V} - \frac{k}{Veq} \quad ,$$

or,

$$\frac{dr}{dt} = k \left(\frac{1}{V} - \frac{1}{Veq}\right) \quad . \tag{3.21}$$

There is a striking similarity between equation (3.21) and equation (3.1). The difference is, however, significant enough to prevent analytical solution by the same method as equation (3.1). Equation (3.21) can be rewritten in the following form:

$$\frac{dr}{dt} = \frac{a}{r^3} - b \quad , \tag{3.22}$$

in which $a = 3k/4\pi$ and $b = k/Veq$. After determination of a common denominator, and rearrangement,

$$\frac{dr}{dt} = \frac{a - br^3}{r^3} \quad ,$$

integration becomes possible

$$\frac{r^3 dr}{(a - br^3)} = \quad dt = t + c \quad ,$$

which is a form consistent with the equation 86, page 410, CRC Standard Math Tables (Selby, 1969). The solution is:

$$t + c = \frac{1}{b} \int dr - \frac{a}{b} \int \frac{dr}{(a + br^3)} \quad . \tag{3.23}$$

The first term of equation (3.23) can be solved and the second term can be replaced with the analytical solution given by equation 74, (Ibid. page 409). This yields:

$$t + c = \frac{1}{b} (r - r_o)$$

$$- \frac{a}{b} \frac{h}{3a} \left[\frac{1}{2} \log \frac{(h + r)^3}{a + br^3} \right.$$

$$\left. + \quad 3 \quad \tan^{-1} \frac{2r - h}{h \quad 3} \right]$$

in which $$h = 3 \frac{a}{b} \quad . \tag{3.24}$$

Modification for the Effects of Surface Tension

Volume change in a mitochondrion is resisted by surface tension (Racker, 1970), elastic forces within the membrane (Trudell, 1977), or damping of the osmotic gradient by the outer membrane (Lemasters, 1978). This requires the modification of the rate equation (3.22) to account for resistance to expansion. The usual way to correct rate equations for the effects of surface tension is to

subtract a term for the resistance. This results in an equation of the following form:

$$\frac{dr}{dt} = \frac{\alpha_1}{r^3} - Kr - \alpha_2 \ , \qquad (3.25)$$

in which K is the membrane's constant of elasticity, and α_1 and α_2 are constants. The middle term implies that the resistance increases linearly with the radius. There is no analytical solution available for equation (3.23). Nevertheless, using a fourth-order Runge-Kutta approximation (Conte, pp. 336-339), it is possible to get a good approximation of r(t) with errors of h^5 (e.g., data taken each 0.5 minutes during a ten-minute assay will yield 3.125×10^{-7} min-error/min).

Probabilistic Model of Light Scatter

As opposed to light scattering methodology, turbidometric measurements have the advantage of avoiding the assumption of an angular distribution function for scattered light. The following treatment describes reduction in light intensity by suspended mitochondria, including both light scatter and absorption. The specific discussion of energy absorption is not included here, but the approach utilized may also find application for description of energy deposition in mitochondrial membranes.

Assuming a spherical mitochondrion (see Figure 2), the radius increases as the following function of volume (Malamed, 1965):

$$r = \left(\frac{3V}{4\pi}\right)^{1/3} \tag{3.26}$$

Correlative assumptions are that the membranes form a spherical shell about the mitochondrion (Wallach, et al., 1966), and that the shell thickness, a, is small compared to the radius, r (actually, a/r = 1/100; Racker, page 21). The volume of the shell is then given by:

$$V_{shell} = 4\pi r^2 a \tag{3.27}$$

Further necessary assumptions are that the total amount of material making up the membrane is constant (no protein or lipid assimilation, fixation, or association over the 10 minute test), and that the density of the material does not change:

$$\text{Mass(gm)} = [\text{Density(gm/cc)}]\,[V_{shell}(\text{cc})] \;;$$

$$\begin{aligned} \text{if:} \quad & d\text{Mass} = 0 \;; \\ \text{and:} \quad & d\text{Density} = 0 \;; \\ \text{then:} \quad & dV_{shell} = 0 \;. \end{aligned} \tag{3.28}$$

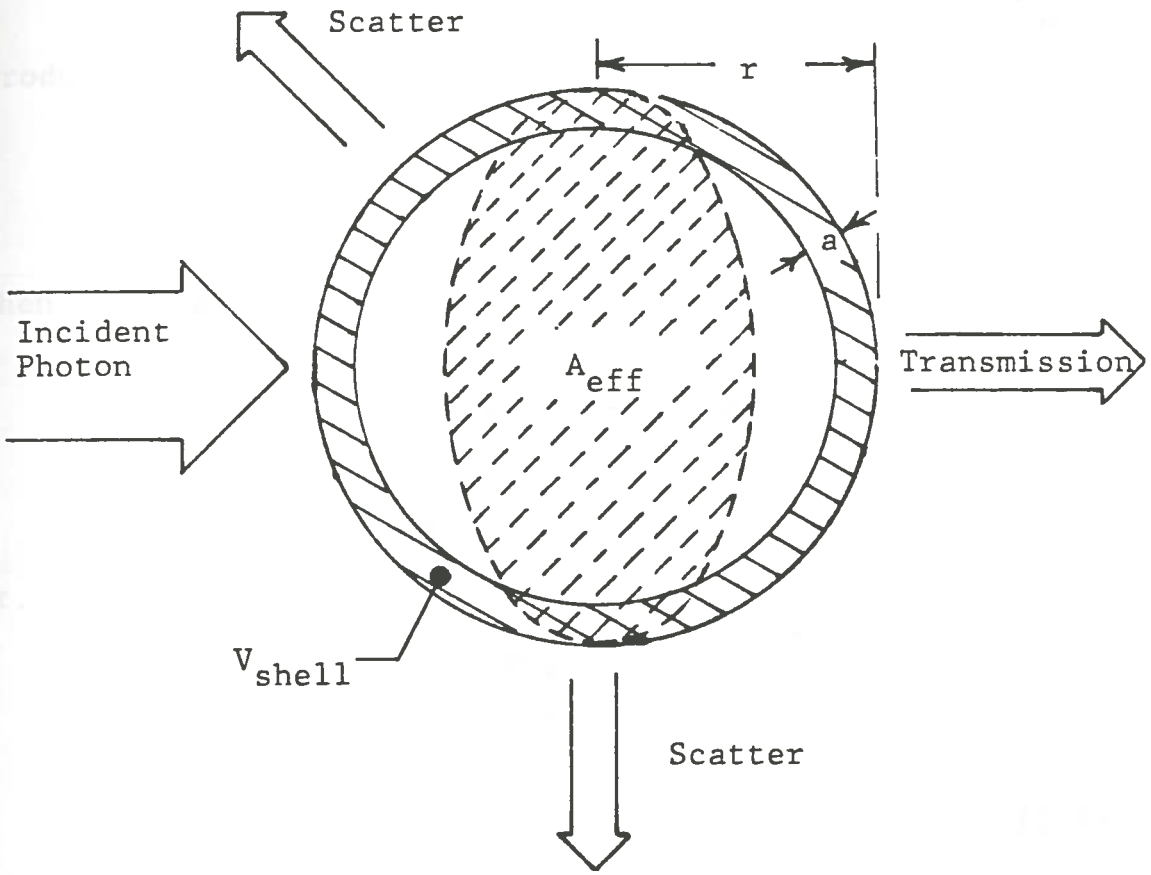

Figure 2. Spherical Mitochondrion

Although the density assumption may appear trivial, the consequence is to allow the quantity "a" to embody all of the membrane structural characteristics, including thickness and conformation (density and compactness). It should be noted that decreases in membrane thickness during swelling have been reported in the literature (Trudell, 1977).

Differentiating equation (3.27) by means of the Product Rule:

$$dV_{shell} = a\ 8\pi r dr + 4\pi r^2 da \quad .$$

Then, by the use of equation (3.28);

$$dV_{shell} = a\ 8\pi r dr + 4\pi r^2 da = 0 \quad ;$$

$$4\pi r^2 da = -\ a\ 8\pi r dr \quad ;$$

or,

$$\frac{da}{a} = -\ \frac{8\pi r dr}{4\pi r^2} \quad ,$$

$$\frac{da}{a} = -\ \frac{2\ dr}{r} \quad . \qquad (3.29)$$

Integrating equation (3.29) yields:

$$\ln(a)\ \alpha\ -\ 2[\ln(r)] \ ;$$

and, by exponentiation

$$a \propto \frac{1}{r^2} \quad . \tag{3.30}$$

Since the swelling is monitored by a spectrophotometer, the change in "thickness", da, of the membrane is critical to the light transmission characteristics of the mitochondrion. If μ_ℓ (Mu) is the linear attenuation coefficient for the mitochondrion, then we can express μ_ℓ as:

$$\mu_\ell = \sigma_T A_{eff} \tag{3.31}$$

in which σ_T is the total microscopic probability for any interaction which would prevent the transmission of light into the sensitive volume of the phototube detector, and A_{eff} is the effective area of the target mitochondrion. Since the mitochondrion is assumed to be spherical, the effective area is proportional to the cross-sectional area (Malamed, 1965):

$$A_{eff} \propto \pi r^2 \tag{3.32}$$

The interaction probability, σ_T, is a function of the density of the material which must be traversed by the light,

$$\sigma_T = f(\text{surface density})$$

in which

$$\text{surface density} = \frac{a(\text{thickness}) \times \text{Mass(gm)}}{4\pi r^2 (\text{surface area})} .$$

Since the amount of material in the membranes is constant:

$$\sigma_T \propto \frac{a}{\pi r^2} \tag{3.33}$$

Substituting equations (3.32) and (3.33) into equation (3.31):

$$\mu_\ell \propto \left(\frac{a}{\pi r^2}\right) (\pi r^2) ,$$

or,

$$\mu_\ell \propto a \quad . \tag{3.34}$$

Combining equations (3.30) and (3.34) leads to the following relationship between the linear attenuation coefficient and the radius:

$$\mu_\ell \propto r^{-2} \tag{3.35}$$

As is conventional for beam attenuation theory (see Glasstone, p. 69), the total macroscopic attenuation

is equal to the sum of the individual microscopic attenuations:

$$\Sigma_{\ell} = p \sum_{i=1}^{N} r_i^{-2} \quad ; \tag{3.36}$$

in which Σ_{ℓ} is the linear macroscopic attenuation coefficient, p is a proportionality constant (which can be adjusted to unity by selection of arbitrary units of radius), r_i is the radius of the i^{th} mitochondrion, and N is the total number of mitochondria in the beam path. It should be noted that this treatment in terms of collision cross-section is, in principle, similar to Mie scattering theory (page 329, Oster; Koch, 1961).

Transmission Characteristics of a Heterogeneous Solution of Mitochondria

One can imagine the possibility of the existance of several discrete groups of mitochondria, which have similar swelling characteristics (Tedeshi, 1965; Willis, unpublished, included in part as Appendix B). This being the case, it is straightforward to write equation (3.36) as

$$\Sigma_{\ell} = p \sum_{i=1}^{N} P_i r_i^{-2} \quad . \tag{3.37}$$

in which P_i is the relative abundance of the i^{th} group of n groups of mitochondria.

The transmission of light as measured by a spectrophotometer is given by the Lambert-Beer relation for uncollided flux, which is, in our case,

$$T = \frac{I}{I_o} = e^{-\Sigma_\ell x} \quad ,$$

in which x is the beam path length; Σ_ℓ is the macroscopic linear attenuation coefficient, or turbidity, τ (Oster, page 322); and T is the fractional transmittance, which is defined as the ratio of the observed intensity, I, to the incident intensity, I_o.

Substitution of equation (3.37) into the Lambert-Beer relation yields

$$T(t) = e^{-(P \sum_{i=1}^{N} P_i r_i^{-2} x)} \qquad (3.38)$$

With unit path length and arbitrary units of r such that p = 1, the following model for the time dependent transmittance is obtained from equation (3.38):

$$T(t) = e^{-\sum_{i=1}^{N} P_i r_i^{-2}} \quad . \qquad (3.39)$$

Equivalently, in terms of volume,

$$T(t) = e^{-\sum_{i=1}^{N} P_i V_i^{-2/3}} \quad . \qquad (3.39a)$$

This treatment is an important restatement of scattering theory for large particles, namely, that as the particle radius increases, the scattering out of the system will decrease (page 333, Oster). This conclusion is neither based on the assumption of an angular scattering distribution function, nor on the fallacious assumption that a decrease in the number of particles in solution per unit volume will occur with an increase in particle radius, as is the current explanation of large particle scatter (page 333, Oster). Nonetheless, the result bears a striking similarity to the result of the classical treatment by Koch (1961; eq. 11, p. 454).

Limitations of the Mathematical Model

The model assumes only osmotically generated swelling. Other modes of swelling may occur simultaneously in the reaction mixture, resulting in distortion of the shape of the swelling curves, as indicated schematically in Figure 3. The consequence of such interference would be the failure of the computer program to properly fit the data, or the imprecise determination of rate constants. Since transport processes have typically fast rates (Harris, 1972) and since oxidative phosphorylation is at a minimum (only endogenous substrates are available to the mitochondria), these interferences are probably minimal.

Another source of interference could come from contamination of the solution by osmotically active

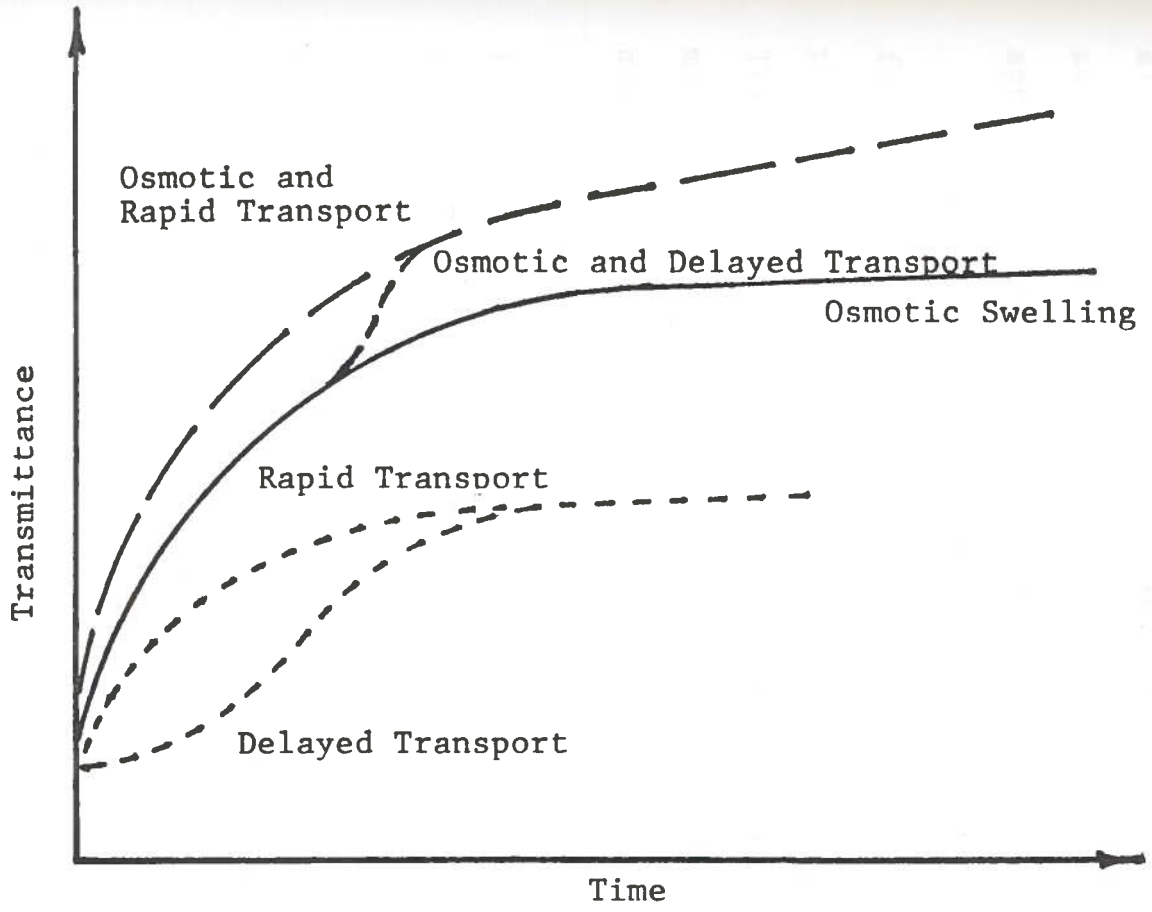

Figure 3. Generalized Swelling Curves

microsomes (Tedeshi, et al., 1963; Wallach, et al., 1966; see also Appendix B). These would contribute to the overall transmittance change observed. The model would account for such contaminants by the inclusion of an appropriate swelling group or groups.

The model does not account for the possibility of fragmentation during the progress of swelling. It is possible to calculate the degree of this process (v.i.). The model can account for a low occurence of intact mitochondria at the onset of swelling through the parameter, P_i.

The final limitation is the source of mitochondria for application of the method. If the radiation dose has been high enough to substantially attenuate the number of peripheral lymphocytes, blood sample size will have to increase proportionately to yield enough mitochondria to produce detectable changes on the spectrophotometer. However, if the radiation dose is high enough to severely reduce the number of circulating lymphocytes, it is already standard techniques.

CHAPTER 4

DOSIMETRIC QUANTITATION

Three preceeding chapters have explained the need for an intrinsic biological dosimeter, presented evidence that lymphocyte mitochondria may satisfy that need, and described the tubidometric study of isolated mitochondria in mathematical detail. It is the intent of this chapter, applying the information from the first three chapters, to devise a dosimetry system of quantification using lymphocyte mitochondria.

In order to make practical use of mitochondrial swelling as a radiation dosimeter, it is necessary to determine a dose-versus-damage function. To accomplish this, mitochondria can be isolated, aliquots can be exposed to a range of radiation doses, and these can be subjected to osmotic swelling. The disturbance of these swelling curves by radiation can be described by a variety of damage indices. Dose-response curves can then be constructed, to select the most precise and sensitive index. It is this sort of generalized treatment which has been applied to the measurement of swelling perturbation in response to other disruptive influences.

Alternatively, the actual effects of radiation damage on the swelling process and its tubidometric

manifestation should be isolated and clearly defined. These pertubations should be measurable quantities which are predictable, reproducible, and understandable in light of the foregoing analytical development.

Once the dose-response function is established, the osmotic swelling of prior-irradiated mitochondria should deviate from the behavior of unirradiated controls in one of two ways. Isolated mitochondria should manifest anomolous swelling curves outright, or should present anomolous dose-response curves upon subsequent radiation exposure.

Quantification of Radiation Effects on Mitochondrial Swelling

If mitochondria exhibit two discrete states, one normal and the other damaged (see Figure 1), the mathematics of Target Theory may be applicable (pp. 136-144, Casarett). The two steps for the application of Target Theory to this system are: 1) the surviving fraction, S, must be determined; and 2) the number of hits per kill and the dose necessary to destroy all but 37%, D_{37}, must be determined.

Determination of the surviving fraction.

A special case of equation (3.39) for the time-dependent transmittance for two groups of mitochondria is:

$$T(t) = e^{-(P_1/r_1^2 + P_2/r_2^2} , \qquad (4.1)$$

in which the radii, r_1 and r_2, and abundances, P_1 and P_2, are defined for intact and damaged mitochondria, respectively.

Using the relationship between "shell thickness," a, and radius, given by equation (3.30) as follows:

$$a \propto 1/r^2 \quad ; \tag{4.2}$$

and substituting into equation (4.1) gives

$$T(t) = e^{-(P_1 a_1 + P_2 a_2)} \quad , \tag{4.3}$$

which can be rearranged to

$$- \ln[T(t)] = P_1 a_1 + P_2 a_2 \quad . \tag{4.4}$$

For the special case of a control, in which none of the mitochondria are damaged, $P_2 = \emptyset$, and at the same time, t,

$$- \ln[T(t)_c] = P_T a_1 \quad , \tag{4.5}$$

in which P_T is the total abundance of mitochondria in the sample. If P_T is arbitrarily defined as unity, equation (4.5) becomes,

$$- \ln[T(t)_c] = a_1 \quad . \tag{4.6}$$

Substitution of equation (4.6) into equation (4.4) yields:

$$- \ln[T(t)] = - P_1 \ln[T(t)_c] + P_2 a_2 \quad , \qquad (4.7)$$

in which P_1 is now the surviving fraction of mitochondria, S. Since damaged mitochondria are assumed to be osmotically inactive, a_2 is time-independent, and if no damage occurs during the swelling process, the term $P_2 a_2$ is constant. Equation (4.7) is more properly presented as follows:

$$\ln[T(t)] = S \ln[T(t)_c] - (1 - S) a_2 \quad ; \qquad (4.8)$$

since the abundance of damaged mitochondria, P_2 plus S equals one. By the relationship between transmittance and absorbance it is possible to restate equation (4.8) as

$$A(t) = S\, A(t)_c + \frac{(1-S)}{2.303}\, a_2 \quad . \qquad (4.8a)$$

It is possible, therefore, to use equation (4.8), or equation (4.8a), as the basis for determining both S, the surviving fraction, and a_2, the "shell thickness" of the damaged group. This method is illustrated in Figure 4.

The slope of control curves should be one, with the intercept at zero. The slopes of damaged samples should be less than one, with intercepts that yield a consistant

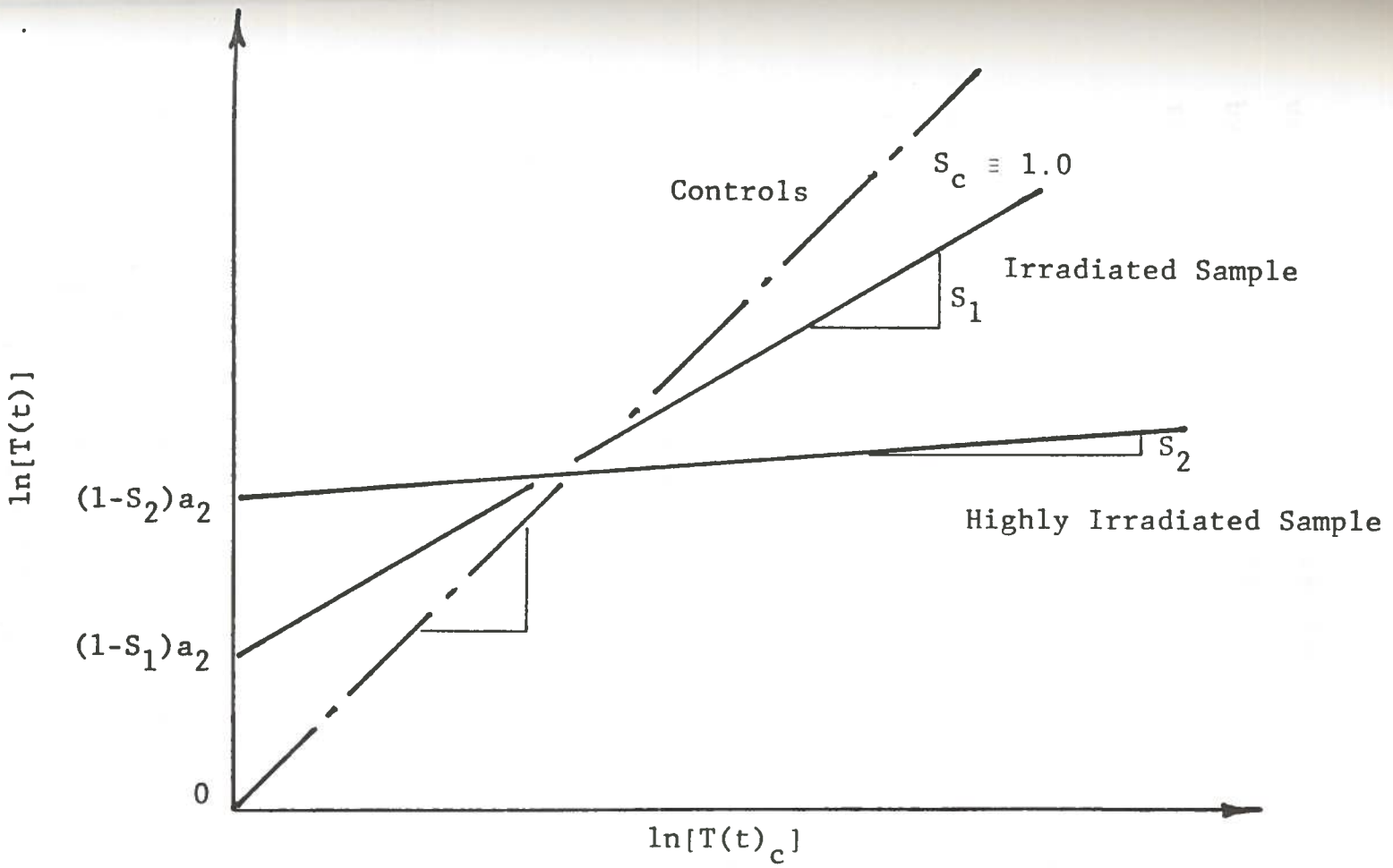

Figure 4. Graphical Determination of Surviving Fraction

value for a_2. This value can be determined independently by the preparation of a totally damaged sample, by the same reasoning as equation (4.6),

$$a_2 = - \ln[T(t)\text{destroyed}] \tag{4.9}$$

This might also be a good way to test the assumption that the damaged mitochondria are osmotically inactive.

It should be noted that timing is especially critical with this method since small timing errors can result in large errors in the sample versus control ratio, especially at early times, when transmittance changes are large and especially important. This method also assumes that the basic process of swelling is either unhampered or nonexistant, which may not be the case. There may be an intermediate level of damage in which swelling proceeds, but at an anomolous rate. In order to examine this possibility, a further treatment of the swelling curves is indicated.

Transformation of swelling curves into volumetric information.

In order to more closely examine the swelling curves, it is necessary to transform the units of transmittance into arbitrary volumetric units. From equation (3.39a) for one group,

$$T(t) = e^{-P(V^{-2/3})} \quad , \tag{4.10}$$

By taking natural logarithms;

$$\ln[T(t)] = -P(V^{-2/3}) \quad ;$$

and simplifying;

$$- \ln[T(t)] = P(V^{-2/3}) \quad ,$$

$$- \frac{\ln[T(t)]}{P} = V^{-2/3} \quad ,$$

and inverting;

$$\frac{P}{- \ln[T(t)]} = V^{2/3} \quad ,$$

and raising to the 3/2 power,

$$\frac{P^{3/2}}{- \ln[T(t)]^{3/2}} = V \quad , \tag{4.11}$$

we can get an equation for V, in terms of transmittance and abundance, P. This can be expressed equivalently,

$$\frac{P^{3/2}}{[A(t)]^{3/2}} = V \quad , \tag{4.11a}$$

in terms of absorbance units. Since the abundance, P, is not known in absolute terms (unless by microscopic

sampling), the volume should be written as:

$$\frac{1}{[A(t)]^{3/2}} = \frac{V}{P^{3/2}} = Q \qquad (4.12)$$

in which the quantity, Q, is defined as the ratio between the volume, and the abundance to the 3/2 power. This ratio can be shown to be identical to the inverse of, the abundance times the shell thickness, a, or

$$Q = \frac{1}{P_a} \quad . \qquad (4.12a)$$

when two Q parameters are compared,

$$\frac{Q_1}{Q_2} = \frac{V_1/P_1^{3/2}}{V_2/P_2^{3/2}} \quad , \qquad (4.13)$$

The ratio is given by equation (4.13).

Conversion of time dependent transmittance data into Q-data will result in numbers which, for a given sample, where $P_1 = P_2$, should be representative of relative volume changes. From this data the magnitude of swelling can be determined.

Determination of first-order rate constants.

By the empirical rate equation for swelling, equation (3.7),

$$V(t) = V_s - V_c e^{-Lt} \quad . \qquad (4.14)$$

Division by the totally swollen volume, V_s, yields

$$\frac{V(t)}{V_s} = 1 - \frac{V_c}{V_s} e^{-Lt}$$

which can be rearranged,

$$(1 - \frac{V(t)}{V_s}) = \frac{V_c}{V_s} e^{-Lt}$$

and reduced to the form:

$$\log \frac{V_c}{V_s} - \frac{Lt}{2.303} = \log (1 - \frac{V(t)}{V_s}) \quad . \qquad (4.15)$$

Equation (4.15) is the equation of a line, and lends itself to the analysis as illustrated by Figure 5. Normalization of the Q-data, that is, division of each Q-value of a sample by the highest achieved Q, will result in the factor $V(t)/V_s$, for the rate constant determination. The intercept is of some use in determining the actual magnitude of swelling, and the relative numerical value of V_s.

Determination of the relative active volume.

Since the mathematical treatment of swelling and light scattering has been statistical, it is possible to describe average properties through the resultant model, using the one-group model.

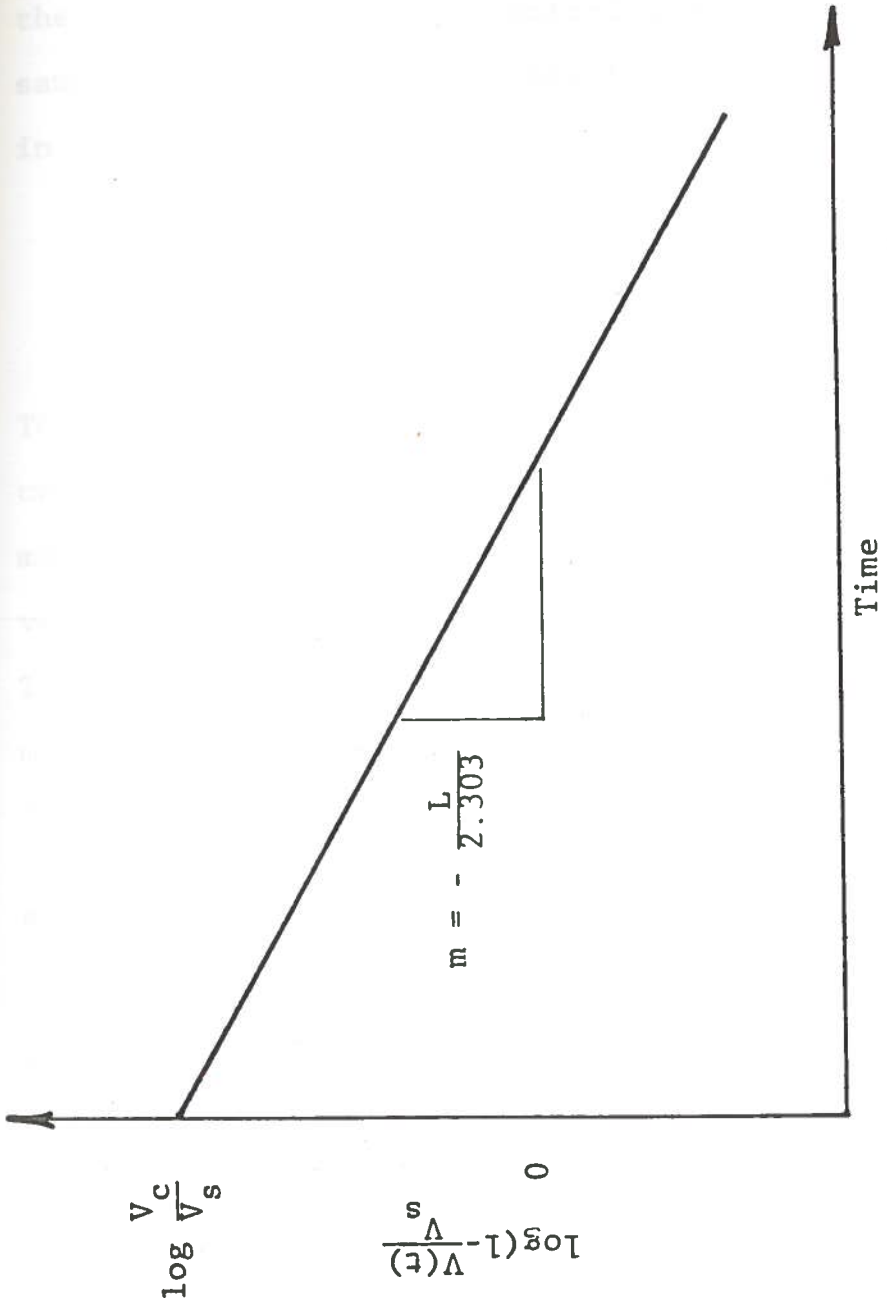

Figure 5. Graphical Determination of First-Order Rate Constant

Using equation (4.13), it is possible to compare the average volume of a given sample at a given time with the average volume of a control (intact) sample at the same time, provided there are the same number of particles in each sample.

$$\frac{Q(t)}{Q(t)_c} = \frac{V}{V_c} \alpha S \quad . \tag{4.16}$$

This relationship is valid only if the swelling process is unchanged from sample to sample, i.e., the rate constant must remain the same. If this is the case, the ratio of volume between sample and control will remain constant. This constant ratio is indicative of the fraction of intact mitochondria in the sample, and must be proportional the S, the surviving fraction.

Application of Target Theory

If mitochondrial damage is, indeed, a two state phenomenon, and if the surviving fraction, S, can be determined, it is a simple matter to analyze the results by means of Target Theory.

As illustrated by the survival curves in Figure 6, a plot of log S-versus-log dose should be constructed. The resultant curve can be interpreted to determine number of hits per kill and inactivation dose, D_{37}, defined as the dose required to inactivate all but 37%.

Another interesting bit of data which can be obtained is the effective target size. By the following relationship,

$$\text{target volume(cc)} = \frac{1}{D_o \times 2 \times 10^{12}} \quad , \qquad (4.17)$$

since D_o is defined as the dose to produce 1 hit per target, and since 1 R will produce 2×10^{12} ionizations per gram (approximately per cc), the target volume can be determined. In the single hit theory, D_o is identical to D_{37}. However, in multihit theory, D_{37} produces m hits per target, where m is the number of hits required for inactivation. Equation (4.17) must be modified, accordingly, to yield:

$$\text{target volume(cc)} = \frac{m}{D_{37} \times 2 \times 10^{12}} \quad . \qquad (4.18)$$

The determination of target volume will give a means of assessment of the validity of this method. Since the sensitive target in this case is assumed to be the mitochondrial membrane, the target volume calculated should correspond with the shell volume, V_{shell}, mentioned previously, or with the volume of some discrete elements of the membrane, such as molecules of the electron transport chain, which are critical to the maintainance of gradients across the membrane.

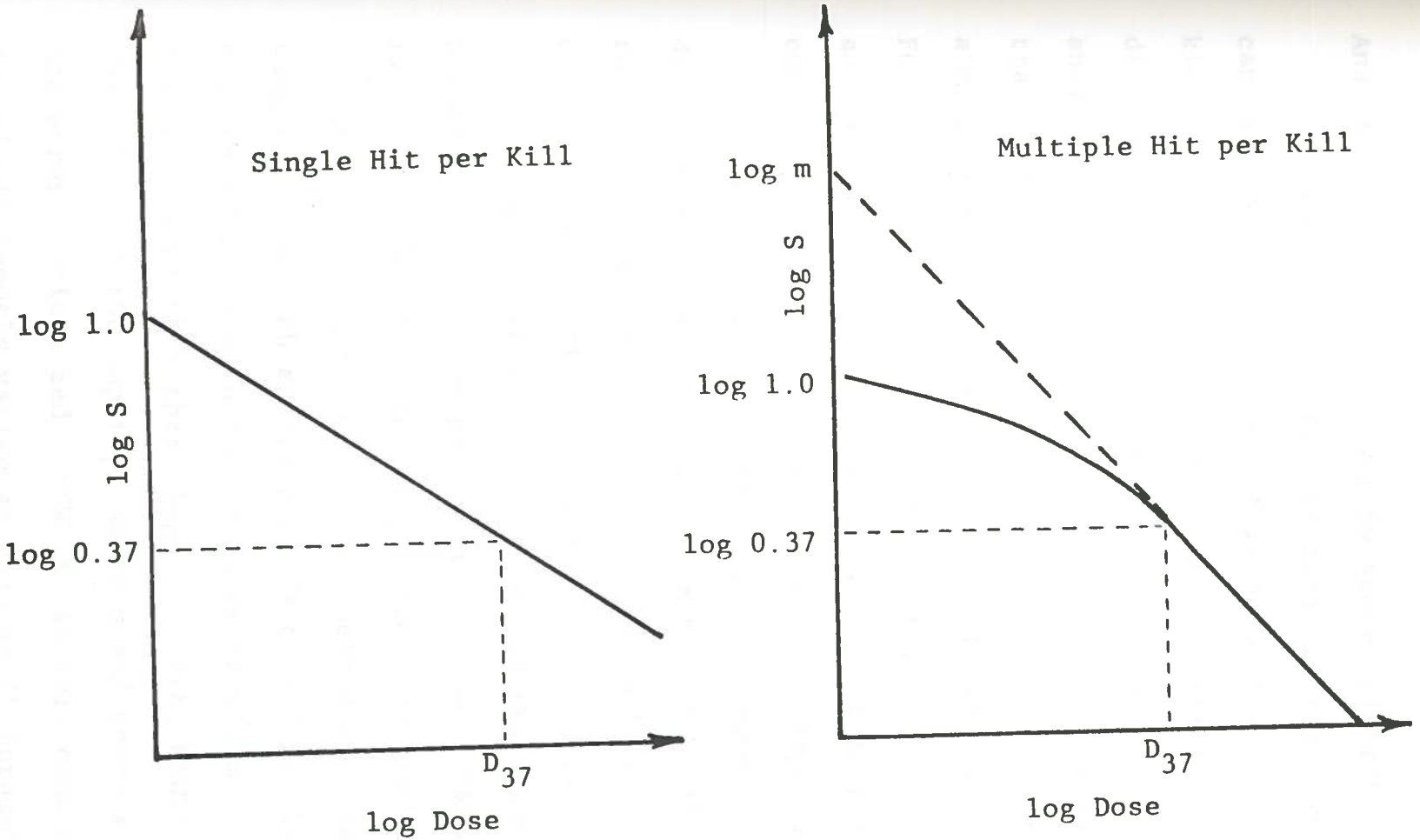

Figure 6. Interpretation of the Dose-Response Curve

Analysis of Swelling Curves by Numerical Methods

Since the analysis of mitochondrial swelling curves can be a monumental task, it is desirable to determine kinetic parameters and conformance of the data to different models by means of electronic computers. The analyses previously detailed in this chapter can easily be transformed into computer programs. In order to provide a more general method of analysis of swelling data, a FORTRAN program was developed. The program consists of an executive program and two subroutines (Figure 7). A complete program listing is included as Appendix C.

The executive program, EXESWL, accepts the input data, generates an initial approximation of the solution, calls the search subroutine, MNWD4A, and handles the output of the solution, once the fit is optimized.

The search subroutine, MNWD4A (MacPhate, 1976) accepts data from the executive program. MNWD4A is an extensively modified version of the algorithm of Powell (1964). This algorithm uses the method of parallel tangents to search an error surface, defined by the subroutine SWELL, and to locate an error minimum. Based on the results of this three-legged search, MNWD4A varies the values of the input parameters and searches again until the error is minimized. MNWD4A, in this configuration, has simultaneously varied as many as 40 parameters, with good results.

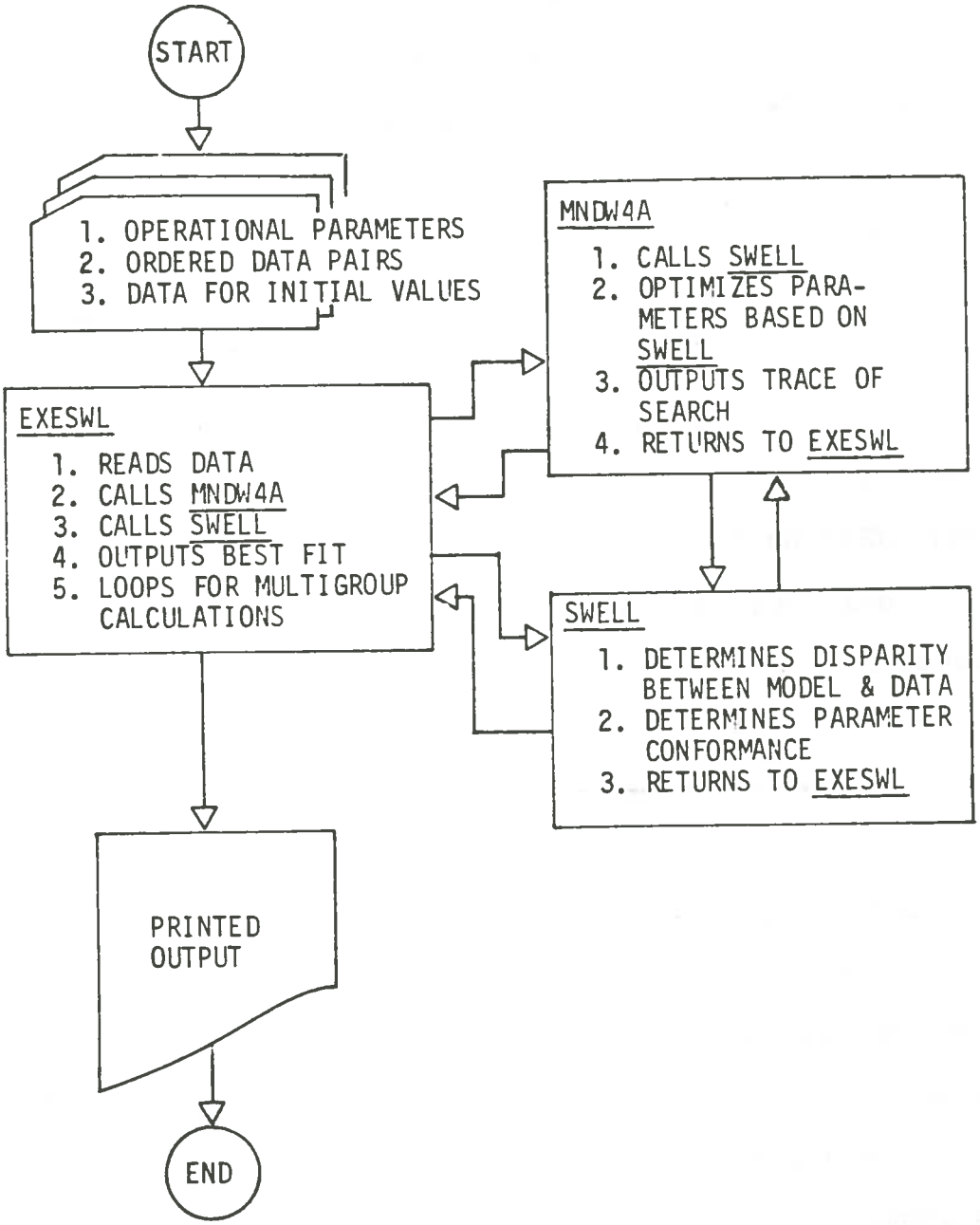

Figure 7. Flowchart of Computer Program

Subroutine SWELL defines an error surface by comparing the result of the tentative parameter values, when substituted into the swelling/transmittance model, against the observed values. SWELL also defines the contraints on the numerical value of the parameters, by adding a penalty function to the overall error of the fit, when the parameters values get out of bounds. The error in the fit is relayed to MNWD4A by the parameter COST.

As soon as the error is minimized, SWELL is called again, this time by EXESWL. The final call to SWELL returns only error in the fit, without the penalty function. EXESWELL uses this error to calculate the standard deviation, outputs the solution, and itterates the process, if multiple terms are to be considered in the model.

With the need for intrinsic biological dosimetry established, the reasoning for the choice of lymphocyte mitochondria as the sensitive organ set forth, an analytical description of the phenomena derived, and a system for quantitative dosimetry detailed, it is now the proper time to discuss the actual methods for the extraction, purification, and analysis of the organelle of interest.

CHAPTER 5

EXPERIMENTAL PROCEDURES

The procedures for the extraction, purification, irradiation, and swelling of lymphocyte mitochondria are divided into modular sections for lymphocyte isolation, mitochondrial extraction, simultaneous irradiation, and swelling. The sections are presented in chronological order. Each section consists of an overview, a protocol, and a technical comments subsection.

Isolation of Lymphocytes from Whole Blood

The purpose of the first protocol is to isolate a high yield of peripheral lymphocytes from whole blood with relatively little contamination by other cell types. The method is a modification of that by Kay and Kayberle (1972), in that the blood was heparinized as described (Demopoullos, 1963) instead of physically defibrinated. The method is rapid and inexpensive, and compares favorably with other methods of lymphocyte isolation (Willis, D., unpublished).

Protocol for lymphocyte isolation.

1) Whole blood is collected in a siliconized glass or plastic flask containing 7500 USP units of heparin (ammonium salt) per liter of blood.

2) Heparinized blood is transferred to 50 ml plastic screw-top centrifuge tubes and centrifuged at 500 x G for 30 minutes, with refrigeration at 5°C.

3) The interfacial buffy coat (white cell layer) is removed by aspiration with a siliconized or plastic Pasteur pipette, without disturbing the underlying red cells. The buffy coat is transferred to plastic centrifuge tubes and is resuspended in an equal volume of Earle's Balanced Salt Solution (EBSS, Earle, 1943).

4) A large plastic syringe (35 ml) filled with cotton fibres acts as an isolation column. The syringe barrel and fibres are washed with EBSS. The washed column is then press-fitted into a 50 ml plastic centrifuge tube. Saran wrap can be wrapped around the syringe barrel to make a complete seal.

5) Approximately 20 ml of buffy coat/EBSS solution is placed on the column using a siliconized pipette. The saturated column is then allowed to incubate for 15 minutes at room temperature.

6) A suspension of lymphocytes and red cells are expressed from the column into the centrifuge tube by insertation of the syringe plunger and compression of the fibres.

7) An equal volume of Tris-buffered, 0.83% ammonium chloride, pH 7.2, is added to the lymphocyte-red cell expression and the mixture is agitated for 5 minutes.

8) Lymphocytes are collected by centrifugation for 15 minutes at 500 X G with refrigeration (2-5^{o}C) in preweighed centrifuge tubes. If the resultant pellet is reddish in color, steps 7) and 8) are repeated.

9) Supernatant is decanted and the isolated lymphocytes are weighed, then resuspended in 0.25 M sucrose, 1 mM Ethylene Diamine (or Dinitrillo) Tetraacetic Acid (EDTA), Tris buffered at pH 7.2. This suspension buffer is referred to as MSB (mitochondrial suspension buffer) throughout the remainder of this chapter.

Technical comments on lymphocyte isolation. The concentration of heparin is important for a good isolation (Campbell, 1964) because an excess will cause coagulation of the lymphocytes, which sometimes traps other types of blood cells. Either silicon-coated or plastic glassware are used to maximize the yield of lymphocytes, which tend to stick to bare glass. The suspension medium, EBSS, is not calcium and magnesium free in order to preserve mitochondrial function, which depends on these divalent metal ions. Cotton fibers are obtained from sterile cotton gauze or cheesecloth. The isolation procedure can be expedited by the use of several columns. Methyl green-

pyronin stain can be used to check purity of the lymphocyte preparation (Kay and Kayberle, 1972; Clark, 1973).

Extraction of Mitochondria from Lymphocytes

The extraction of mitochondria from lymphocytes was achieved by homogenization and differential centrifugation in isoosmotic sucrose. Detailed discussion of this method and alternative approaches are set forth in Appendix B.

Protocol for extraction of mitochondria.

1) Suspended lymphocytes are collected at 500 X G with refrigeration for 15 minutes. After discarding the supernatant, lymphocytes are resuspended in fresh MSB.

2) Lymphocytes are homegenized to rupture the cell membrane by means of a hand operated Dounce homogenizer. Homogenization is conducted in an ice bath for 15 minutes or until no intact lymphocytes are visible under light microscope. Homogenate is transferred to glass centrifuge tubes with plastic inserts.

3) Homogenate is centrifuged at 500 X G for 10 minutes with refrigeration, to collect nuclei and cell debris. Mitochondria remain in suspension. This step can be repeated.

4) Suspended motochondria and microsomes are pipetted off into glass centrifuge tubes. Cell debris pellet can be resuspended and recentrifuged to improve yield. Suspended motochondria are collected at 4000 X G

for 10 minutes refrigerated. Microsomes remain in suspension.

5) After discarding the supernatant, the mitochondrial pellet is resuspended in MSB and pelleted by centrifugation at 8700 X G for 10 minutes with refrigeration. Steps 3) and 4) can be repeated for increased purity.

6) After discarding the supernatant, mitochondria are resuspended in minimal volume of MSB and are refrigerated.

7) Protein concentration is determined by means of a modified Biuret assay, which assumes an extinction coefficient of 0.095 for 1 mg/3 ml volume of Biuret complex.

8) Mitochondria are diluted to 0.75 mg/ml extractant protein concentration and 1 mg/ml Bovine Serum Albumin (BSA), using 4 mg/ml BSA in MSB and MSB as diluents.

Technical comments on mitochondrial extraction.

Homogenization of lymphocytes is especially easy because of their adhesion to the glass walls of the homogenizer. Additional washing is performed if the pellet appeared visually impure. Because of the low temperature of the sample, incubation with Biuret reagent was allowed to proceed at room temperature for a full 60 minutes before observation with the spectrophotometer at 540 nm.

Since the incubation time is so long, the protein assay is run in duplicate to avoid unnecessary delays. The addition of BSA to the mitochondrial fraction is a well-known measure designed to prevent the degenerative tendancy of the organelle outside the cell (Spenser and Horton, 1978). The low temperatures maintained during centrifugation should be sufficient to avoid damage to the membranes from hydrostatic pressure (Wattiaux-deConinck, et al., 1977).

There is one final consideration which has bearing on the method of extraction of lymphocyte mitochondria to be used as intrinsic biological dosimeters. There may be an increase in the fragility of the organelle associated with radiation damage. Since the homogenitation procedure used here is rather rough on the organelles, only intact mitochondria tend to be isolated, causing interpretational difficulties (Locher, et al., 1978). This problem has been surmounted by the method of Jennings, et al. (1969), which uses an enzyme Nagarse. This method has demonstrated the ability to isolate damaged as well as intact mitochondria. This method should be used when isolating lymphocyte mitochondria for dosimetry.

Irradiation of Isolates and Dosimetry

In order to provide simultaneous irradiation at a large range of exposures, the ^{60}Co irradiation facility at LSU Nuclear Science Center was used. The irradiation configuration is illustrated in Figure 8.

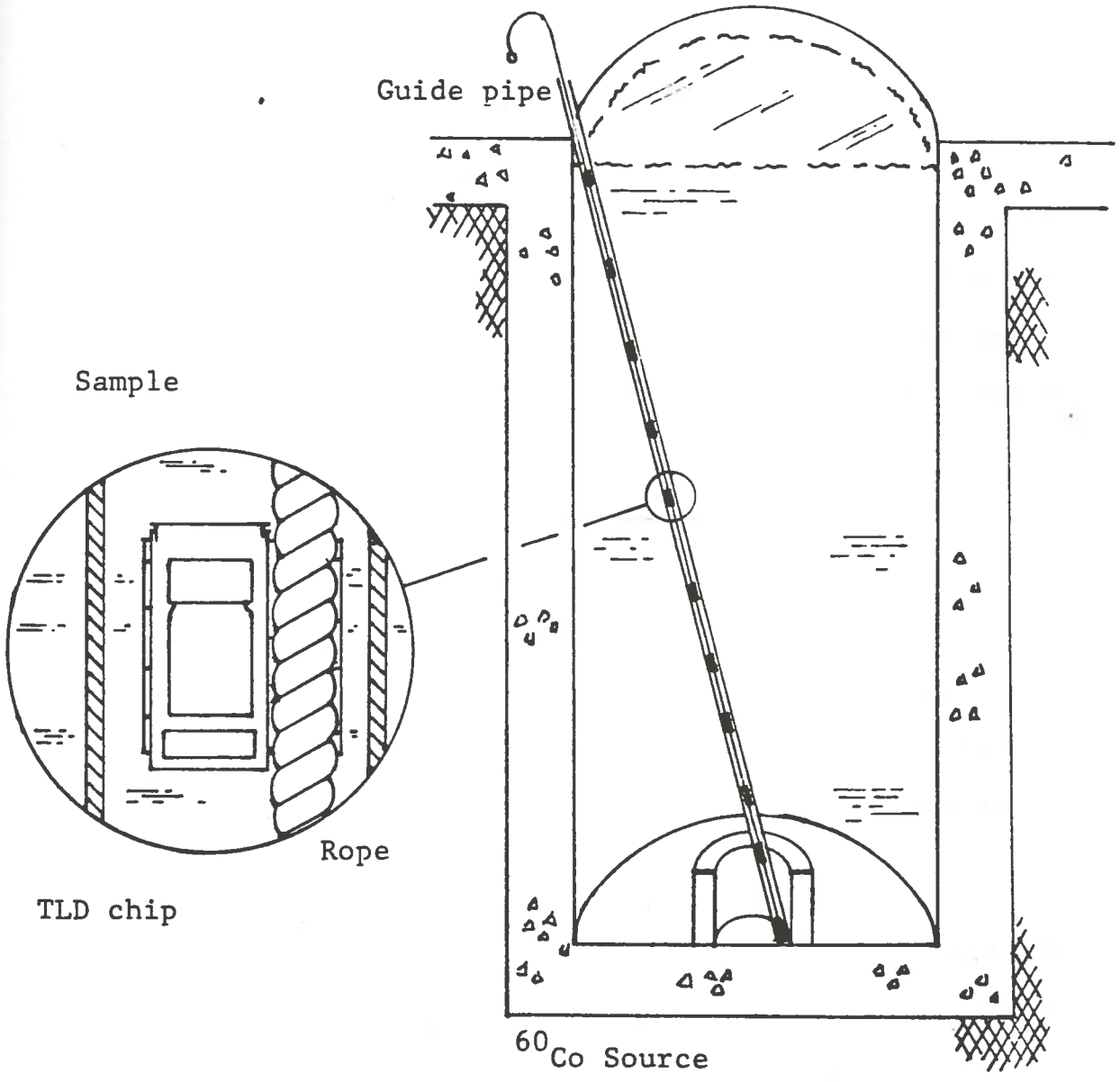

Figure 8. Co^{60} Irradiator Facility

Sample containers (bunnies) were attached to a weighted rope at premeasured positions. Single CaF_2:Mn Thermoluminescent Dosimeters (TLD), cleared of residual excited electrons by overnight heating at 400°C, were heat-sealed inside short pieces of plastic tubing and placed inside each bunny. Individual screw-top 1/2 dram glass bottles, to hold about 1.5 ml of sample each, were filled with water for a field check and were placed inside each bunny. The entire apparatus was quickly introduced into the water-filled irradiation tank by means of a pre-placed polyvinyl chloride (PVC) pipe, open at both ends, which acts as a guide to provide relatively reproducible geometry. When emplacing the PVC pipe, care was taken to allow water to fill the pipe to avoid compromising the biological shield. After irradiation for a timed interval the rope assembly was raised, placed on an ice bath, and transferred to a spectrophotometer. The TLD's were read at 24 hours post-irradiation to constitute a record of relative exposure absorbed by each individual sample.

Induction and Observation of Swelling

The purpose of this procedure is to subject the mitochondria to a set of conditions which will cause a reproducible response as evidence of the mitochondria's degree of integrity. The strip chart preserves a record of this response for later reduction and analysis.

Protocol for swelling.

1) A double beam spectrophotometer is zeroed at 546 nm using 3 ml cuvettes each containing the reaction mixture (0.5 ml BSA at 6 mg/ml; 0.5 ml potassium phosphate monobasic, KH_2PO_4, 0.24 M; 0.5 ml KCl, 1.2 M; and 0.5 ml Tris, 0.12 M pH 7.2) plus 1 ml BSA at 1 mg/ml in MSB to act as the sham sample.

2) The sample cuvette is cleaned and replaced in the spectrophotometer. The 1.5 ml mitochondrial sample is added to the cuvette and the initial absorbance is recorded.

3) The sample is removed from the cuvette; the cuvette is cleaned; and 2 ml of reaction mixture are added to the cuvette.

4) One ml of the mitochondrial sample is added to the cuvette; the strip chart is turned on as a record of the start time; and the cuvette can be covered and inverted several times for mixing. The cuvette is returned to the sample chamber which, when closed begins recording of data.

5) After 10 minutes the test is terminated. The sample is recoverable in its present state. The entire process is repeated for the suceeding samples.

Technical comments of swelling. The procedure for mitochondrial swelling comes from Hunter and Smith (1967). See also Packer, 1967. It is called "pseudoenergized" swelling because of the attempts to correlate it to energy

function in mitochondria. Nevertheless, by the judicious choice of reaction conditions the method manages to produce 3-4 times the magnitude of simple osmotic swelling (Jung, et al., 1977). This is because of the rapid transport of ions in the reaction medium into the mitochondrion, which in turn causes increased water uptake.

The reaction mixture and sample are rather viscous, so that mixing may be a problem. Experience has shown that this mixing problem is observable in 1 ml cuvettes, but not in 3 ml cuvettes.

The viscosity of the solution can be significantly reduced by the use of mannitol instead of sucrose (50% lower viscosity) in the MSB, or by the reduction of BSA or deletion of BSA altogether.

Reproducible mixing and more accurate initiation timing can be provided by a crude sample injection system based on the "stopped-flow" concept.

CHAPTER 6

EXPERIMENTAL RESULTS AND DISCUSSION

Using the experimental methods outlined in Chapter 5, peripheral lymphocytes and mitochondria were obtained, irradiated and subjected to conditions to cause swelling. The resultant swelling data were reduced as described in Chapter 4. The presentation of these results is in chronological order.

Discussion of Experimental Procedures

Whole blood was obtained from aortic puncture of a single, freshly-killed cow at a local slaughter house. Because of the brief duration of the experiment, no antibiotics were added to the suspension media. The red cell expansion was repeated to minimize the number of remaining erythrocytes, and was followed by a wash in MSB. This wash was to remove as much hemoglobin on mitochondria (Pettengill, 1974). The purity of the lymphocyte preparation was checked microscopically after staining with Janus Green B (Brenner, 1949). The yield of lymphocytes was approximately 10 gram wet weight/liter whole blood.

The degree of homogenization of the lymphocytes was checked with and without staining by Janus Green B (Clark, 1973) by phase contrast microscopy. Protein was determined by the method of Gornal, et al. (1949), using

TABLE 1

Dosimetry Results

Distance (cm) from bottom	Dose (rad) in 2 min exposure					
	Field Checks			Range Finding	Experiment (estimated)	From Fig. 3
	1	2 (5 min)	2 (2 min)			
50				(1000)		
60		1.970	788			
70		.980	392			
75				(100)	(100)	(275)
80		.586	234.4		(78)	(200)
85					(53)	(145)
90	36.4	.254	101.6		(35)	(105)
95					(25)	(75)
100		.151	60.4		(18)	(55)
105					(13)	(40)
110	9.7	.63	25.2	(10)	(10)	(28)
115					(7)	(21)
120		33.4	13.36		(5)	(15)
125					(4)	(10)
130	3.19	19.7	7.88		(3)	(8)
135						
140		6.8	2.72		(2)	(4)
150	1.05	5.32	2.128	(1)	(1)	(2)
160		2.76	1.104			
170	.49	.09(?)	--			
180		.77	.308			
190	.25	.40	.16			
200		.25	.10			
210	.035	.12	.048			
220		.06	.024	(.1)		

TABLE 1 (cont'd)

Distance (cm) from bottom	Dose (rad) in 2 min exposure					
	Field Checks			Range Finding	Experiment (estimated)	(from Fig. 3)
	1	2 (5 min)	2 (2 min)			
230	.0164	.00				
240		.00				
250	.0171	.45				
260		.38				
270	.0107	.38				
280		.38				
290	.0098	.37				
300		.37				
310	.0176					
350	.0109					
370	.0112					
390	.0125					
410	.0230					
430	.0178					
450	.0195					
Empty pan	.25	.27				
Remarks:		recalibrated after 240 cm	Calibrated from #2		estimated (TLD reader broken)	estimated

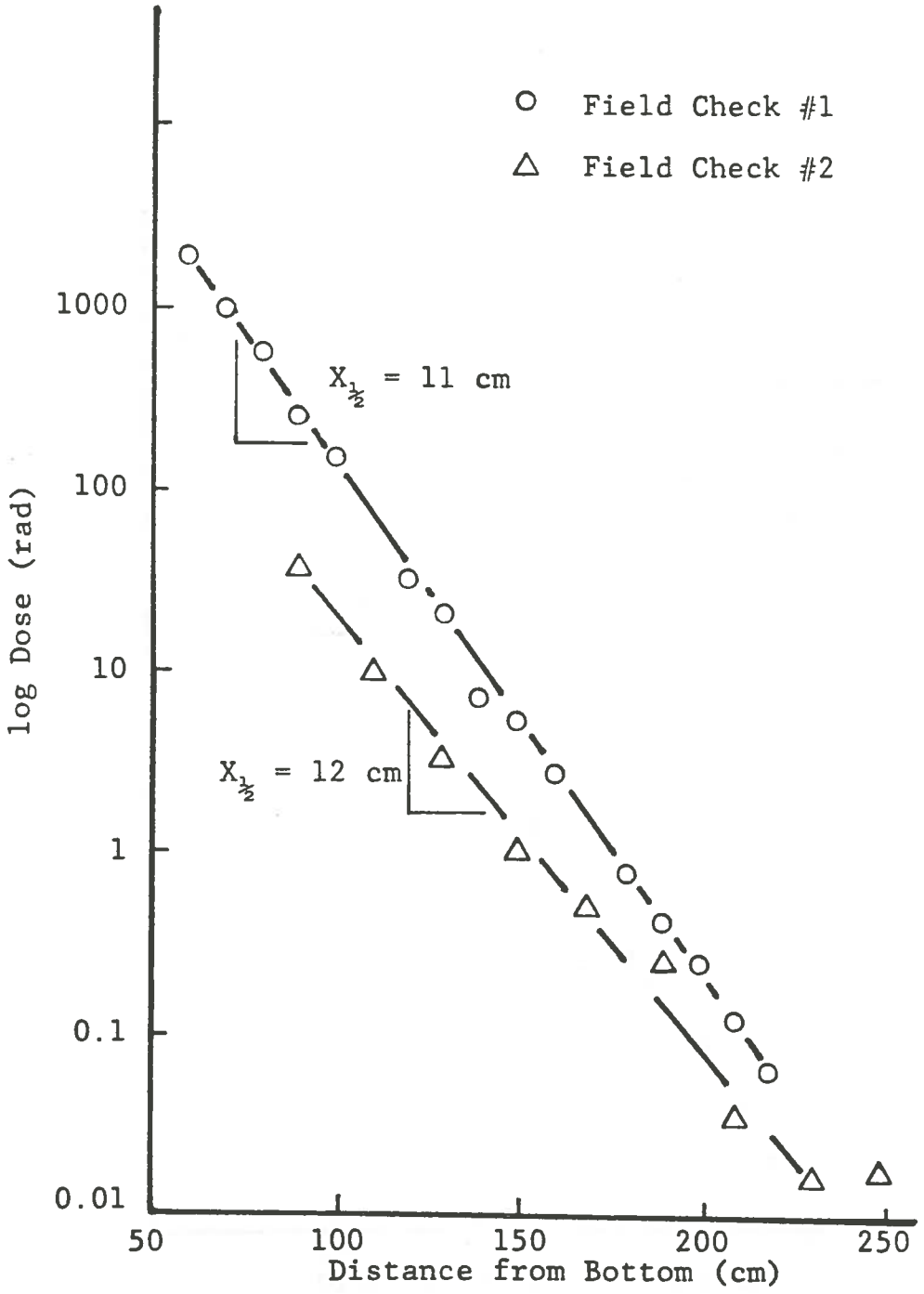

Figure 9. Radiation Field Check

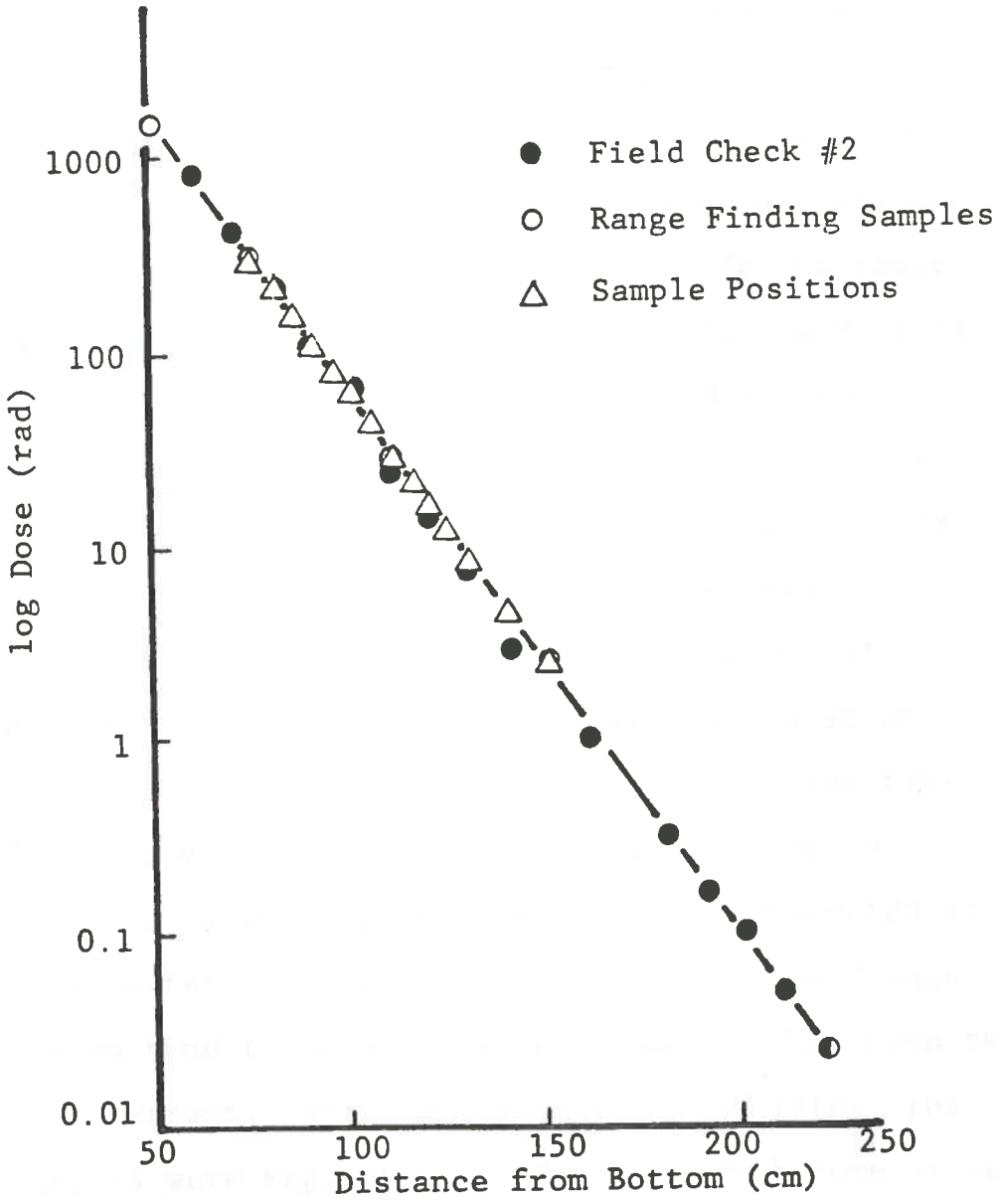

Figure 10. Two-minute Exposure Calibration Graph

BSA as a standard. The yield of mitochondrial protein was approximately 30 μg/ml whole blood, or 0.3% of the lymphocyte wet weight. Since a 0.75 mg sample is used in the swelling assay, 25 ml whole blood is required per sample. The total reaction volume is 3 ml, so the possibility of a microadaptation is not unrealistic.

A field check with water phantoms was conducted as previously described. The results of the field check are presented in Table 1 and Figure 9. The half-thickness calculated for water and radiation of 1.25 MeV (average energy per disintegration for ^{60}Co), from Figure 9 is 11 cm which is in good agreement with accepted values.

In order to provide a bracketting of irradiated samples, the first sample which was swollen was a control. This sample was followed by the most highly irradiated sample and the other samples in decreasing order of exposure. The last sample which was read was also an unirradiated control. The order of assessment was two-fold: If there was significant degeneration over the waiting time for swelling, this would be demonstrated to its fullest extent in the controls, and any time damage effect would tend to mask radiation damage rather than to amplify its effect. While one sample was swelling, the other samples were kept on ice. The spectrophotometer was was chamber at ambient temperature. Samples were not morphologically characterized post irradiation.

A range-finding study of five samples indicated that the swelling curves exhibited abnormalities around the 10 rad dose. Positions were chosen to bracket this area.

Swelling curves were manually digitized with a 0.5 minute step size. The tabulated data is presented in Table 2. It is obvious from these data that there is a decreasing trend of transmittance with increasing dose.

The data were subsequently transformed into Q-data, by the use of equation (4.12). These data are reported in Table 3. From this data it is evident that the magnitude of the volume changes is relatively constant, about 1.52 X start volume.

In order to determine the first order rate constants, the data were further reduced by normalization, as described previously. Data suitable for use in equation (4.15) is presented in Table 4. The rate constants were determined by a linear-least-squares variation of Figure 5. Graphs of the form of Figure 5 were prepared for visual inspection. These graphs are included as Figures 11-16. The values of the rate constants do not vary significantly from the average value of 0.406 + 12% min^{-1}. Variations between samples and nonlinearity of the graphs can best be understood by reference to the well-known dependence of the rate constant on temperature,

TABLE 2. Digitized Swelling Data

Sample	C1	C2	S1	S2	S3	S4	S5	S6
Dose (rad)	0	0	2	4	8	11	15	20
Time (rad)				PERCENT TRANSMITTANCE				
0.5	55	57	53	49	45	47	43	43
1.0	60	58	55	51	47	48.5	45.5	45
1.5	62.5	59	56	52	48.25	50	47	47
2.0	63	59.5	57	53	49.5	51	48	48
2.5	63.5	60	57.7	54	50.2	52	49	49
3.0	64	60.5	58.2	54.5	50.8	52.4	49.5	49.75
3.5	64.3	60.8	58.6	55	51.2	52.8	50	50.25
4.0	64.6	61.1	58.8	55.3	51.5	53.2	50.5	50.8
4.5	64.8	61.4	59	55.5	51.7	53.4	50.75	51.2
5.0	65	61.6	59.2	55.7	51.8	53.6	50.9	51.5
5.5	65.1	61.7	59.4	55.9	51.9	53.8	51	51.8
6.0	65.25	61.8	59.6	56.1	52	54	51.1	52
6.5	65.4	61.9	59.7	56.3	52	54.2	51.2	52.25
7.0	65.5	62	59.8	56.5	52	54.3	51.3	52.5
7.5	65.6	62	59.9	56.7	52	54.4	51.4	52.7
8.0	65.75	62.1	60	56.8	52	54.5	51.5	52.9
8.5	65.9	62.1	60.1	56.9	52	54.6	51.6	53
9.0	66	62.2	60.2	57	52	54.7	51.7	53.1
9.5	66.1	62.2	60.3	57	52	54.7	51.8	53.2
10.0	66.2	62.3	60.4	57	52	54.7	51.9	53.3
10.5	66.3	62.3	60.5	57.1	52	54.7	52	53.4

TABLE 2. (continued)

Sample Dose (rad) Time (rad)	S7 28	S8 40	S9 55	S10 75	S11 100	S12 140	S13 200	S14 275
				PERCENT TRANSMITTANCE				
0.5	49	39	30	49	35	39	27	12
1.0	51	42	33	50	38	41	32	15
1.5	52.4	43.5	35	51	40.5	42	35	17.3
2.0	53.3	44.8	37	51.4	41.8	43	36.8	19
2.5	54	45.6	38	51.8	43	43.8	38	19.8
3.0	54.5	46.2	38.7	52	43.6	44.2	39	20.4
3.5	55	46.8	39.4	52.1	44.2	44.7	39.7	21
4.0	55.4	47.2	40.4	52.2	44.6	45	40.3	21.6
4.5	55.8	47.6	40.7	52.3	45	45.3	40.8	22
5.0	56	47.9	41	52.3	45.4	45.6	41.2	22.3
5.5	56.2	48.1	41.3	52.2	45.7	45.8	41.6	22.6
6.0	56.4	48.2	41.6	52.2	45.9	45.9	41.9	22.9
6.5	56.8	48.3	41.8	52.1	46.1	46	42.2	23.1
7.0	56.9	48.4	42	52	46.2	46	42.5	23.2
7.5	57	48.5	42.2	51.9	46.3	46.1	42.8	23.3
8.0	57.1	48.6	42.4	51.8	46.4	46.1	43	23.4
8.5	57.2	48.7	42.5	51.7	46.5	46.2	43.4	23.5
9.0	57.3	48.8	42.6	51.5	46.6	46.2	43.4	23.7
9.5	57.4	48.8	42.7	51.3	46.7	46.3	43.6	23.9
10.0	57.5	48.9	42.8	51.2	46.8	46.3	43.8	24.0
10.5	57.6	48.9	42.9	51.1	46.9	46.3	44	24.1

TABLE 3. "Q" Values

Sample Dose (rad) Time (rad)	C1 0	C2 0	S1 2	S2 4	S3 8	S4 11	S5 15	S6 20
				Q VALUES				
0.5	7.56	8.29	6.91	5.80	4.90	5.33	4.51	4.51
1.0	9.57	8.69	7.56	6.32	5.33	5.68	5.00	4.90
1.5	10.84	9.12	7.91	6.61	5.62	6.05	5.33	5.33
2.0	11.12	9.34	8.29	6.91	5.93	6.32	5.56	5.56
2.5	11.42	9.57	8.57	7.22	6.11	6.61	5.80	5.80
3.0	11.72	9.81	8.77	7.39	6.27	6.73	5.93	5.99
3.5	11.91	9.95	8.94	7.56	6.38	6.85	6.05	6.12
4.0	12.10	10.10	9.03	7.66	6.46	6.97	6.19	6.27
4.5	12.23	10.26	9.12	7.73	6.52	7.03	6.25	6.38
5.0	12.36	10.36	9.20	7.81	6.55	7.09	6.30	6.46
5.5	12.42	10.41	9.29	7.88	6.58	7.16	6.32	6.55
6.0	12.52	10.47	9.39	7.95	6.61	7.22	6.35	6.61
6.5	12.63	10.52	9.43	8.02	6.61	7.29	6.38	6.68
7.0	12.69	10.57	9.48	8.10	6.61	7.32	6.41	6.76
7.5	12.79	10.57	9.52	8.18	6.61	7.36	6.44	6.82
8.0	12.87	10.63	9.57	8.21	6.61	7.39	6.46	6.88
8.5	12.97	10.63	9.62	8.25	6.61	7.42	6.49	6.91
9.0	13.04	10.68	9.66	8.29	6.61	7.46	6.52	6.94
9.5	13.12	10.68	9.71	8.29	6.61	7.46	6.55	6.97
10.0	13.19	10.73	9.76	8.29	6.61	7.46	6.58	7.00
10.5	13.26	10.73	9.81	8.33	6.61	7.46	6.61	7.03
Q_s/Q_o	1.75	1.29	1.42	1.44	1.35	1.40	1.47	1.56

TABLE 3. (continued)

Sample Dose (rad) Time (rad)	S7 28	S8 40	S9 55	S10 75	S11 100	S12 140	S13 200	S14 275
				Q VALUES				
0.5	5.80	3.82	2.64	5.80	3.25	3.82	2.33	1.13
1.0	6.32	4.32	2.99	6.05	3.67	4.15	2.87	1.34
1.5	6.73	4.66	3.25	6.32	4.07	4.32	3.25	1.50
2.0	7.00	4.86	3.52	6.44	4.29	4.51	3.50	1.63
2.5	7.22	5.02	3.67	6.55	4.51	4.66	3.67	1.70
3.0	7.39	5.15	3.78	6.61	4.62	4.74	3.82	1.74
3.5	7.56	5.28	3.89	6.64	4.74	4.84	3.93	1.79
4.0	7.70	5.37	4.05	6.67	4.82	4.90	4.03	1.84
4.5	7.84	5.46	4.10	6.70	4.90	4.96	4.12	1.88
5.0	7.91	5.53	4.15	6.70	4.98	5.02	4.18	1.90
5.5	7.99	5.58	4.20	6.67	5.04	5.06	4.25	1.93
6.0	8.06	5.60	4.25	6.67	5.08	5.08	4.31	1.95
6.5	8.21	5.63	4.29	6.64	5.13	5.11	4.36	1.97
7.0	8.25	5.65	4.32	6.64	5.15	5.11	4.41	1.98
7.5	8.29	5.68	4.36	6.58	5.17	5.13	4.47	1.99
8.0	8.33	5.70	4.40	6.55	5.19	5.13	4.51	2.00
8.5	8.37	5.73	4.41	6.52	5.21	5.15	4.54	2.00
9.0	8.41	5.75	4.43	6.46	5.24	5.15	4.58	2.02
9.5	8.45	5.75	4.45	6.41	5.26	5.17	4.62	2.04
10.0	8.49	5.77	4.47	6.38	5.28	5.17	4.66	2.05
10.5	8.56	5.77	4.49	6.35	5.30	5.17	4.70	2.06
Q_s/Q_o	1.58	1.51	1.70	1.09	1.63	1.35	2.02	1.82

TABLE 4. Normalized Volumetric Data

Sample Dose (rad) Time (rad)	C1 0	C2 0	S1 2	S2 4	S3 8	S4 11	S5 15	S6 20
				$(1 - Q/Q_s)$				
0.5	.430	.227	.296	.304	.259	.280	.318	.359
1.0	.278	.190	.229	.241	.194	.239	.244	.303
1.5	.183	.150	.194	.207	.150	.189	.194	.242
2.0	.161	.130	.155	.171	.103	.153	.159	.209
2.5	.139	.108	.126	.133	.076	.114	.123	.175
3.0	.116	.086	.106	.113	.051	.098	.103	.140
3.5	.102	.073	.089	.092	.035	.082	.085	.129
4.0	.088	.059	.080	.080	.023	.065	.063	.103
4.5	.078	.049	.070	.072	.014	.058	.055	.093
5.0	.068	.035	.062	.062	.009	.050	.047	.081
5.5	.063	.030	.053	.054	.005	.040	.044	.068
6.0	.056	.024	.043	.046	--	.032	.039	.060
6.5	.048	.020	.039	.037	--	.029	.035	.050
7.0	.043	.015	.034	.028	--	.019	.030	.038
7.5	.035	.015	.030	.018	--	.013	.026	.030
8.0	.029	.009	.025	.014	--	.009	.023	.021
8.5	.022	.009	.019	.010	--	.005	.018	.017
9.0	.017	.005	.015	.005	--	--	.014	.013
9.5	.011	.005	.010	.005	--	--	.009	.001
10.0	.005	--	.005	.005	--	--	.005	.004

TABLE 4. (continued)

Results of Linear Least-Square Fit for Preceding Data								
Correlation	.972	.997	.984	.984	.993	.949	.986	.981
Intercept (V_c/V_s)	.399	.307	.344	.447	.444	.295	.335	.522
Slope k(min^{-1})	.360	.429	.357	.439	.768	.402	.368	.406

Note: Average k is .430 $\pm$ 24%. Discarding 53 results in an average k of .406 $\pm$ 12%.

TABLE 4. (continued)

Sample Dose (rad) Time (rad)	S7 28	S8 40	S9 55	S10 75	S11 100	S12 140	S13 200	S14 275
				$(1 - Q/Q_s)$				
0.5	.322	.338	.412	.087	.387	.261	.504	.451
1.0	.262	.251	.334	.047	.308	.197	.389	.350
1.5	.214	.192	.276	.005	.232	.164	.309	.272
2.0	.182	.158	.216	--	.191	.128	.255	.209
2.5	.156	.130	.183	--	.149	.099	.219	.175
3.0	.137	.108	.158	--	.128	.098	.187	.155
3.5	.117	.085	.134	--	.106	.083	.164	.131
4.0	.101	.069	.098	--	.091	.064	.143	.107
4.5	.084	.054	.087	--	.075	.052	.123	.087
5.0	.076	.042	.076	--	.060	.041	.111	.078
5.5	.067	.033	.065	--	.049	.029	.096	.063
6.0	.055	.029	.053	--	.041	.017	.083	.053
6.5	.041	.024	.045	--	.032	.012	.072	.044
7.0	.036	.021	.038	--	.028	.012	.062	.039
7.5	.031	.016	.029	--	.025	.008	.049	.034
8.0	.027	.012	.020	--	.021	.008	.040	.029
8.5	.022	.007	.018	--	.017	.004	.034	.029
9.0	.017	.003	.013	--	.011	--	.026	.019
9.5	.013	.003	.009	--	.007	--	.017	.010
10.0	.008	--	.005	--	.004	--	.009	.005

TABLE 4. (continued)

Results of Linear Least-Square Fit for Preceding Data								
Correlation	.993	.986	.991	--	.990	.995	.983	.981
Intercept (V_c/V_s)	.398	.464	.555	--	.480	.352	.590	.521
Slope $k(min^{-1})$	.351	.490	.417	--	.423	.497	.354	.390

Note: Average k is .430 $\pm$ 24%. Discarding 53 results in an average k of .406 $\pm$ 12%.

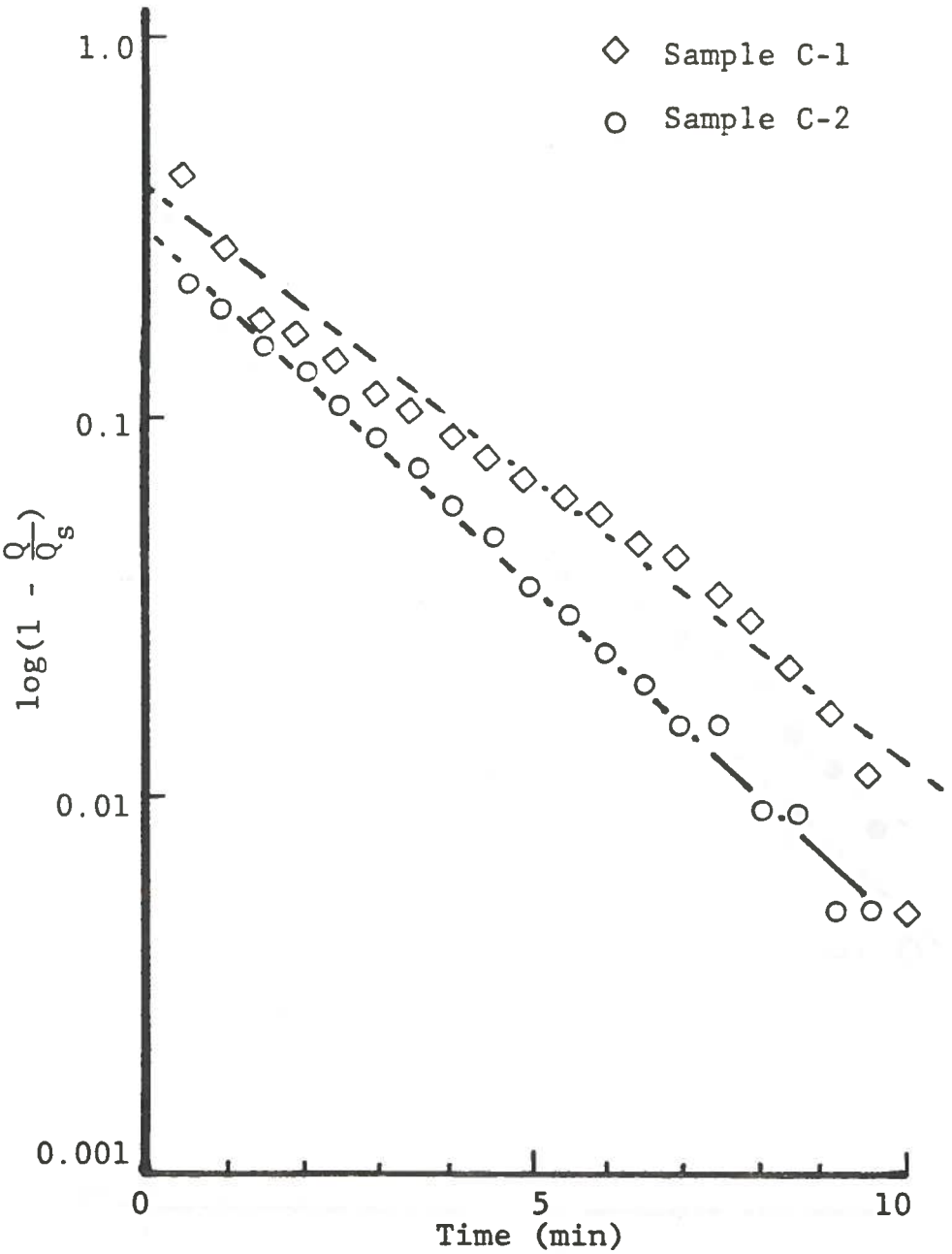

Figure 11. Swelling Rate Constant Determinations for Samples C1 and C2.

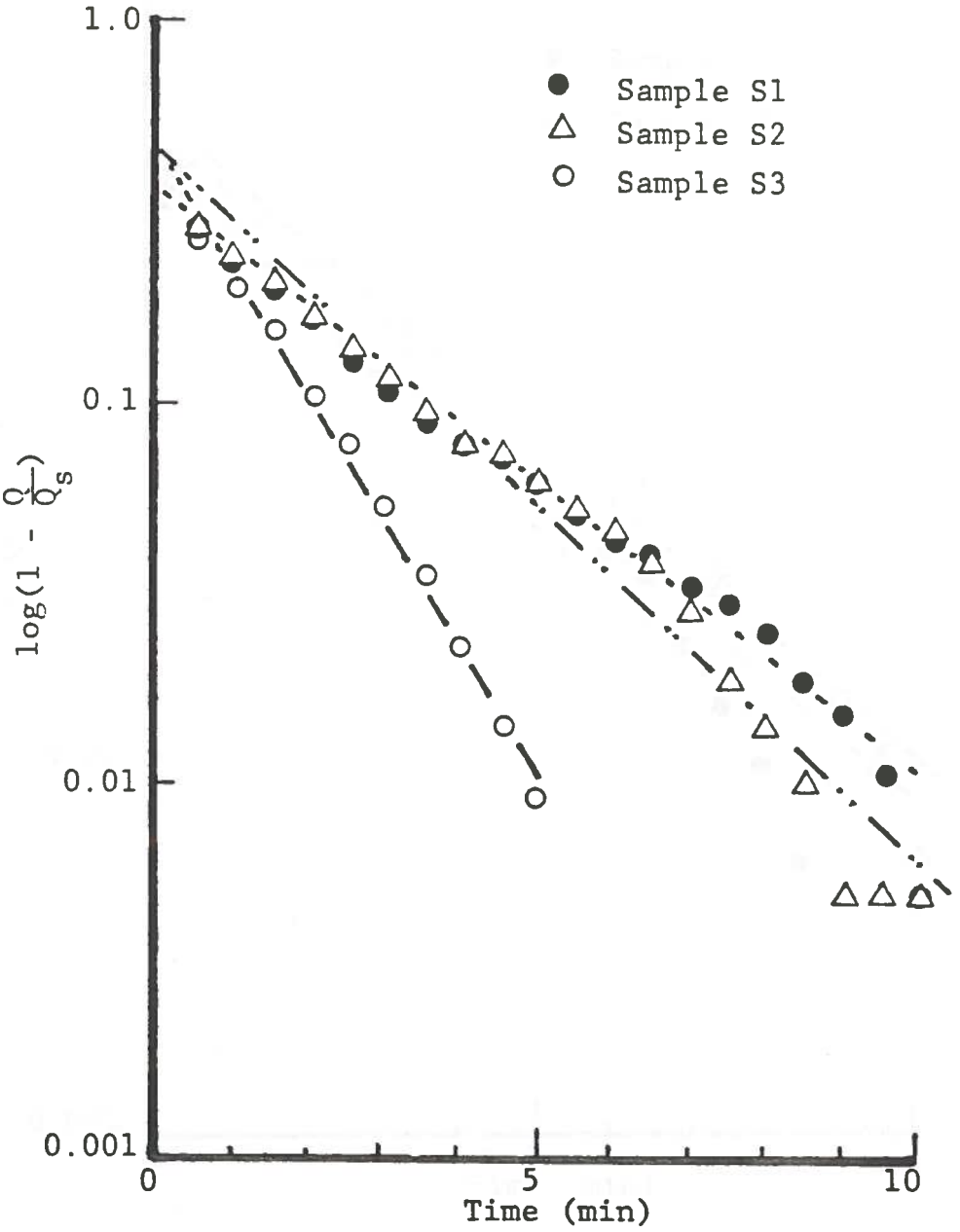

Figure 12. Swelling Rate Constant Determination for Samples S1-S3.

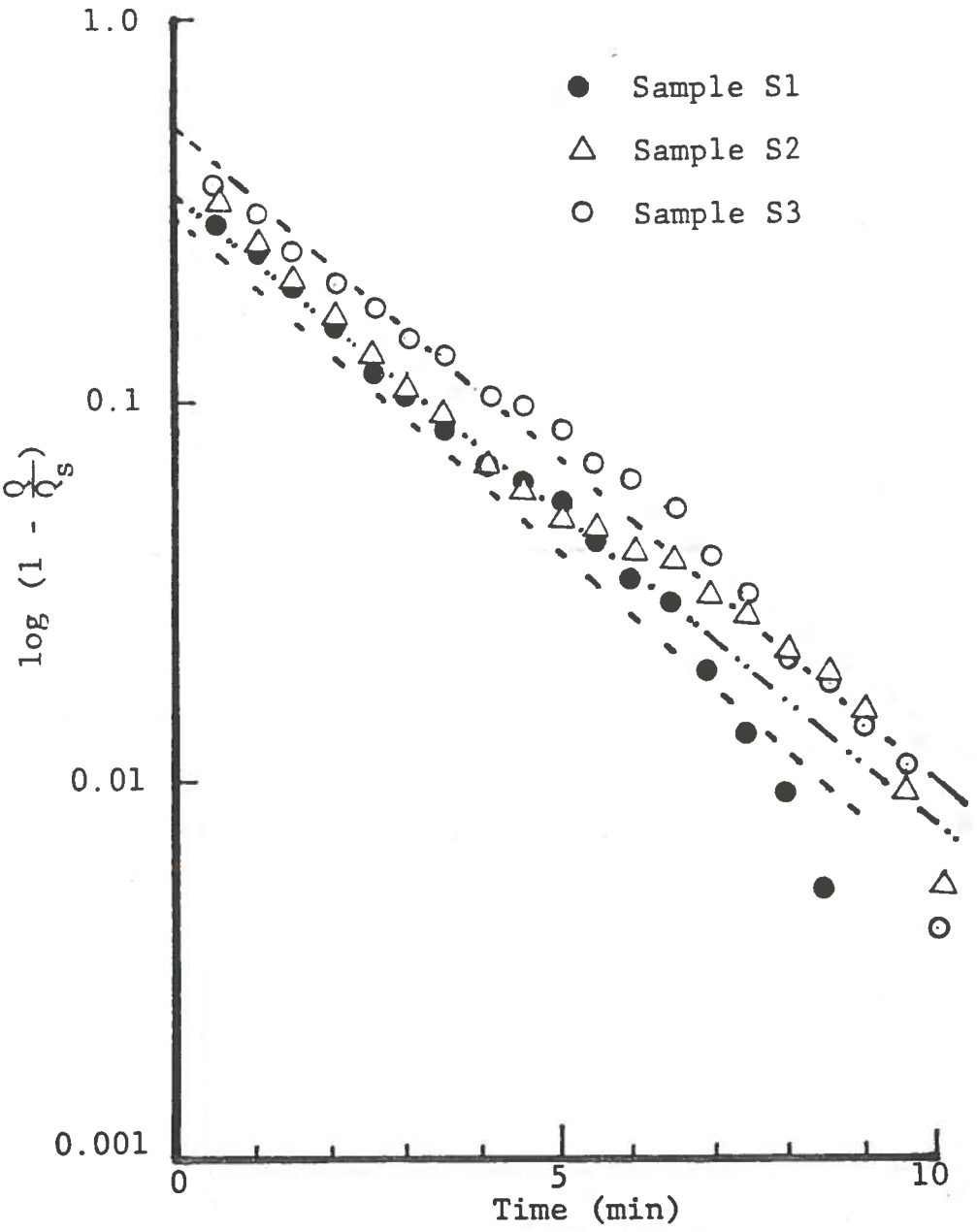

Figure 13. Swelling Rate Constant Determinations for Samples S4-S6.

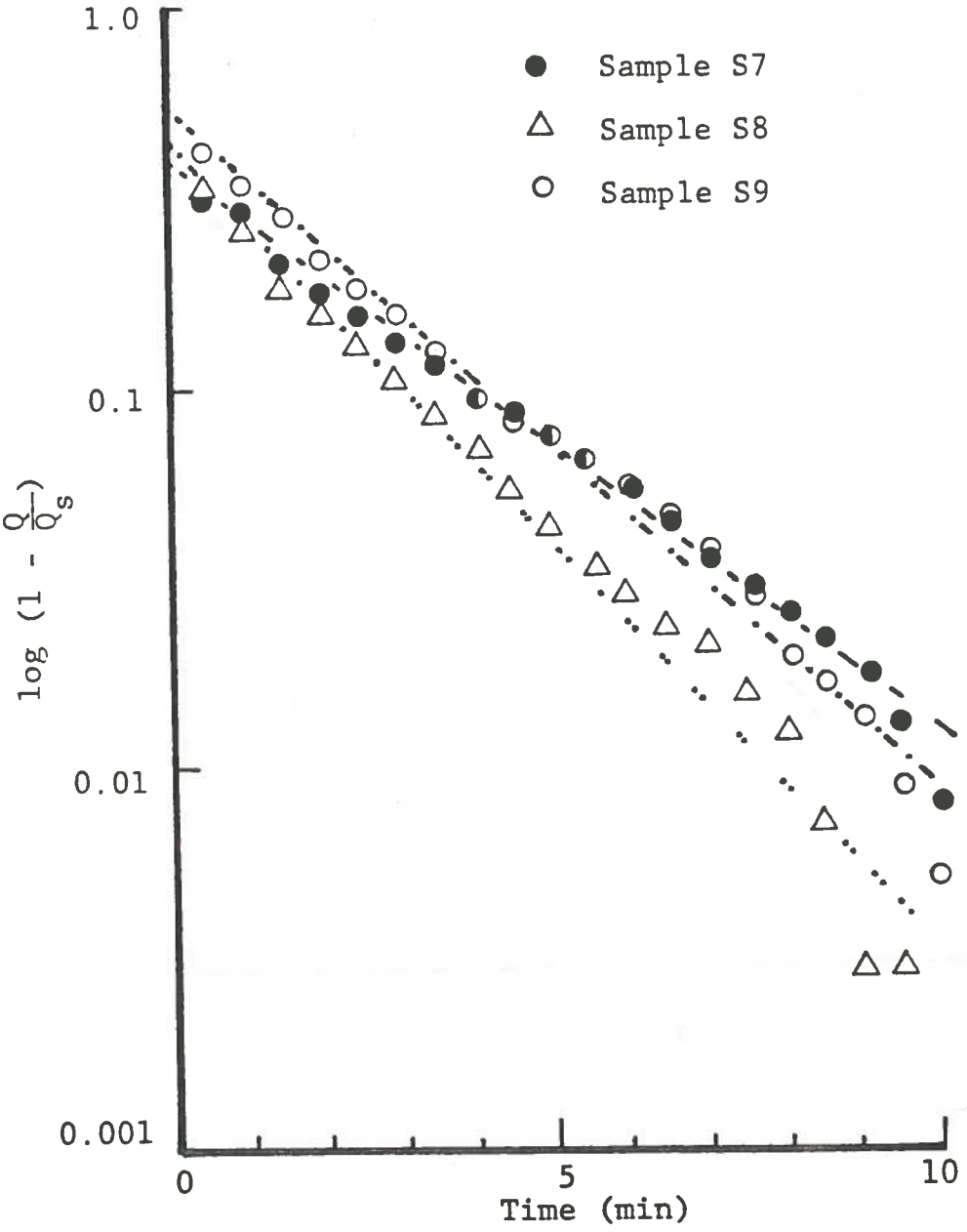

Figure 14. Swelling Rate Constant Determinations for Samples S7-S9.

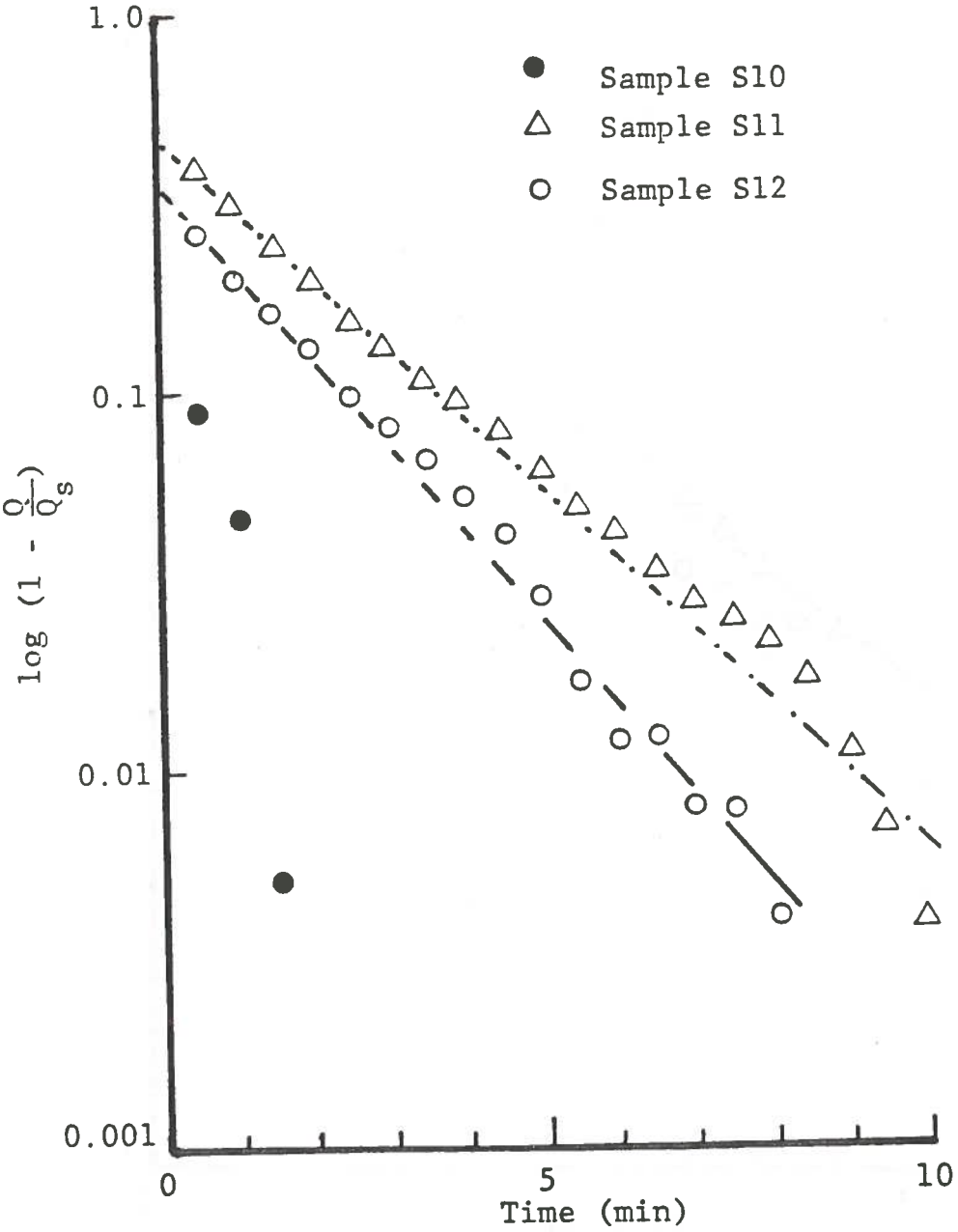

Figure 15. Swelling Rate Constant Determinations for Samples S10-S12.

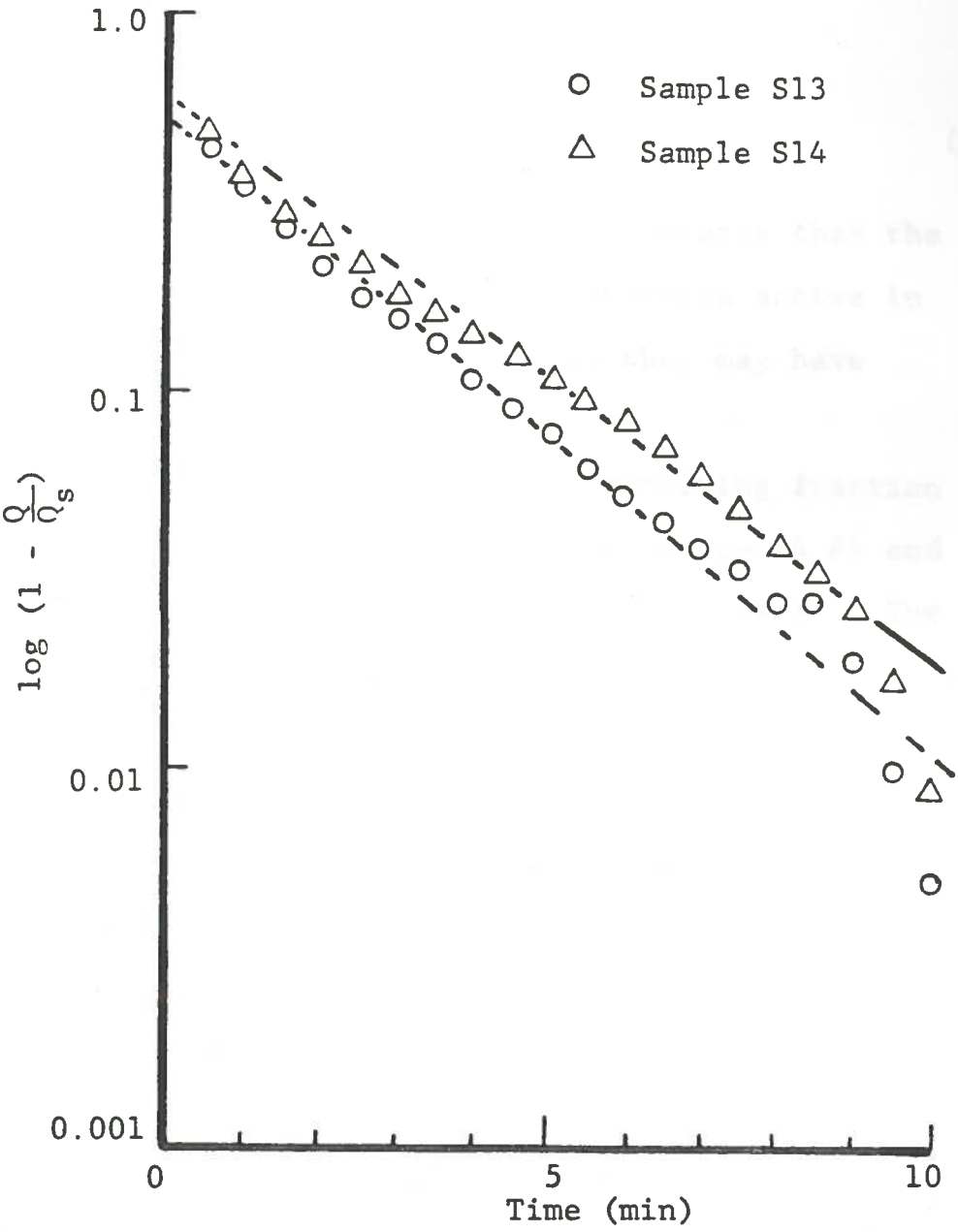

Figure 16. Swelling Rate Constant Determinations for Samples S13 and S14.

as illustrated by the Arrhenius equation (Daniels and Alberty, 1966) which is

$$k = Ae^{-E_a/RT} \tag{6.1}$$

The agreement of the rate constants indicates that the permeability to water of those mitochondria active in swelling is unaffected by any damage they may have received from the radiation.

An attempt to determine the surviving fraction directly from the relation given by equation (4.8) and Figure 4 was unsuccessful, as shown in Figure 17. The slope of these curves, as revealed by statistical analysis (see Table 5), increases with radiation dose, rather than the expected trend. Figure 18 depicts the dose dependence of the reciprocal of the slope, which bears an uncanny resemblance to the typical survival curve in Figure 6. The inset of Figure 18 hints at a possible cause for the failure of the direct method. The parameter a_2 from equation 4.7 is not constant, as assumed. Either damage occurs during swelling or the transition from the osmotically active state to inactive is not a simple, discrete phenomenon, and intermediate swelling of damaged mitochondria may occur.

Using equation (4.16) and the average Q values of the controls, the data were again transformed. This

TABLE 5. Data for the Direct Determination of S

Sample	C1	C2	S1	S2	S3	S4	S5	S6
Dose (rad)	0	0	2	4	8	11	15	20
Time (rad)				-ln[T(t)]				
0.5	.598	.562	.635	.713	.799	.755	.844	.844
1.0	.511	.545	.598	.673	.755	.724	.787	.799
1.5	.470	.528	.580	.654	.729	.693	.755	.755
2.0	.462	.519	.562	.635	.703	.673	.734	.734
2.5	.454	.511	.550	.616	.689	.654	.713	.713
3.0	.446	.503	.541	.607	.677	.646	.698	.698
3.5	.442	.498	.534	.598	.669	.639	.688	.688
4.0	.437	.493	.531	.592	.664	.631	.677	.677
4.5	.434	.488	.528	.589	.660	.627	.669	.669
5.0	.431	.485	.524	.585	.658	.624	.664	.664
5.5	.429	.483	.521	.582	.656	.631	.658	.658
6.0	.427	.481	.518	.578	.654	.616	.654	.654
6.5	.425	.480	.516	.574	.654	.612	.649	.649
7.0	.423	.478	.514	.571	.654	.611	.644	.644
7.5	.422	.478	.512	.567	.654	.609	.641	.641
8.0	.419	.476	.511	.506	.654	.607	.637	.637
8.5	.419	.476	.509	.564	.654	.605	.635	.635
9.0	.416	.475	.507	.567	.654	.603	.633	.633
9.5	.414	.475	.506	.562	.654	.603	.631	.631
10.0	.412	.473	.504	.562	.654	.603	.629	.629
10.5	.411	.473	.503	.560	.654	.603	.627	.627

TABLE 5. (continued)

Linear Least Square Fit of ln T(t) versus ln T(C_2) For Preceding Data						
Correlation	.994	.997	.987	.994	.990	.998
Intercept (V_c/V_s)	- .139	- .213	- .180	- .186	- .256	- .477
Slope $k(min^{-1})$	1.36	1.63	1.716	1.662	1.918	2.336
Intercept divided by slope	- .102	- .126	- .105	- .112	- .134	- .204

TABLE 5. (continued)

Sample	S7	S8	S9	S10	S11	S12	S13	S14
Dose (rad)	28	40	55	75	100	140	200	275
Time (rad)				-ln[T(t)]				
0.5	.713	.942	1.204	1.050		.942	1.309	2.120
1.0	.673	.868	1.109	.968		.892	1.139	1.897
1.5	.646	.832	1.050	.904		.868	1.050	1.754
2.0	.629	.803	.994	.872		.844	1.000	1.661
2.5	.616	.785	.968	.844		.826	.968	1.619
3.0	.607	.772	.949	.830		.816	.942	1.590
3.5	.598	.759	.931	.816		.805	.924	1.561
4.0	.591	.751	.906	.807		.799	.909	1.532
4.5	.583	.742	.899	.799		.792	.896	1.514
5.0	.580	.736	.892	.790		.785	.887	1.501
5.5	.576	.732	.884	.783		.781	.877	1.487
6.0	.573	.730	.877	.779		.779	.870	1.474
6.5	.566	.728	.892	.774		.777	.863	1.465
7.0	.564	.726	.868	.772		.777	.856	1.461
7.5	.562	.724	.863	.770		.774	.849	1.457
8.0	.560	.722	.858	.768		.774	.844	1.452
8.5	.559	.719	.856	.766		.772	.839	1.448
9.0	.557	.717	.853	.764		.772	.835	1.440
9.5	.555	.717	.851	.761		.770	.830	1.431
10.0	.553	.715	.849	.759		.770	.826	1.427
10.5	.552	.715	.846	.757		.770	.821	1.423

TABLE 5. (continued)

Linear Least Square Fit of $\ln[T(t)]$ versus $\ln[T(C_2)]$ For Preceding Data							
Correlation	.997	.990	.995	.987	.995	.982	.982
Intercept (V_c/V_s)	- .251	- .382	- .935	- .659	- .104	-1.393	-1.822
Slope $k(min^{-1})$	1.701	2.305	3.752	2.978	1.834	4.673	6.825
Intercept divided by slope	- .148	- .166	- .249	- .211	- .057	- .298	- .267

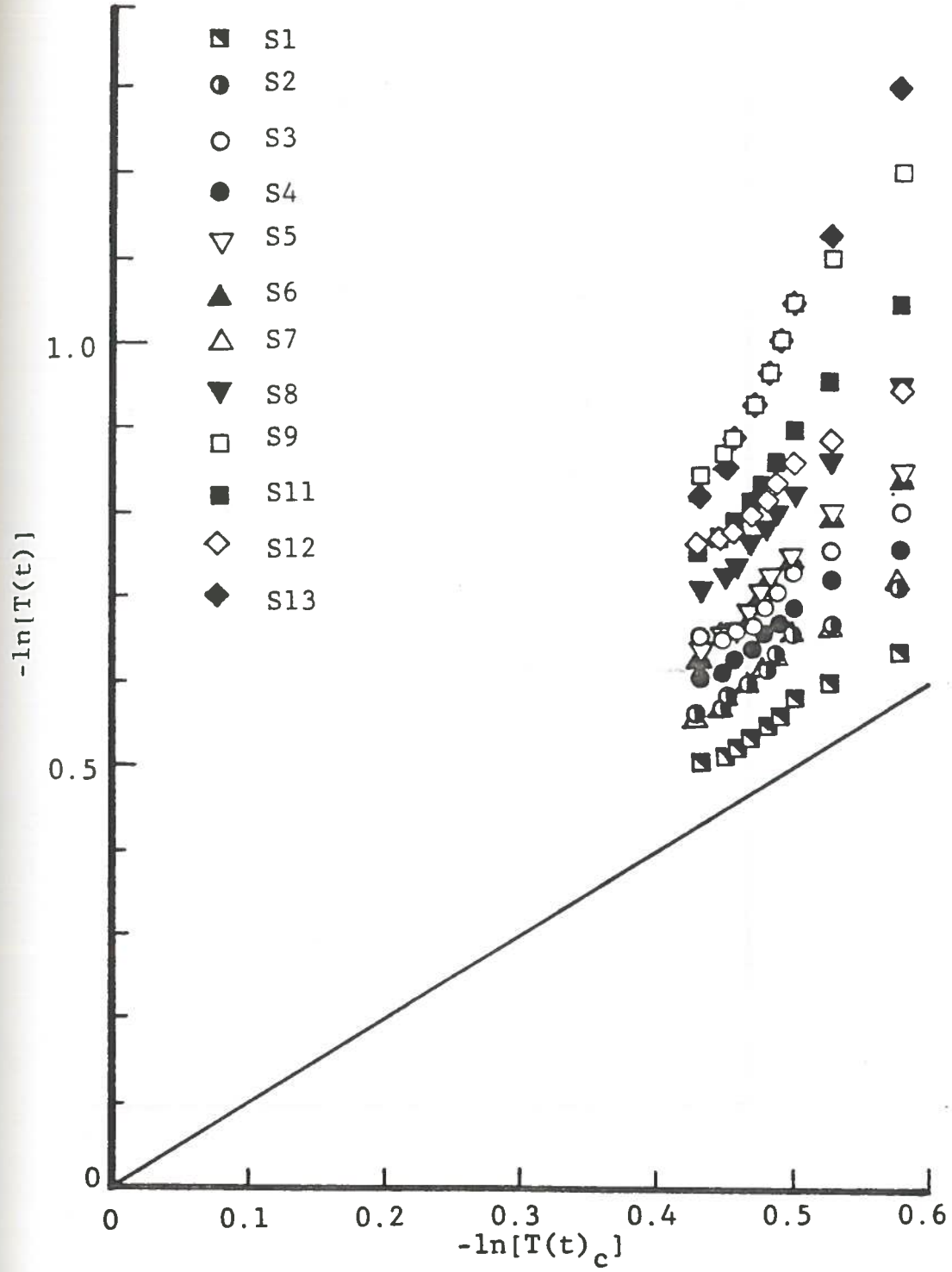

Figure 17. Direct Determination of S

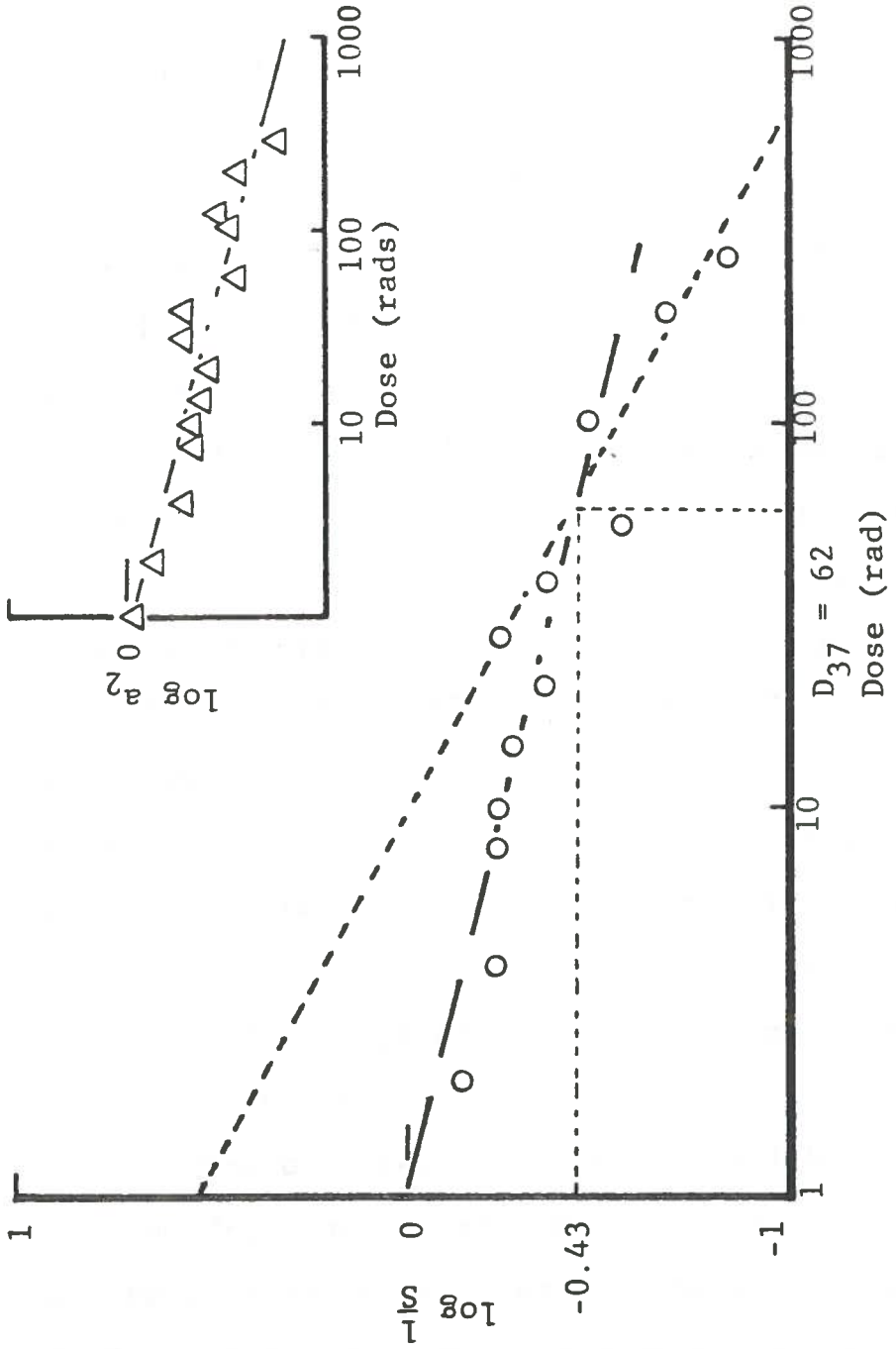

Figure 18. Dose Response of Parameters from Table 5.

transformation is a means of expressing the fraction of active mitochondria, or another expression for S. The S values thus determined are reported in Table 6. Notice that the value obtained shows little variation within a given sample but large variation with increasing dose. Also note the small variation between the control values. These observations are consistent with the arguments detailed in Chapter 4 that this value is indeed the surviving fraction, S.

The values given for S can therefore be plotted by the method of Figure 6 and evaluated with respect to target theory. This plot is reproduced as Figure 19. The scatter of data on this plot is significant enough to prevent definitive analysis by Target Theory, but a rough approximation is possible. The shape of the curve appears to exhibit a knee at about 100 rads. This shape is consistent with the multiple hit/multiple site model.

Extrapolation of the 'linear' region past the knee yields an intercept of about 0.73 which corresponds to a value of 5.4 hits (sites) per kill.

The dose necessary to kill all but 37% of the mitochondria can be read from the graph directly. Because of the scatter in this region, there is some uncertainty in the value. The value is apparently between 100 and 165 rads, regardless of the assumed shape of the curve.

TABLE 6. Q/Q_c Values (S)

Sample Dose (rad) Time (rad)	Q_c 0^c	C1 0	C2 0	S1 2	S2 4	S3 8	S4 11	S5 15	S6 20
					Q/Q_c				
0.5	7.93	.952	1.04	.870	.730	.617	.671	.568	.568
1.0	9.13	1.05	.952	.826	.694	.585	.621	.546	.541
1.5	9.98	1.09	.917	.794	.662	.562	.606	.535	.535
2.0	10.23	1.09	.909	.813	.676	.578	.617	.543	.543
2.5	10.50	1.09	.909	.820	.690	.581	.629	.552	.552
3.0	10.77	1.09	.909	.813	.685	.581	.625	.549	.556
3.5	10.93	1.09	.909	.820	.690	.585	.625	.552	.559
4.0	11.10	1.09	.909	.813	.690	.581	.629	.559	.565
4.5	11.25	1.09	.909	.813	.690	.581	.625	.556	.568
5.0	11.36	1.09	.909	.813	.690	.578	.625	.556	.568
5.5	11.42	1.09	.909	.813	.690	.578	.629	.552	.575
6.0	11.50	1.09	.909	.820	.690	.575	.629	.552	.575
6.5	11.58	1.09	.909	.813	.694	.571	.629	.552	.578
7.0	11.63	1.09	.909	.813	.694	.568	.629	.552	.581
7.5	11.69	1.10	.901	.813	.699	.565	.629	.552	.585
8.0	11.75	1.10	.901	.813	.699	.562	.629	.549	.585
8.5	11.80	1.00	.901	.813	.699	.559	.629	.549	.585
9.0	11.86	1.10	.901	.813	.699	.559	.629	.549	.585
9.5	11.90	1.10	.901	.813	.694	.556	.625	.549	.585
10.0	11.96	1.10	.901	.813	.694	.552	.625	.549	.585
10.5	12.00	1.11	.893	.820	.694	.552	.621	.552	.585
Average S		1.09	.920	.820	.694	.571	.629	.552	.568

TABLE 6. (continued)

Analysis of Q/Q_c Values	Linear Least Squares for Preceding Data					
	Mean	Standard Dev.	Fit of Q/Q_e Data	Correlation	Slope	Intercept
all points incl.	.586	≠.286 (38.9%)	all points included	.857	-.223	.859
w/out C1	.553	≠.191 (34.5%)	w/out S10	.892	-.235	.865
w/out C1, S14	.580	≠.163 (28.2%)	w/out S10, S7	.935	-.234	.850
w/out C1, C2, S14	.554	≠.136 (24.6%)	w/out S10, S7 & S4	.933	-.232	.844

TABLE 6. (continued)

Sample Dose (rad) Time (rad)	S7 28	S8 40	S9 55	S10 75 Q/Q_c	S11 100	S12 140	S13 200	S14 275
0.5	.730	.483	.333	.741	.410	.483	.294	.143
1.0	.694	.474	.328	.662	.402	.455	.314	.147
1.5	.676	.461	.326	.633	.408	.433	.326	.150
2.0	.685	.476	.344	.629	.420	.441	.342	.159
2.5	.690	.478	.350	.625	.429	.444	.350	.162
3.0	.685	.478	.351	.613	.429	.441	.355	.162
3.5	.690	.483	.356	.606	.433	.442	.360	.164
4.0	.694	.483	.365	.602	.435	.441	.364	.166
4.5	.699	.485	.365	.595	.437	.441	.366	.167
5.0	.694	.488	.365	.588	.439	.442	.368	.167
5.5	.693	.488	.358	.585	.442	.442	.372	.169
6.0	.693	.488	.370	.581	.442	.442	.375	.170
6.5	.709	.488	.370	.575	.442	.441	.377	.170
7.0	.709	.488	.372	.571	.442	.439	.379	.170
7.5	.709	.488	.372	.562	.442	.439	.383	.170
8.0	.709	.485	.375	.559	.442	.437	.383	.170
8.5	.709	.485	.373	.552	.442	.437	.385	.169
9.0	.709	.485	.373	.543	.442	.435	.386	.170
9.5	.709	.483	.375	.538	.442	.435	.388	.172
10.0	.709	.483	.373	.535	.441	.433	.394	.172
10.5	.714	.481	.375	.529	.442	.431	.392	.172
Average S	.699	.483	.366	.585	.433	.441	.362	.165

TABLE 6. (continued)

Analysis of Q/Q_c Values	Linear Least Squares for Preceding Data					
	Mean	Standard Dev.	Fit of Q/Q_e Data	Correlation	Slope	Intercept
all points incl.	.586	≠.286 (38.9%)	all points included	.857	-.223	.859
w/out C1	.553	≠.191 (34.5%)	w/out S10	.892	-.235	.865
w/out C1, S14	.580	≠.163 (28.2%)	w/out S10, S7	.935	-.234	.850
w/out C1, C2, S14	.554	≠.136 (24.6%)	w/out S10, S7 & S4	.933	-.232	.844

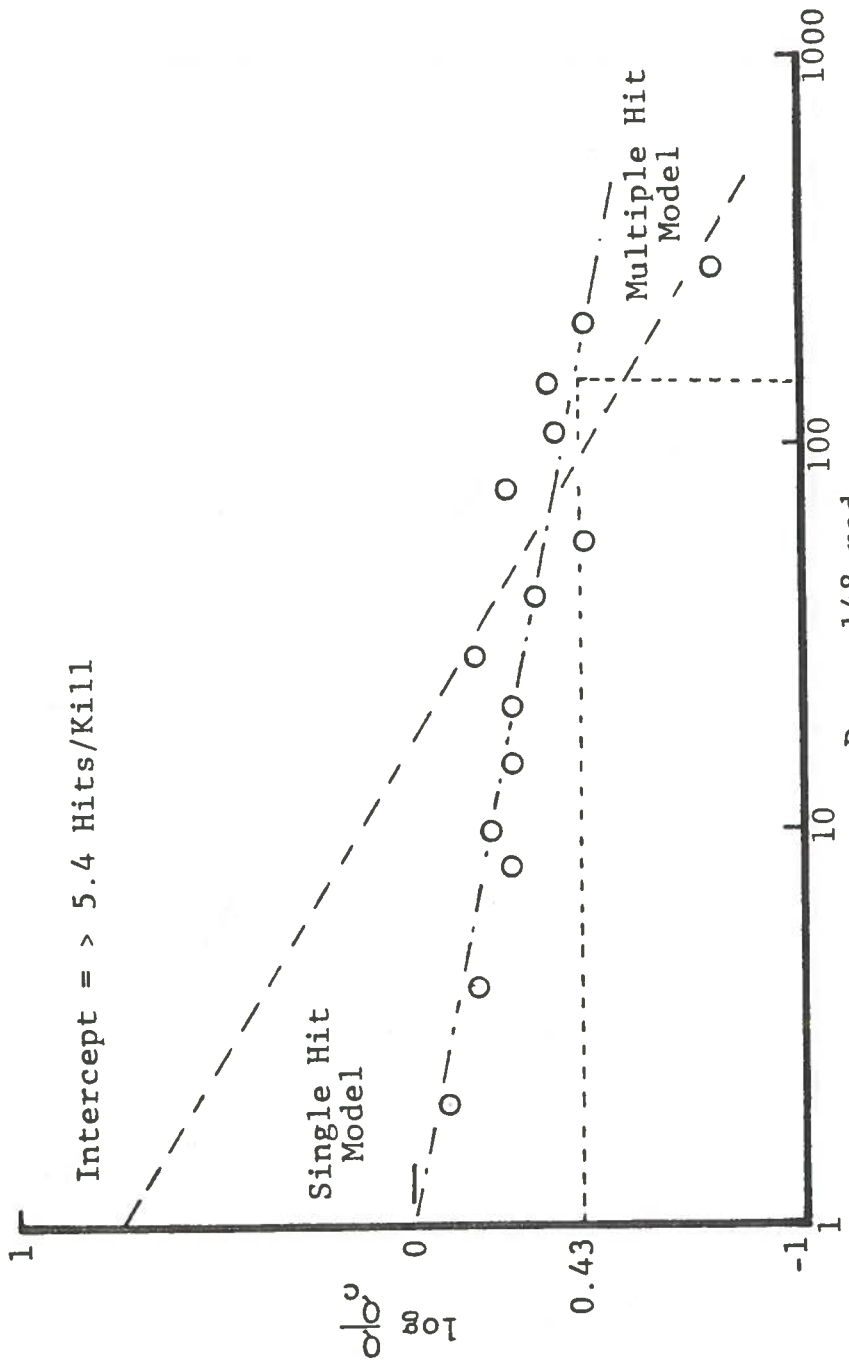

Figure 19. Survival Curve Based on Q/Q_c

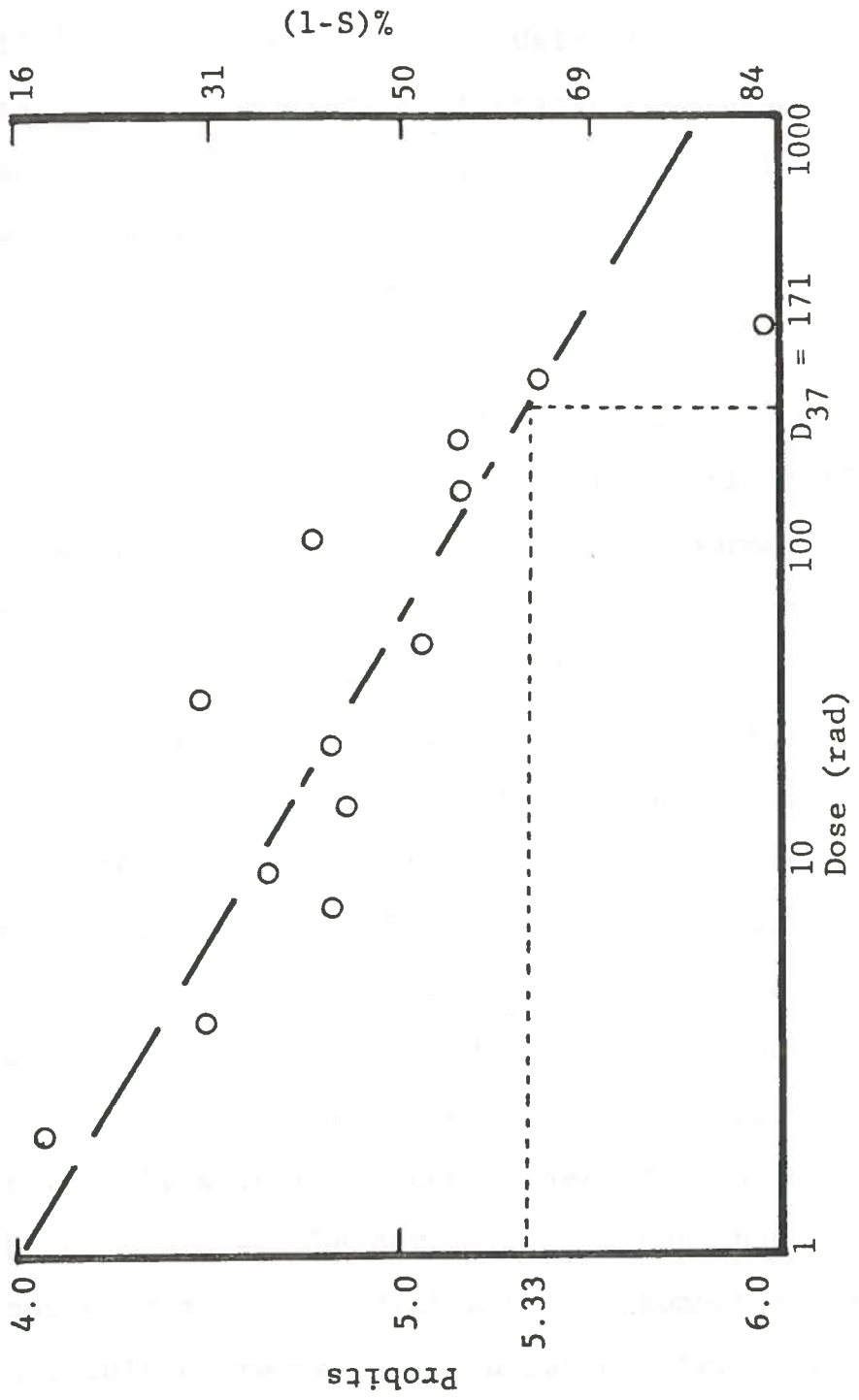

Figure 20. Log/Probit Dose-Effect Curve

By equation (4.18), the using the values reported above, the target size is calculated to be between 1.6 x 10^{-14} and 2.7 x 10^{-14} cc. Using the assumptions of the mathematical treatment of Chapter 3, the volume of the spherical shell formed by the membranes is 5.5 x 10^{-14} cc, with the average dimensions reported by Racker (1970).

The data from Table 6 were analyzed by Probit Transformation (Litcchfield and Wilcoxon, 1949), depicted in Figure 20. The percentages of damaged mitochondria (unity minus the surviving fraction, times 100%), were taken to represent the area under a Normal Distribution function between negative infinity and a point, c. The probit values, which can be obtained from a table or read directly from a special type of graph paper, are numerically equivalent to the Normal Deviation at the point, c, times 100. Analysis by this method yields a D_{37} value of 171 rads, and an LD_{50} value of 46 rads.

The swelling data was further analyzed by means of the computer program described previously. The data generated by the computer-derived solution agrees favorably with the actual observed data, as illustrated by Figure 19. The deviations in the shape of the observed curve from that predicted by the computer solution may be a result of temperature variation, transport phenomena (see Figure 3), or nonideal variation in shape with swelling.

The results of the single term model computer runs are summarized in Table 7. There appears to be no pattern to the variation in the computer program's ability to fit the data with the prescribed model, as evidenced by the similarities in the standard deviations. Increasing the number of terms to a maximum of ten had little effect in the overall fit of the model.

The rate constants determined are similar in value and uniformity to those obtained by the graphical method. The parameter for the overall change in volume also shows little variation, especially when normalized by division by the parameter for the totally swollen volume.

The final volume is the parameter which reflects the effect of increased radiation dose. When the final volume parameter for a sample is divided by the final volume for the control, the result is very similar numerically to the Q/Q_c value, which was used as the survival fraction, S. A plot of the values versus dose, presented in Figure 22, yields a D_{37} of 178 rads, and approximately 4 hits per kill. The target sizes, 2.8×10^{-15} cc and 1.1×10^{-14} cc, for the single hit and multiple hit models respectively, are in close agreement with values determined by the other methods.

It is of some interest to examine the results of the two term model, since the rationale for radiation damage involves the transition to a condensed, osmotically

TABLE 7. Summary of Computer Results

Sample	C1	C2	S1	S2	S3	S4	S5	S6
Dose (rads)	0	0	2	4	8	11	15	20
Parameter	BEST-FIT VALUE							
P (abundance)	.997	.998	.998	.998	.998	.997	.997	.998
S (swollen size)	3.67	3.08	2.78	2.38	1.89	2.13	1.87	2.02
C (volume change)	.208	.860	.962	.860	.683	.758	.727	.856
K (rate constant)	.702	.371	.402	.367	.612	.409	.472	.330
Standard Deviation	.457	.051	.158	.130	.097	.098	.140	.132
C/S	.057	.279	.346	.361	.361	.356	.389	.424
$S/\bar{S}$ controls (survival fraction)	1.08	.913	.824	.705	.560	.631	.554	.599

TABLE 7. (continued)

Sample Dose (rads) Parameter	S7 28	S8 40	S9 55	S10 75	S11 100	S12 140	S13 200	S14 275
				BEST-FIT VALUE				
P (abundance)	.998	.997	.997	.997	.997	.998	.998	.997
S (swollen size)	2.44	1.64	1.28	1.87	1.50	1.47	1.32	.581
C (volume change)	.906	.684	.634	.432	.715	.481	.774	.315
K (rate constant)	.337	.470	.386	1.29	.450	.454	.402	.452
Standard Deviation	.139	.128	.148	.402	.176	.072	.443	.247
C/S	.371	.417	.495	.231	.447	.327	.586	.542
$S/\bar{S}$ controls (survival fraction)	.723	.486	.379	.554	.444	.436	.391	.172

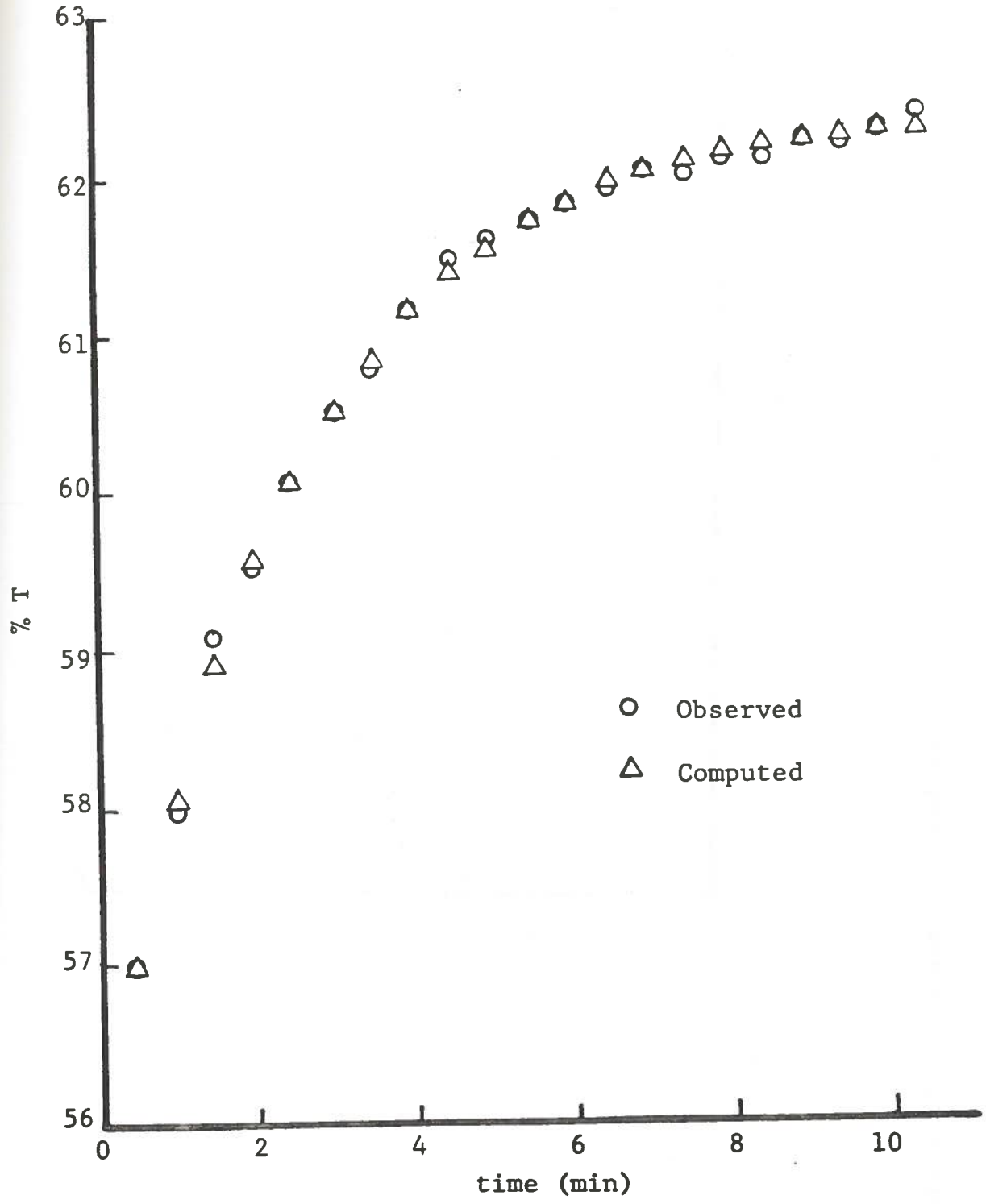

Figure 21. A Typical Swelling Curve Sample C-2

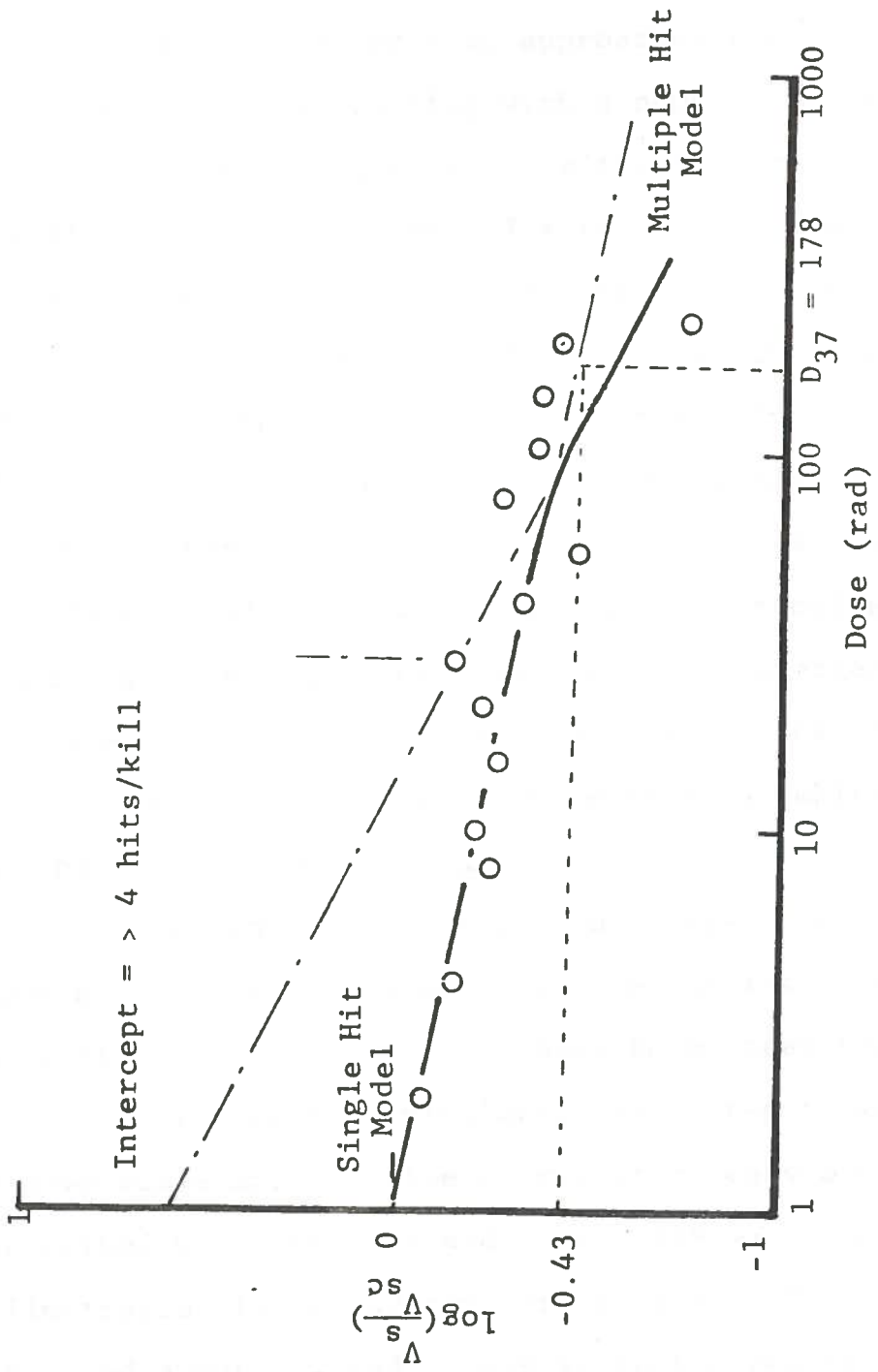

Figure 22. Computer-Derived Swollen Volume Parameter Versus Dose

inactive state. The program approaches the problem of multiple groups by starting with a number of identical groups and attempting to improve the fit by unequal modification of the terms. The results of the two term model were either to find no fit better than the two identical group case, or to force one group to assume a "dummy" role, that is, to swell very slowly, or not at all, or to swell a large amount very rapidly in order to avoid participation of that group in the calculations. This inconclusive result can probably be remedied by demanding more significant figures for convergence. Nevertheless, the result is supportive of the idea of a background of relatively inactive material which does not participate in swelling.

One anomolous swelling curve was observed. That sample, S-10, was delayed after the initiation of swelling, so that the reaction was followed to a later than normal time. An interesting similarity was noted between the sample curve and the time course of a leaky osmometer described by Katchalsky and Curran (1967). Their illustration is reproduced here as Figure 23. The sample received about D_{37} rads; this is in the region where the mitochondria have each received, on the average a destructive dose.

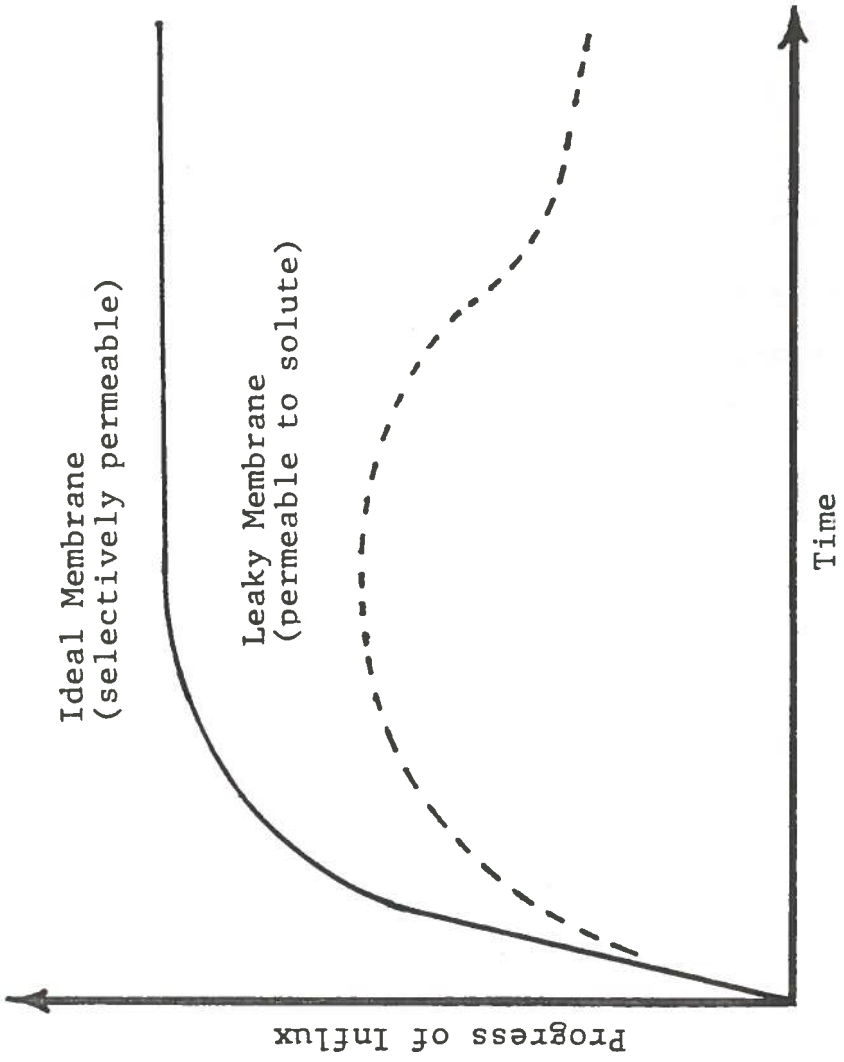

Figure 23. Time Course of a Leaky Osmometer

There is a very basic limitation on the use of mitochondrial damage as an indication of radiation damage. Mitochondrial damage can be caused by a variety of things from the isolation method to pathological conditions of the subject. The use of mitochondrial dosimetry will probably be limited to the screening of suspected exposure subjects. There may also be a time limit on the damage information carried by the mitochondria in vivo because of membrane repair mechanisms. These subjects are beyond the scope of this thesis.

CHAPTER 7

SUMMARY AND CONCLUSIONS

The introduction of this thesis critically examined the conventional methodology for the evaluation of personnel radiation dose. The contention was made that lymphocyte mitochondria might be suitable as a limiting indicator of radiation dose. The reasoning behind the selection of lymphocyte mitochondria as the candidate for an intrinsic biological dosimeter was explored in some detail in the second chapter. It was suggested that radiation might have some effect on the osmotic properties of the mitochondria, as evidenced by some change in their swelling response. Emphasis was placed on the significance of this damage, since energy production by the mitochondrion is dependent on the integrity of the inner mitochondrial membrane.

In order to detect changes in mitochondrial swelling, a detailed mathematical analysis of the process, and its manifestation by nephelometry, was presented in Chapter 3. The results of this treatment include an important restatement of classical scattering theory, which is derived in a simple manner, without the inappropriate assumptions of the conventional method, yet which bears

striking resemblence to the classical result. A method for the application of the theoretical treatment of swelling to the quantitation of radiation dose was described in Chapter 4. The means to analyze the mitochondrial "survival" curves by conventional Target Theory is also revealed.

Experimental methods for the isolation and analysis of lymphocyte mitochondria were outlined in Chapter 5, including the method of irradiation and dosimetry. The results of actual experiments involving the irradiation of isolated mitochondria were reported and discussed in Chapter 6. The data do not allow an unambiguous choice between single hit and multiple hit mechanisms. Analysis by either method, however, reveals a target size on the order of magnitude of the volume occupied by the mitochondrial membranes.

The theoretical upper and lower limits of detection by this method of dosimetry can be inferred from Figure 19. The variation between survival fractions determined for nonirradiated controls was 0.070. The lowest credible difference that could be measured between samples is about twice this value or 0.14. A difference of 0.14 from the control value of 1.00 gives a survival fraction of 0.86, which corresponds to a radiation dose of 2.25 rad on the survival curve. This is, therefore,

the theoretical lower limit of detection. The upper limit of detection would be the dose at which the surviving fraction could not be reliably distinguished from zero, or S = 0.14. This fraction corresponds to a dose of over 1000 rads if the single hit mechanism is correct, or 250 rads, if the damage is by multiple hits.

In addition, the following conclusions can be made:

Peripheral lymphocyte mitochondria can be obtained in quantity and quality suitable for dosimetric purposes.

Osmotic swelling traced by nephelometry, can reveal information about radiation damage to these mitochondrial isolates.

The first-order rate constant for the swelling process can be derived from the reaction time course, but derivation in the linearity of these determinations implies that the process is not strictly first-order.

Attempts to calculate the surviving fraction, S, directly demonstrate that the two-state model is not an entirely adequate description of the radiation damage phenomenon.

The osmotically active volume, Q/Q_c, provides useful information about the surviving fraction.

The numerical method of analysis of the data, by the FORTRAN program is capable of providing the same information about rate constants and degree of damage.

It is clear that a degree of radiation damage to isolated mitochondria can be quantitated through the analytical methodology presented in this thesis. The observation of the loss of osmotic activity at low doses of radiation, viewed in light of the mechanistic discussion of the action of uncouplers of oxidative phosphorylation (Chapter 2), implies that radiation acts to violate the structural integrity of the mitochondrial membranes. In this respect, peripheral lymphocyte mitochondria may indeed fulfill the need for an intrinsic biological dosimeter. However, there are several critical uncertainties about the use of these organelles for personnel dosimetry.

Is it possible to isolate mitochondria from peripheral lymphocytes without perturbing the existant proportions of damaged and functional mitochondria? The enzymatic isolation procedure of Jennings et al. (1969) should be used to isolate mitochondria from lymphocytes which have been irradiated in vivo or in the form of whole blood, using good dosimetry, and the analytical methodology applied to these organelles. If the survival curves are similar to those of the irradiated isolates, further investigations are in order.

At what rate does the organism repair or replace the damaged mitochondria? The biological half-life for mitochondrial constituents is about 20 days, which places an upper limit to the usefulness of this method, but repair could be affected more rapidly. Whole animal irradiations with delayed sampling would answer this question.

What modifications of this methodology can provide increased reliability for the measurement of mitochondrial damage? Experiments should be done using temperature-controlled conditions during swelling, with reproducible mixing using pseudo-stopped-flow sample injection. Following swelling, samples should be morphologically characterized with phase-contrast, or, better still, electron microscopy. The measurement of oxidative phosphorylating ability would provide another measure of mitochondrial functional integrity.

Is there another method of analysis of the functional integrity of the mitochondrial population which may supplant the swelling analytical method for quantitation of mitochondrial damage? Organelle electrophoresis (mentioned in Appendix B) may provide a simpler method for the study of the mitochondrial survival. Experiments to determine the effect of radiation on the

migration pattern of mitochondrial suspensions should be conducted. It is expected that effects similar to those of uncouplers will be observed. This method has the advantage of physically separating mitochondrial sub-populations for further study.

REFERENCES

Bacq, Z. M. and Alexander, P. (1966) Fundamentals of Radiobiology, 2nd ed, Pergamon Press, NY. 562 pps.

Brenner, S. (1949) S. Afr. J. Med. Sci. 14,13-19.

Campbell, D. H. (1964) Methods in Immunology, W. A. Benjamin, Inc., New York. p. 248.

Casarett, A. P. (1968) Radiation Biology, Prentice-Hall, Inc., Englewood Cliffs, NJ. 368 pps.

Chance, B. and Williams, G. R. (1955) J. Biol. Chem. 217, 409-427.

Chen, L. H. and Chang, M. L. (1978) J. of Nutri. 108(10), 1616-1620.

Clark, G. ed. (1973) Staining Procedures, 3rd ed., William Wilkins, Baltimore, MD.

Coggle, J. E. (1971) Biological Effects of Radiation, Springer-Verlag, NY. 149 pps.

Cottier, H., Roos, B., and Barandun, S. (1963) In Cellular Basis and Aetiology of Late Somatic Effects of Ionizing Radiation. A Symposium in 1962, Academic Press, Inc., NY. pps. 113-118.

Daniels, F. and Alberty, R. A. (1966) Physical Chemistry, 3rd ed., John Wiley & Sons, Inc., NY. 767 pps.

Davis, J. T. (1967) In Methods in Enzymology, X, ed. Estabrook and Pullman, Academic Press, NY. p. 114.

Dugle, D. L., Gillespie, C. J., and Chapman, J. D. (1976) Proc. Nat. Acad. Sci. US 73(3),809-812.

Duniec, J. T. and Thorne, S. W. (1977) J. of Bioen. and Biomem. 9,223-235.

Earl, W. R. (1943) J. of Nat. Canc. Inst. #4,165-212.

Elkind and Whitmore (1967) The Radiobiology of Cultured Mammalian Cells, Gordon and Breach, NY. 615 pps.

Fine, P. E. M. (1978) Lancet Sept. 23,659-662.

Fremlin (1980) Ambio. IX #2, pps. 60-62.

Fowler, B. A. and Woods, J. S. (1977) Exp. and Mol. Path. 27,403-412.

Gebicki, J. M. and Hunter, F. E., Jr. (1964) J. Biol. Chem. 239(2),631-639.

Geraci, J. P., Jackson, K. L., Christensen, G. M., Parker, R. G., Fox, M. M. and Thrower, P. D. (1974) Rad. Res. 59(1),247.

Glasstone, S. and Sesonske, A. (1967) Nuclear Reactor Engineering, Van Nostrand Reinhold Co., NY. 830 pps.

Gornal, A. G., Bardawill, C. J., and David, M. M. (1949) J. of Biol. Chem. 177,751.

Hanson, K. P. and Komar, V. E. (1978) Studia Biophysica 68,237-242.

Harada (1978) Nutr. Rep. Int. 18(5),559-568.

Harman, J. W. and O'Hegarty, M. T. (1962) Exp. and Mol. Path. 1,573-588.

Harris, T. E. (1972) Transport and Accumulation in Biological Systems, University Park Press; Baltimore, MD. 454 pps.

Holtzman, D., Lewiston, N., Herman, M. M., Desantel, M., Brewer, E., and Robin, E. (1978) J. of Neurochem. 30,1409-1419.

Hunter and Smith (1967) In Methods in Enzymology X, ed. Estabrook, Academic Press, NY. p. 689.

Jennings, et al. (1969) Lab. Invest. 20. pps. 548-557.

Katchalsky, A. and Curran, P. F. (1967) Nonequilibrium Thermodynamics in Biophysics, 2nd ed., Harvard Univ. Press, Cambridge, MA. 248 pps. (see page 121)

Kay, H. D. and Kaeberle, M. L. (1972) In vitro 7(6),387-390.

Koch, A. L. (1969) Biochimica et Biophysica Acta 51,429-441.

Koelliker (1888) Zur Kenntris der Quergestreiften Muskelfasern", Z. Wiss. Zool. 47,689-710.

Land, C. E. (1980) Science 209,1197-1203.

Latimer, P. (1979) Biop. J. 27,117-126.

Lemasters, J. J. (1978) F.E.B.S. Lett. 88(1),10-14.

Lehninger, A. L. (1963) Physiol. Rev. 42,467-515.

Lehninger, A. L. (1975) Biochemistry, 2nd ed., Worth Pub., NY. 1104 pps.

Litchfield, J. T., Jr., and Wilcoxon (1949) J. Pharm. and Exp. Therapeut. 96,99-113.

Lochner, A., Anlinskas, T., Kotze, J. C. N., and Gevers, W. (1978) S. Afr. J. of Sci. 74,168-171.

MacPhate, A. J. (1976) Personal communication.

Madhavanath, U. (1976) Health Phys. 30(3),296-299.

Malamed, S. (1965) Zeitschvift fur Zelltorscheng 65,10-15.

Michael, et al. (1980) Science 208,1267-1269.

Mihai, C., Dinesca, G., and Popesca, A. (1973) Revue Roumaine de Biochemie 10(3),191-201.

Mitchell, P. (1965) Biol. Rev. 41,445-487.

Mitchell, P. (1979) Science 206(4423),1148.

Mustea, I., Bara, A., Petrescu, I., and Reversz, L. (1978) Br. J. Cancer 37, Suppl. III, 159-162.

Nohl, H. and Hegner, D. (1978a) Eur. J. Biochem. 82,563-567.

Nohl, H. and Hegner, D. (1978b) F.E.B.S. Lett. 89(1),126-130.

Orlov, S. N., Malkov, Y. A., Rebrov, V. G., and Danilov, V. S. (1976) Biofizika 21(2),276-279.

Oster, G. (1948) Chem. Rev. 43(2),319-365.

Packer, L. (1963) J. of Cell. Biol. 18,487-494.

Packer, L. (1967) In Methods in Enzymology X, ed. Estabrook, Academic Press, NY. p. 685.

Pauly, H., Packer, L., and Schwan, H. P. (1960) J. Biop. and Bioc. Cytol. 7(4),589-602.

Pauly, H. and Packer, L. (1960) J. Biop. and Bioc. Cytol. 1(4),603-611.

Pettengill, H. J. (1974) "Adenosine Triphosphate Production of Mitochondria During and After X-irradiation", Disseration, University of Michigan. 104 pps.

Porter, C. W., Mikles-Robertson, F., Kramer, D., and Dave, C. (1979) Canc. Res. 39,2414-2421.

Powell, M. J. D. (1964) Computer Journal 7(2),155-162.

Racker, E. (1970) Membranes of Mitochondria and Chloroplasts, Van Nostrand Reinhold, NY, ACS Monograph #165. 322 pps.

Reed, K. C. (1972) Anal. Bioc. 50,206-212.

Rees, D. J. (1967) Health Physics, Butterworth and Co., Ltd., Cambridge. 242 pps.

Schrader, G. T. and Dimopoullos, G. T. (1963) Am. J. of Vet. Res. 24(99),283-286.

Segreto, C., Matera, A., and Ludwig, F. C. (1974) Rad. Res. 59(1),293.

Selby, S. M. ed. (1969) CRC Standard Math Tables 17th ed., Chemical Rubber Co., Ohio. 724 pps.

Silberstein, E. B., Ewing, C. J., Bahr, G. K., and Kerelakes, J. G. (1974) Rad. Res. 59(1),658-664.

Spencer, J. A. and Horton, A. A. (1978) Exp. Geront. 13, 227-232.

Tamura, H. and Sugiyama, Y., and Sugiyama, T. (1974) Rad. Res. 59(1),653-657.

Tarr, J. S., Jr. and Gamble, J. L., Jr. (1966) Am. J. Physiol. 211(5),1187-1191.

Tedeshi, H., James, J. M. and Anthony, W. (1963) J. of Cell Biol. 18,503-518.

Tedeshi, H. (1965) J. of Cell Biol. 25,229-242.

Trudell, J. R. (1977) Bioc. Biop. Acta 470,509-510.

von Wagenheim, K. H. (1976) In Radiation and Cellular Control Processes ed. J. Kiefer, Springer-Verlag, NY. 321 pps.

von Wagenheim, K. H. (1976) J. of Theor. Biol. 59,205-222.

Wallach, D. F. H., Kamat, V. B., and Gail, M. H. (1966) J. of Cell Biol. 30,601-621.

Watson, J. D. (1970) Molecular Biology of the Gene, 2nd ed., W. A. Benjamin, Inc., Menlo Park, CA. 662 pps.

Wattiaux-deConinck, S., Dubois, F., and Wattiaux, R. (1977) Bioc. and Biop. Acta 471,421-435.

Willis, C. E. (unpublished) Oral Research Proposition for Ph.D, Biophysical Sciences, Univ. of Houston. (Included as Appendix B).

Willis, D. G. (unpublished) A Survey of Current Strategies for Quantitative Isolation of Peripheral Lymphocytes. (Included as Appendix A).

Witkin, E. M. (1969) Ann. Rev. of Gen. 3,525-552.

APPENDICES

APPENDIX A

A SURVEY OF CURRENT STRATEGIES FOR QUANTITATIVE ISOLATION OF PERIPHERAL BLOOD LYMPHOCYTES

Diana G. Willis

Most lymphocyte isolation procedures begin with preliminary processing of whole blood. Whole blood is collected in siliconized glassware or plastic containers, otherwise the lymphocytes will adhere to the glass and be lost (Wildy and Ridley, 1958). Anticoagulants such as heparin or citrate are used, or the blood is defibrinated either by passage through an ion exchange column (Greenwalt, 1962), or the use of wooden applicator sticks (Kay and Kayberle, 1972). Low speed centrifugation of the blood now produces three characteristic phases. At bottom, the erythrocyte layer comprises about 46% of the total blood volume. On top of the red cell pack a thin, buff colored layer, called the "buffy coat," forms, comprising 19% of the total volume and containing the lymphocytes, granulocytes, and leucocytes. The supernatant resulting from such a low speed centrifugation is known as the serum. Collection of the buffy coat is then accomplished by simple aspiration or by the "floatation method" (Burrin et al., 1965). Much of this fraction is made up of contaminating platelets, granulocytes, and erythrocytes which must be removed by further processing.

Perhaps the most widely used method of separating the lymphocytes from the other buffy coat material is by isopycnic density gradient centrifugation. This involves layering the buffy coat on a preformed gradient containing erythrocyte clumping agents, such as Ficoll/Hypaque (Boyum, 1968) or Sodium Metrizoate-Ficoll (Laissue et al., 1975), and then centrifuging at high rotor speed to equilibrium. At equilibrium, the lymphocytes form a band at the point in the gradient which matches their own density, and any contaminating erythrocytes from a pellet at the bottom of the tube. The lymphocytes are then collected by aspiration or drainage of the tube and are resuspended in the appropriate balanced salt solution for analysis.

The fiber method applies the difference in adsorption of lymphocytes and granulocytes to nylon (Greenwalt, 1962) or cotton fibers (Kay and Kaeberle, 1972) in order to exclude granulocytes from the suspension. Unlike the glass bead (Garvin, 1961) and glass wool columns (Johnson and Garvin, 1959) from which the lymphocytes had to be eluted with a chelating agent, the lymphocytes can pass freely through the fiber columns while the granulocytes and platelets are retained. Removal of erythrocytes may be accomplished by a variety of hemolysis techniques (Fallon et al., 1962; and Marks et al., 1962). The cotton fiber technique has been combined with the Ficoll-Hypaque procedure with good results (Kay et al., 1976).

Once isolated, the lymphocytes must be characterized with respect to their homogeneity and functional integrity. Purity of the suspensions can be determined histologically (Clark, 1973) using Wright-stained smears or by observation of live cells using phase contrast microscopy (Rabinowitz, 1964). The functional state of the extracted lymphocytes can be established by observation of their ameboid mobility; their phagocytic ability, as evidenced by the engulfing of polystyrene beads; trypan blue staining, in which non-viable cells become stained; and by the presence or absence of the ability to conduct oxidative metabolism, as indicated by oxygen consumption observed on the Warburg manometer or oxygen polarimeter.

Methods which require isopycnic focusing call for extended periods of high speed centrifugation, typically 12 hours or more. These also require ready access to sophisticated ultracentrifugation equipment. Laissue et al. (1976) report yields of greater than 75% leucocytes with less than 1% erythrocytes and platelets present, and no contaminating granulocytes following isopycnic focusing in a liquid silicon solution. Trypan blue positive cells were rarely observed. Similarly, Yakir et al. (1977) were able to isolate 1 to 2 x 10^6 lymphocytes/ml of peripheral blood in suspensions containing 80 to 90% lymphocytes using the Ficoll-Hypaque gradient. Suspensions with greater purity can be produced in shorter times with

relatively crude equipment by fiber column methods. Concentrated suspensions of 0.5 to 3 x 10^6 lymphocytes/ml can be produced by passage through a nylon fiber column (Greenwalt et al., 1962). These isolates can be stored satisfactorily for 14 to 21 days. Yields of 10^6 lymphocytes/ml whole can be obtained with less than 1% contaminating granulocytes after incubation in a simple cotton fiber column (Kay and Kayberle, 1972). Trypan blue exclusion of cells indicates 94 to 100% viability. Greater than 10^6 lymphocytes/ml whole blood are obtained by combination of the cotton fiber and isopycnic focusing, resulting in suspensions of 92 to 94% pure lymphocytes. Exclusion of Trypan blue indicates 97 to 100% viability (Kay et al., 1976).

Because of the lack of significant improvement over the cotton fiber method by the combination method; and due to the speed, simplicity, and minimal equipment requirements of the cotton fiber column; and the obviation of the exposure of the cells to the high centrifugal forces inherent in isopycnic focusing; the method of Kay and Kaeberle (1972) should come into widespread use and, ultimately, become the method of choice for isolating pure, viable samples of peripheral lymphocyte tissue.

REFERENCES FOR APPENDIX A

Boyum, A. (1968) Separation of lymphocytes and erythrocytes by centrifugation. Scandinavian Journal of Clinical Laboratory Investigations, 21,77.

Burrin, D. A., Keppie, J. and Smith, H. (1966) The isolation of phagocytes and lymphocytes from bovine blood and the effect of their extracts on the growth of Brucella abortus. British Journal of Exploratory Pathology, 47,70-75.

Cassen, B., Hitt, J. and Hays, E. F. (1958) Journal of Laboratory Clinical Methods, 52,778.

Clark, G., ed. (1973) Supravital Staining. In: Staining Procedures used by the Biological Stain Commission, 3rd edition, pp. 133-135. Williams and Wilkins Company, Baltimore.

Davis, J. T. (1967) A technique for the isolation of mitochondria from bovine lymphocytes. In: Methods in Enzymology. Volume X, pp. 114-117. Academic Press, New York.

Fallon, H. J., Frei, E., Davidson, J. D., Trier, J. S. and Burk, D. (1962) Leukocyte preparations from human blood: evaluation of their morphologic and metabolic state. Journal of Laboratory and Clinical Medicine, 59,779.

Garvin, J. E. (1961) Adhesive properties of human leukocytes on a glass bead column. Federation Proceedings, 20, 71.

Greenwalt, T. J., Gajewski, M. and McKenna, J. L. (1962) A new method for preparing buffy coat-poor blood. Transfusion, 2,221-229.

Jago, M. (1956) British Journal of Haematology, 2,439.

Johnson, T. M. and Garvin, J. E. (1959) Separation of lymphocytes in human blood by means of glass wool columns. Proceedings of the Society of Experimental Biology in Medicine, 2,333.

Kay, H. D. and Kaeberle, M. L. (1972) A simplified method for isolating bovine lymphocytes, in vitro, 7,#6, 387-390.

Kay, H. D., Thota, H. and Sinkovics, J. (1976) A comparative study on *in vitro* cytotoxic reactions of lymphocytes from normal donors and patients with sarcoma to cultured tumor cells. Clinical Immunology and Immunopathology, 5,218-234.

Laissue, J. A., Joel, D. and Sipe, C. (1976) Large monocytid cell in mononuclear cell fraction of bovine blood. American Journal of Veterinary Research, 37, 307-308.

Marks, P. A., Burka, E. R. and Schlesinger, D. (1962) Protein synthesis in erythroid cells. I. Reticulocyte ribosomes active in stimulating amino acid incorporation. Proceedings of the National Academy of Sciences, USA, 48,2163.

Rabinowitz, Y. (1964) Separation of lymphocytes, polymorphonuclear leukocytes and monocytes on glass columns, including tissue culture observations. Blood, 23,811-828.

Yakir, Y., Kook, A. and Schlesinger, M. (1977) Effect of thymic humoral factor on intracellular levels of cyclic AMP in human peripheral blood lymphocytes. Israel Journal of Medical Sciences, 13,1191-1196.

Wildy, P., and Ridley, M. (1958) Separation of human lymphocytes from blood. Nature 182,1801.

APPENDIX B

MITOCHONDRIAL HETEROGENEITY*

Background

The purity, homogeneity, and functional integrity of the "mitochondrial" fraction obtained by differential centrifugation of single tissue homogenates has been a matter of discussion since the introduction of the subcellular fractionation procedure by Bensley and Hoer (1934). In order to avoid contamination by smaller particulates occurring in the homogenates, at that time collectively referred to as microsomes, elaborate fractionation schedules were devised (Novikoff, et al., 1953). Some degree of heterogeneity within the mitochondrial fraction was initially reported by Kuff and Schneider in 1957 with respect to succinate dehydrogenase. Werkheiser and Bartley (1957) separated the mitochondrial fraction into "heavy, light, and fluffy" subfractions by means of differential centrifugation through 0.25 M sucrose. The heavy subfraction was found to contain twice the sarosine dehydrogenase activity of the light subfraction (Frisell, et al., 1965). Meanwhile, careful investigations with density gradient centrifugation (Beaufey, et al., 1964)

---

*Taken from an oral research proposition, University of Houston, 1979 by Charles E. Willis.

revealed the presence of two other biological particles, the lysosomes and peroxisomes, in the "mitochondrial" fraction, as well as fragments of the plasma membrane and endoplasmic reticulum (microsomes). Even when corrections were applied to account for the effects of this contamination, differences in biochemical behavior were noted in rat liver mitochondrial subfractions under normal and regenerating conditions (Gear, 1965a,b). Heterogeneity was also observed in yeast mitochondria (Matile and Bahr, 1968). The short (18.5 days) biological half-life observed for mitochondria when compared to the life of the cell (Fletcher and Sanadi, 1961; Beattie, et al., 1967) led some investigators to expect variation in the mitochondrial population within a tissue with respect to age and biochemical composition, while others (de Duve, 1967) maintained that any observed heterogeneity was the result of contamination by other organelles and soluble proteins, or differential fragmentation during the isolation procedure. Patterns of protein incorporation among the subfractions suggested that the light mitochondria might be incomplete, immature organelles; the heavy mitochondria normal; and the fluffy population a combination of regenerating and degenerating mitochondria (Katyare, et al., 1970). More recently, similarly obtained arbitrary subfractions of insect flight muscle mitochondria were demonstrated to be heterogeneous with

respect to phospholipid turnover (Novak, et al., 1979). Pickett, et al. (1976), isolated light and heavy mitochondria on a continuous Ficoll gradient, and although unable to resolve them into discrete subpopulations, found them to be heterogeneous with respect to capacity for oxidative phosphorylation. Murfitt, et al. (1978), used gradients of Metrizamide to separate upper and lower bands of myocardial mitochondria, and noted differences in morphology and oxidative phosphorylation. Functional differences in the absence of osmotic effects is supported by the work of Thompson, et al. (1974) using H_2O/D_2O gradients. Recently, (Wattiaux-de Coninck, et al., 1977), the validity of any isolation method based on centrifugation has been challenged due to the observation that the hydrostatic pressure generated by centrifugation could cause structural damage to the mitochondrial membranes. The extent of this process can be monitored by measurement of the free malate dehydrogenase activity in the supernatant, which is normally low since this enzyme is retained in the matrix of intact mitochondria. The effect of pressure on mitochondria is well known; early studies (Beaufay, et al., 1964) report that mitochondria exhibit a second isopycnic point following exposure to dense sucrose solutions. Recently (Higgins, et al., 1978), heterogeneity in mitochondrial function has been observed between morphologically distinct structures within the

same organ. Since much of work on mitochondrial heterogeneity has been done using homogenates of liver, a notably heterogeneous organ (Jungermann and Sasse, 1978), the question of mitochondrial heterogeneity within a single, homogeneous cell type has not been clearly answered.

An important characteristic of mitochondria is that each individual organelle is a discrete genetic entity (Shatz et al., 1964; Borst and Kroon, 1968, Bogenhagen and Clayton, 1977). By virtue of its closed, circular, supercoiled DNA, the mitochondrion is a potential vector for transmission of genetic variation, reminiscent of the "determinant" theory of August Weismann (p. 10, Fulton and Klein). A multitude of mutants have been catalogued and mapped onto the mitochondrial genomes of several species of higher organisms (Tzagoloff and Macino, 1979). The direct transcription products include ribosomal RNA's and tRNA's (which could account for variation in protein incorporation rates), and mRNA's which code for cytochrome oxidase subunits, Cytochrome b and subunits of the reversible ATPase complex (a defect in any one of which might also lead to alterations in the stochiometry of oxidative phosphorylation) (Schatz and Mason, 1974; Mitchell, 1979). Mitochondria are also important structures for the translation of nuclear messenger RNA's (Kisselev, et al., 1975), not only for

some of their own functional components, but also for use by the entire cell (Irwin, et al., 1978). Elaborate coordination schemes have been devised to explain the interaction between nuclear and mitochondrial genes (Freedman and Chan, 1978). Though melting and renaturation studies indicate little or no heterogeneity in mtDNA from green alga (Ryan, et al., 1978), heterogeneity of mtDNA from higher organisms has been observed with regard to primary structure, quarternary structure (see below) and general physical characteristics. MtDNA from various species has been found to differ in buoyant density (Strassberg, et al., 1974), base composition, pyrimidine clustering, and occurrence of "odd" bases (Vanyushin and Kirnos, 1977). A unique mtDNA was found to occur in the sterile "S" cytoplasm of maize by electron microscopy and electrophoresis in agarose gels (Pring, et al., 1977), and later the diversity of mtDNA's from normal maize cytoplasms was established (Levings and Pring, 1977) by means of restriction endonuclease digests. Synenki, et al. (1978) have reported the occurrence of multiple discrete size classes of mtDNA from soybean. MtDNA is known to exist in several forms with regard to "quaternary" structure. These forms include catenated (interlocked) dimers (Hudson and Vinograd, 1967; Clayton and Vinograd, 1967), circular dimers (associated with abnormal cellular states such as cancer; Smith and Vinograd, 1973), as well as monomeric

and replicative forms (Kasumatsu, et al., 1971). Relative occurrence of these forms has been found to vary between tissues and with aging (Piko and Matsumoto, 1977; Piko and Meyer, 1978), and between normal and malignant tissues (Clayton, et al., 1968; Clayton and Vinograd, 1969). Gillum and Clayton (1978) reported that the displacement loop initiation sequence (7.5 S mtDNA) of the replicative form exists as a family of discrete lengths. One proposed mechanism for this phenomenon is that the parental duplex molecules are heterogeneous in the D-loop region. The most straightforward means of detecting heterogenity in the primary structure of mtDNA is through the use of restriction endonuclease digests. In this way, microheterogeneity has been detected in the circular dimer form as compared to the monomeric and catenated forms of mouse LD (cultured cells) and human cells, (Robberson, et al., 1977). Two types of mtDNA were found within a single strain of rat, though no individual rats were found to possess both types. Other rat strains exhibited either one or the other type mtDNA (Hayashi, et al., 1978a; Kroon, et al., 1978; Buzzo, et al., 1978). The restriction pattern trait shows strict maternal inheritance (Hayashi, et al., 1978b), and the results were confirmed for natural populations (Avise, et al., 1979). Maki and Cummings (1977) demonstrated the power of the restriction digest technique when they used mtDNA's to distinguish

between interspecies hybrids of Paramecium aurelia. Though Ascites tumor cell mtDNA's were shown to differ from normal host cell mtDNA's (Hayashi, et al., 1978c), Potter, et al. (1975) detected no difference from different organs of the same individual domestic farm animal. Highlighting the controversy, recently Coote, et al., (1979) demonstrated heterogeneity between mtDNA's of different tissues from the same individual animal. The question remains whether the preparations of mtDNA used as substrate for the restriction digests are single molecular clones or represent mixtures of different molecules. The usual way of resolving the question is to sum up the lengths of the fragments, as determined by comparison with the migration of "known" fragments, and see if it approximates the length of the intact molecule. Even though the sum of the major fragments may approximate the intact length, there exist certain "minor" bands which are difficult to locate and may represent heterogeneity within single preparations of mtDNA. Though the stochiometry of the bands can be determined with some difficulty, accurate methods of quantitation (Pulleyblank, et al., 1977; Willis and Gray, unpublished) are not in general use, so that the relative molar ratios of the bands, which should be one-to-one for a homogeneous molecule, completely digested where all bands are resolved, is usually not measured.

If there are indeed discrete subclasses of different-sized mitochondria, it may be possible to separate them, either analytically or preparatively, by electrophoresis. The electrophoretic mobility of mitochondria was first measured by means of free boundary electrophoresis using a modified Tiselius apparatus (Thompson and McLees, 1961). Evidence showed that the net negative charge borne by the mitochondria was due to membrane binding of $HPO_4^{=}$. Electrophoretic mobilities of mitochondria were measured under a variety of conditions of pH and toxicity, and isoelectric pH's were measured (Plummer, 1965) using themicroelectrophoretic apparatus of Gittens and James (1960). Another microelectrophoretic apparatus (Bangham, et al., 1958) was used to compare the properties of heavy, light, and "fluffy" mitochondrial fractions under normal (Katyare, et al., 1970) and abnormal (Koppikar, et al., 1972) conditions. These efforts were largely unsuccessful in detecting significant heterogeneity, probably because of the short path length for observation (too small for marginal differences to be manifested) and because of the arbitrary nature of the fractionations by differential centrifugation (which allows cross-contamination which distorts the averaging of observations in these microdeterminations). Modified zonal electrophoresis on paper was effective in demonstrating the effect of incouplers on mitochondrial properties,

but lacked the resolution necessary to quantify the results (Valdivia, et al., 1973). Continuous flow electrophoresis (Bier, 1957) has been used preparatively to fractionate crude subcellular homogenates (Hannig, 1964a,b; 1967), and was successful in separating mitochondria from microsomes, nuclei, and chloroplasts, but lacked the resolution necessary to detect heterogeneity in mitochondrial population. Under optimal conditions, continuous flow electrophoresis has demonstrated a degree of mitochondrial heterogeneity (Ryan, et al., 1971). A simpler method which holds more promise for the resolution of mitochondrial subclasses is zonal density gradient electrophoresis (Svensson and Valmet, 1955; Brakke, et al., 1968). The use of this method has been restricted to the visual determination of electrophoretic mobility of mitochondria already partially purified by discontinuous density gradient electrophoresis (Vos, et al., 1968). Preliminary results with continuous linear gradients indicate that all of the mitochondrial subfractions obtained by differential centrifugation contain heterogeneously migrating populations of mitochondria.

REFERENCES FOR APPENDIX B

Avise, J. C., Lansman, R. A., and Shade, R. O. (1979) Genetics 92,279-295.

Bangham, A. D., Flemans, R., Heard, D., and Seaman, G. V. F. (1958) Nature 182,642-644.

Beattie, D. S., Basford, R. E., and Koritz, S. B. (1967) JBC 242(20),4581-4586.

Beaufay, H., Jaques, P., Bandhuin, P., Sellinger, O. Z., Berthet, J. and DeDave, C. (1964) Bioc. J. 92,184-205.

Bensley, R. R., and Hoerr, N. L. (1934) Anat. Rec. 60, 449-455.

Bier, M. (1957) Science 125,1084-1085.

Bogenhagen, D. and Clayton, D. (1977) Cell 11,719-727.

Borst and Kroon (1969) Int. Rev. Cytol. 26,108.

Brakke, M. K., Allington, R. W., and Langille, F. A. (1968) Anal. Bioc. 25,30-39.

Buzzo, K., Fonts, D. L. and Wolstenholme, D. R. (1978) PNAS US 75(2),909-913.

Clayton, D. A., Smith, C. A., Jordan, J. M., Teplitz, M., and Vinograd, J. (1968) Nature 220(5171),976-979.

Clayton, D. A. and Vinograd, J. (1967) Nature 216,652.

Clayton, D. A. and Vinograd, J. (1969) PNAS US 62,1077-1084.

Coote, J. L., Szabados, G., and Work, T. S. (1979) FEBS Lett. 99(2),266-260.

DeDuve, C. (1967) In Meth. in Enz. X ed., Estabrook, Academic Press, NY. p. 7.

Fletcher, M. J. and Sanadi, D. R. (1961) BBA 51,356-360.

Freedman, J. A. and Chan, S. H. P. (1978) Mol. and Cell. Bioc. 19(3),135-146.

Frisell, W. R., Patwardhan, M. V., and MacKenzie, C. G. (1965) JBC 240(4),1829-1835.

Fulton, C. and Klein, A. O. (1976) Explorations in Developmental Biology, Harvard Univ. Press, Cambridge, MA. 704 pps.

Gear, A. R. L. (1965a) Bioc. J. 95,118-137.

Gear, A. R. L. (1965b) Bioc. J. 97,532-539.

Gillum, A. M. and Clayton, D. A. (1978) PNAS US 75(2), 677-681.

Hannig, K., et al. (1964a) Z. Naturforsch. 19b,1972.

Hannig, K. (1964b) Dissertation. Munich.

Hannig, K. (1967) In Electrophoresis; Theory, Methods, and Applications. II. ed. Bier, Academic Press, NY. pps. 464.

Hayashi, J., Yonekawa, H., Gotoh, O., Motohashi, J. and Tagashira, Y. (1978a) BBRC 81(3),871-877.

Hayashi, J., Yonekawa, H., Gotoh, O., Wantanabe, J., and Tagashira, Y. (1978b) BBRC 83(3),1032-1038.

Hayashi, J., Yonekawa, H., Gotoh, O., Motohashi, J. and Tagashira, Y. (1978c) Canc. Lett. 4,125.

Higgins, E. S., Seibel, H., Friend, W., and Rogers, K. S. (1978) Proc. of Soc. for Exp. Biol. and Med. 158, 595-598.

Hudson, B. and Vinograd, J. (1967) Nature 216,647-657.

Irwin, C. C., Malkin, L. I., and Morris, H. P. (1978) Canc. Res. 38,1584-1588.

Jungermann, K. and Sasse, D. (1978) TIBS Sept. p. 198-202.

Katsumatsu, H., Robberson, D. L., and Vinograd, J. (1971) PNAS US 68(9),2252-2257.

Katyare, S. S., Fatterpaker, P., and Sreenivasan, A. (1970) Bioc. J. 118,111-121.

Kisselev, O. I., Gaitskhoki, V. S., and Neifakh, S. A. (1975) Mol. and Cell Bioc. 6(2),149-153.

Koppikar, S. V., Katyare, S. S., Fatterpacker, P., and Sreenivasan, A. (1972) Exp. Cell Res. 73,501-502.

Kroon, A. M., deVos, W. M., and Bakker, H. (1978) BBA 519,269-273.

Kuff and Schneider (1954) JBC 206,677.

Levings, C. S., III and Pring, D. R. (1977) J. of Hered. 68,350-354.

Maki, R. A. and Cummings, D. J. (1977) Plasmid 1,106-114.

Matile, P. H. and Bahr, G. F. (1968) Exp. Cell Res. 52, 301-307.

Mitchell, P. (1979) Science 206(4423),1148.

Murfitt, R. R., Stiles, J. W., Powell, W. J., Jr., and Sanadi, D. R. (1978) J. of Mol. and Cell Cardio. 10,109-123.

Novak, F., Norakova, O., and Kubista, V. (1979) Insect Bioc. 9,389-396.

Novikoff, A. B., Podber, E., Ryan, J., and Noe, E. (1953) J. of Histoc. and Cytoc. 1(1),27-46.

Pickett, C. B., Cascarano, J., and Johnson, R. (1977) J. of Bioenerg. and Biomemb. 9,271-282.

Piko, L. and Matsumoto, L. (1977) NAR 4(5),1301-1314.

Piko, L., Meyer, R., Eipe, J., and Costea, N. (1978) Mech. of Aging & Devel. 7,351-365.

Plummer, D. T. (1965) Bioc. J. 96,729-732.

Potter, S. S., Newbold, J. E., Hutchinson, C. A., III, and Edgell, M. H. (1975) PNAS US 72(11),4496-4500.

Pring, D. R., Levings, C. S., III, Hu, W. W. L., and Timothy, D. H. (1977) PNAS US 74(7),2904-2908.

Pulleyblank, D. E., Shure, M., and Vinograd, J. (1977) NAR 4(5),1409.

Robberson, D. L., Wilkins, C. E., Clayton, D. A., and Doda, J. N. (1977) NAR 4(5),1315-1338.

Ryan, K. J., Kalant, H., and Thomas, E. L. (1971) J. Cell Biol. 49,235-246.

Ryan, R., Grant, D., Chiang, K., and Swift, H. (1978) PNAS US 74(7),3268-3272.

Schatz, G. Halsbrunner, E. and Tuppy, H. (1964) BBRC 15(2), 127-132.

Schatz, G. and Mason, T. L. (1979) Ann. Rev. Bioc. 43, 51-87.

Smith, C. A. and Vinograd, J. (1973) Canc. Res. 33,1065-1070.

Strasberg, P. M., Davidson, M. M. L., Wallace, R. B., and Freeman, K. B. (1974) Exp. Cell Res. 89,399-401.

Svensson, H. and Valmet, E. (1955) Sci. Tools 2(1),11-13.

Thompson, T. E. and McLees, B. D. (1961) BBA 50,213-223.

Thompson, T. E., Nance, S. L., and Tollaksen, S. L. (1974) Arch. Bioc. and Biop. 160,130-134.

Synenki, R. M., Levings, C. S., III, and Shah, D. M. (1978) Plant Physiol. 61,460-464.

Tzagoloff, A. and Macino, G. (1979) Ann. Rev. Bioc. 48, 419-441.

Valdivia, E., Pease, B., Gabel, C., and Chan, V. (1973) Anal. Bioc. 51,146-151.

Vanyushin, B. F. and Kirnos, M. D. (1976) BBA 475,323-336.

Vos, J., Kuriyana, K., and Roberts, E. (1968) Brain Res. 9,224-230.

Wattiaux-deConninck, S., Dubois, F., and Wattiaux, R. (1977) BBA 471,421-435.

Werkheiser, W. C. and Bartley, W. (1957) Bioc. J. 66,79-91.

APPENDIX C

FORTRAN LISTING OF EXESWL AND ADJUNCT SUBROUTINES

Direct computer printouts for EXESWL, the executive program; SWELL, the error subroutine; and MNWD4A, the search subroutine, are reproduced in their entirity in this section.

```
C       WILLIS EXECUTIVE PROGRAM-COMPUTER CURVE FITTING-SWELLING MODEL I
C     SAMPLE S-6  DOSE  20 RAD
      LOGICAL SWITCH
      EXTERNAL SWELL,MNWD4A
      DIMENSION X(40),DM(1720),XIN(40)
      COMMON SWITCH,NCP,NX,PCT(50),T(50)
      COMMON  NUM,L,FUD(4)
      INTEGER CYC
      READ 1, NCP,NX,NT
    1 FORMAT (3I5)
C     THE FIRST DATA CARD CONTAINS NCP,NX,NT
C         NCP IS THE NUMBER OF VARIABLE PARAMETERS IN EACH TERM OF THE
C              MODEL
C         NX IS THE NUMBER OF DATA POINTS TO BE FIT BY THE MODEL
C         NT IS THE LARGEST NUMBER OF TERMS TO BE CONSIDERED
      READ (5,2) (T(I),PCT(I),I=1,NX)
    2 FORMAT(V)
C     DATA IS READ OFF CARDS AS ORDERED PAIRS OF TIME AND TRANSMITTANCE
C         FROM SPECTROPHOTOMETRIC OBSERVATIONS AS RECORDED BY STRIP
C         CHART
      READ 3, (TIN,TONE)
    3 FORMAT (2F7.4)
      ESS = 1/((-ALOG((PCT(NX))/100.0))**1.5)
      SEE = ESS-(1/((-ALOG(TIN))**1.5))
      CAY = -ALOG((ESS-(1/((-ALOG(TONE))**1.5)))/SEE)
C     SINGLE STRAIN APPROXIMATIONS FOR THE VARIABLE PARAMETERS ARE READ
      DO 9000 L=1,NT
      NUM=NCP*L
      NN=NUM+3
      CYC=6*NUM
      I=0
```

```
      DO 100 I=1,L
      XIN(4*I-3)=1.0/L
      XIN(4*I-2)= ESS
      XIN(4*I-1)= SEE
  100 XIN(4*I)= CAY
      FOR THIS MODEL,ASSUMING FOUR VARIABLE PARAMETERS PER TERM,
C         APPROPRIATE STARTING VALUES ARE FED TO THE SEACH ROUTINE.
C     THESE INITIAL VALUES ARE BASED ON SINGLE STRAIN APPROXIMATIONS
C     THE MORE TERMS TO BE CONSIDERED,THE MORE INITIAL VALUES ARE
C         GENERATED. THEY ARE READ INTO THE 'XIN' ARRAY
C
      SWITCH=.FALSE.
      CALL MNWD4A(NUM,SWELL,X,FM,XIN,7,7,CYC,2020,D1)
      MNWD4A IS A SEARCH SUBROUTINE WHICH VARIES THE XIN ARRAY TO
      MINIMIZE THE MODEL'S ERROR AS CALCULATED BY THE SWELL SUBROUTINE
C      THE PROPER CALL FOR THE MNWD4A SUBROUTINE INCLUDES:
C          NUM-THE NUMBER OF PARAMETERS BEING FITTED AT THIS PARTICULAR
C          TIME
C          SWELL-THE SUBROUTINE WHICH KEEPS THE PARAMETERS WITHIN
C          SPECIFICATIONS AND CALCULATES THE DIVERGENCE FROM THE MODEL
C          X-THE NAME OF THE STORAGE ARRAY FOR THE DERIVED SOLUTION
C          FM-THE NAME OF THE STORAGE PLACE FOR THE ERROR OF THE FIT
C          XIN-THE NAME OF THE INITIAL INPUT ARRAY
C          -THE NUMBER OF SIGNIFICANT DIGITS REQUIRED FOR SATISFACTORY
C          SOLUTION OF THE PARAMETERS
C          -THE NUMBER OF SIGNIFICANT DIGITS NEEDED FOR SATISFACTORY
C          SOLUTION OF THE ERROR FUNCTION
C          -TOTAL ALLOWED FUNCTION EVALUATIONS BEFORE TERMINATION(LAST
C          -TWO DIGITS ARE LEAST EVALUATIONS ALLOWED PER SEARCH CYCLE,
C          WHERE DD=20)
C          -MAXIMUM NUMBER OF SEARCH CYCLES ALLOWED,USUALLY =5*NUM
C          D1- THE NAME OF AN ARRAY CONTAINING AT LEAST NUM*(NUM+3)
C          DECLARED SPACE FOR USE AS A WORKING MEMORY FOR MNWD4A
C
```

```
      SWITCH=.TRUE.
      CALL SWELL( FT,X )
      PRINT 4, L,FT,FM
    4 FORMAT(1HO,'NUMBER OF STRAINS=',I3,'   FIT=',E12.4,'   FORM=',E12.4)
      J=0
      DO 200 J=1,L
      JK=(4*J)
      JC=(4*J-1)
      JS=(4*J-2)
      JP=(4*J-3)
      PRINT 5, J,X(JP),J,X(JS)
  200 PRINT 6, J,X(JC),J,X(JK)
    5 FORMAT(1HO,'P(',I3,')=',E15.6,'  S(',I3,')=',E15.6)
    6 FORMAT(1HO,'C(',I3,')=',E15.6,'  K(',I3,')=',E15.6)
      STD=0
      STD=SQRT(FT/(NX-1))
 9000 PRINT 7, STD
    7 FORMAT(1HO,'STANDARD DEVIATION=',E15.6)
   99 CONTINUE
      STOP
      END
      SUBROUTINE SWELL(COST,X )
      LOGICAL SWITCH
      COMMON SWITCH,NCP,NX,PCT(50),T(50)
      COMMON  NUM,LL,FUD(4)
      DIMENSION X( 55),P(10),ESS(10),SEE(10),CAY(10)
C     PROSPECTIVE VALUES OF X ARE MAPPED ONTO THE APPROPRIATE PARAMETER
C          ARRAYS
      I=0
      DO 300 I=1,LL
      P(I)=X(4*I-3)
      ESS(I)=X(4*I-2)
      SEE(I)=X(4*I-1)
  300 CAY(I)=X(4*I)
```

```
C       P IS THE RELATIVE ABUNDANCE OF STRAIN I PRESENT IN THE SAMPLE
C       S IS THE TRANSMITTANCE CONTRIBUTION OF TOTALLY SWOLLEN STRAIN I
C       C IS THE CHANGE IN TRANSMITTANCE MADE BY STRAIN I
C       THE UNITS OF P,S,AND C ARE PERCENT TRANSMITTANCE
C       K IS THE EXPONENTIAL SWELLING RATE CONSTANT FOR STRAIN I
C       VARIABLES ARE CONSTRAINED TO LIMITS BY  APPLICATION OF A PENALTY
C           FUNCTION TO THE OVERALL ERROR OF THE FIT
        COST=0
        M=0
        DO 1000 M=1,NX
        PCTCC=0
        L=0
        SOME=0
        DO 500 L=1,LL
        THIN=0
        OSMO=0
        OSMO=(FSS(L)-SEF(L)*EXP(-CAY(L)*T(M)))**2
        THIN=P(L)/(OSMO**.3333)
  500   SOME=SOME+THIN
        PCTCC=100*EXP(-SOME)
        TM=T(M)
        PCTM=PCT(M)
        IF(SWITCH)PRINT 8,TM,PCTM,PCTCC
      8 FORMAT(140,'TIME=',F5.1,'  OBS PCT=',F6.2,'  CALC PCT=',F6.2)
 1000   COST=COST+(PCTCC-PCT(M))**2
        IF(SWITCH)RETURN
C       IF THE ERROR IN THE FIT IS MINIMIZED,SWELL RETURNS ABSOLUTE ERROR
        BIG = 120000
        PEN=0
        J=0
        DO 400 J=1,LL
        TOTAL=0
        K=0
```

```
      TNS = 0.00
      DO 350 K=1,LL
      IF(CAY(K).LT.0)CAY(K)=0
  350 TOTAL=TOTAL+P(K)
      TNS = (ESS(J))/((ESS(J))-(SEE(J)))
      IF(TNS.LT.1.00)PEN = PEN + BIG*(1.00-TNS)**2
      IF(TNS.GT.10.0)PEN = PEN + BIG*(10.0-TNS)**2
      IF(TOTAL.LT.1.00)PEN=PEN+BIG*(1.00-TOTAL)**2
      IF(TOTAL.GT.1.00)PEN=PEN+BIG*(1.00-TOTAL)**2
      IF(P(J).LT..005)PEN=PEN+BIG*(.005-P(J))**2
      IF(P(J).GT..995)PEN=PEN+BIG*(.995-P(J))**2
      IF(ESS(J).GT.10.0)PEN=PEN+BIG*(10.0-ESS(J))**2
      IF(ESS(J).LT.(SEE(J)+.05))PEN=PEN+BIG*(ESS(J)-.05-SEE(J))**2
      IF(SEE(J).GT.(ESS(J)-.05))PEN=PEN+BIG*(ESS(J)-.05-SEE(J))**2
      IF(SEE(J).LT..050)PEN=PEN+BIG*(.050-SEE(J))**2
C     THE NEXT TWO CARDS ARE APPROPRIATE FOR DATA W/TIME IN MINUTES
      IF(CAY(J).LT..01)PEN=PEN+BIG*(CAY(J)-.01)**2
  400 IF(CAY(J).GT.10.0)PEN=PEN+BIG*(CAY(J)-10.0)**2
C     THE OVERALL ERROR OF THE PROSPECTIVE MODEL IS CALCULATED INCLUDING
C         CONFORMITY TO CONSTRAINTS
      COST = COST + PEN
      RETURN
      END
      SUBROUTINE MNWD4A( N,COST,X,FM,XIN,NX,NC,UIT1,NEM,DM)
C     N= ORDER OF THE PARAMETER SPACE TO BE SEARCHED OVER
C     COST= THE NAME OF THE SUBROUTINE SUBPROGRAM THAT COMPUTES THE
C           COST FUNCTION.  SUBROUTINE XXXX( CF,X )
C                           DIMENSION X(1)
C                           INCLUDE DECLARATIONS OF COMMON BLOCK INFO
C     X= NAME OF THE ARRAY IN WHICH THE SOLUTION POINT IS TO BE STORED
C     FM= THE NAME OF THE SIMPLE VARIABLE INTO WHICH THE SOLUTION COST
C         IS TO BE STORED
C     XIN = NAME OF THE ARRAY INTO WHICH THE CALLING PROGRAM HAS PLACED
C          AN INITIAL ESTIMATE FOR THE SOLUTION.
```

```
C       NX= NUMBER OF SIGNIFICANT DIGITS NEEDED FOR CONVERGENCE IN X.
C       NC= NUMBER OF SIGNIFICANT DIGITS NEEDED FOR CONVERGENCE IN COST.
C       NITM=(ABS NITM = MAX NUMBER OF SEARCH CYCLES ALLOWED )
C            = 5*N ( IF NITM LT ZERO NO PRINT OUT )
C       NFM=  ( TWO LEAST SIGNIFICANT DIGITS = NUMBER OF FUNCTION EVALUATIONS
C            ALLOWED ON ANY GIVEN RELATIVE MINIMUM SEARCH )
C            ( TOTAL VALUE = TOTAL NUMBER OF FUNTION EVALUATIONS
C            ALLOWED BEFORE AN ABNORMAL TERMINATION )
C            THUS, NFM=1020 WOULD ALLOW A TOTAL OF 1020 FUNCTION
C            EVALUATIONS, BUT WOULD ALLOW A MAX OF 20 EVALUATIONS
C            RELATIVE MINIMUM SEARCH...
C       DM=  WORKING SPACE = NAME OF AN ARRAY WITH AT LEAST N*(N+3)
C            DECLARED SPACE
      DIMENSION X(N),XIN(N),DM(N, N),F(5),G(5)
      DOUBLE PRECISIOND,H,HMX,PI,S1,S2,A,B,C,TESTX
     &                 ,DABS,DSQRT,TOLX
      LOGICAL NEW,ONCE,NORYTE,REFYN,REVRS,PLEN
      INTEGER P
      EQUIVALENCE (EPSXS,EPSXW )
      DATA ALW/.5/
      DATA A1,A2/.5,.5/
      NORYTE = NITM.LT.00
      REFYN = .FALSE.
      REVRS = .FALSE.
      ONCE = .FALSE.
      EPSX = 0.1**NX
      EPSC = 0.1**NC
      EPSXW = SQRT( EPSX )
      EPSCW = SQRT( EPSC )
      NITMAX = IABS( NITM )
      MXFT = ( NFM/100 )*100
      MXFR = NFM-MXFT
      IF( MXFR.NE.00 ) GOTO 20
      MXFR = 20
```

```
 20 NFR = 00
    NFT = 00
    NS = 00
    IT = 00
    MP1 = 01
    DO 100      J = 1,N
    X(J) = XIN(J)
100 DM(J,N+2) = XIN(J)
    FPST = 1.E3P
    ASSIGN 190 TO IRT
    GOTO 53
190 FM = F(01)
195 DO 196      J=1,N
196 DM(J,N+3) = ABS( X(J) )*EPSXS
200 NEW = .TRUE.
210 IF( IT.GE.NITMAX ) GOTO 9000
    IF( NFT.GE.MXFT ) GOTO 2000
    IT = IT + 01
    IF( .NOT. NEW ) GOTO 230
    RNS = 1.D/( NS + 01 )
    NS= 00
    REVRS = .NOT.REVRS
    DO 220      I=1,N
    DO 215       J=1,N
215 DM(I,J) = 0.0
    DM(I,N+3) = DM(I,N+3)*RNS
    J=I
    IF( REVRS ) GOTO 220
    J= N-I+01
220 DM(I,J) = DM(I,N+3) + EPSXS
230 DO 240      J = 1,N
240 DM(J,N+1) = X(J)
    IF( NORYTE ) GOTO 250
    ASSIGN 250 TO KRRYT
```

```
      GOTO 9005
250   R = 00
      TOLX = EPSXW
      TOLC = EPSCW
      ASSIGN 300 TO KB1000
300   R = R+ 01
      RLEN = R.LE.N
      IF( RLEN ) GOTO 1000
      TOLX = EPSX
      TOLC = EPSC
      AXT = 0.
      DO 310     J=1,N
      DM(J,R) = X(J)-DM(J,N+1)
      TXT = ABS( DM(J,R) )/( ABS( X(J) )+EPSXW )
      IF( TXT.LE.AXT ) GOTO 310
      AXT = TXT
310   CONTINUE
      IF( AXT.LE.EPSXW ) GOTO 8000
      IF( EPST-FM.LE.EPSCW*( ABS( FM )+EPSCW ) ) GOTO 8000
      EPST = FM
      ASSIGN 400 TO KB1000
      GOTO 1000
400   AMX=0.0
      DO     403    I=1,N
      AXP = 0.0
      AXI = 0.0
      DO      402    J=1,N
      AXI = AXI + DM(J,I)*DM(J,R)
402   AXP = AXP + DM(J,I)*DM(J,I)
      AXP = ABS( AXI/SQRT( AXP ) )
      IF( AXP.LE.AMX ) GOTO    403
      AMX = AXP
      IMX = I
```

```
  403 CONTINUE
      DO 410      I=IMX,N
      DO 410      J=1,N
  410 DM(J,I) = DM(J,I+1)
      NEW = ABS( TXT*AXT ) .LE. EPSXW
      GOTO 210
 1000 NFR = 00
      AL = ALW
      IF( ABS( AL ).LT. TOLX ) AL = TOLX
      H = AL
      F(1) = FM
      D(1) = 0.
      D(2) = H
      M = 01
      MP1 = 2
      ASSIGN 1100 TO IRT
      ASSIGN 53 TO JUMP
      GOTO 50
 1100 IF( F(2).LE.F(1) ) GOTO 1200
      H = -H
      GOTO 1300
 1200 H = H + H
 1300 MP1 = 3
      HMX = 10.*H
      D(3) = H
 1350 ASSIGN 1400 TO IRT
      GOTO 50
 1400 M = 3
      MP1 = 4
 1500 A = 0.
      B = 0.
      C = 0.
      DO 1600 I=1,M
      PI = F(I)
```

```
      S1 = 0.
      S2 = 0.
      DO 1580 J=1,M
      IF( J.EQ.I ) GOTO 1580
      PI = PI/( D(I)-D(J) )
      S1 = S1 + D(J)
      IF( M.EQ.3 ) GOTO 1580
      IF( J.EQ.M ) GOTO 1580
      L = J+01
      DO 1560 K=L,M
      IF( K.EQ.I ) GOTO 1560
      S2 = S2 + D(J)*D(K)
1560  CONTINUE
1580  CONTINUE
      A = A + PI
      B = B + S1*PI
      IF( M.EQ.3 ) GOTO 1600
      C = C+ S2*PI
1600  CONTINUE
      IF( M.EQ.4 ) GOTO 1700
1650  IF( A.GT.0. ) GOTO 1900
      IF( M.EQ.4 ) GOTO 4000
      M = 2
      MP1 = 3
2000  L = 1
      DO 2020 J=2,M
2020  IF( F(J).GT.F(L) ) L=J
      IF( F(MP1).GT.F(L) ) GOTO 4000
      D(L) = D(MP1)
      F(L) = F(MP1)
      IF( M.NE.2 ) GOTO 2040
      D(3) = D(3) + H
      H = H + H
      HMX = HMX + HMX
```

```
      GOTO 1350
2040  IF( M.EQ.4 ) GOTO 1500
2041  M = 4
      MP1 = 5
      GOTO 1500
1800  D(MP1) = 0.5*B/A
      GOTO 3007
1700  IF( A.NE.0. ) GOTO 1750
      A = -B
      B = -C
      GOTO 1650
1750  A = 3.*A
      D(5) = B*B - A*C
      IF( D(5).GE.0. ) GOTO 1760
      D(5) = 0.
1760  D(5) = ( B+ DSQRT( D(5) ) )/A
3000  IF( (D(MP1)-D(M)-HMX)*HMX .LE. 0. ) GOTO 3010
      D(MP1) = D(M) + HMX
      HMX = HMX + HMX
3010  ASSIGN 3020 TO IRT
      GOTO 50
3020  TESTX = TOLX*( DABS( D(MP1) ) +TOLX )
      TESTC = TOLC*( ABS( F(MP1) )+TOLC )
      J = 0
      DO 3030  I=1,M
      IF( DABS( D(I)-D(MP1) ).LE.TESTX ) GOTO 4000
      IF( ABS( F(I)-F(MP1)).GT.TESTC) GOTO 3030
      J = J+01
3030  CONTINUE
      IF( J.GT.02 ) GOTO 4000
      IF( M.GT.04 ) GOTO 2000
      GOTO 2041
   50 DO  51   J=1,N
   51 X(J) = DM(J,N+2) + DM(J,R)*D(MP1)
      GOTO JUMP,(53,4020)
```

```
   53 CALL COST( F(MP1),X )
      NFR = NFR + 01
      IF( NFR.GT.MXFR ) GOTO 4000
   52 GOTO IRT,(1100,1400,3020,190)
 4000 DO 4010    I=1,M
      IF( F(I).GE.F(MP1) ) GOTO 4020
      MP1 = I
 4010 CONTINUE
      IF( MP1.EQ.M+01 ) GOTO 4020
      ASSIGN 4020 TO JUMP
      GOTO 50
 4020 AL = D(MP1)
      FM = F(MP1)
      TXT =  A1 + A2*ABS( AL )
      IF( RLEN ) GOTO 4015
      TXT = 1.0 + AL
 4015 DO 4030    J=1,N
      DM(J,N+2) = X(J)
 4030 DM(J,R) = DM(J,P)*TXT
      IF( RLEN ) GOTO 4035
      DO 4032    J=1,N
 4032 DM(J,N+3) = DM(J,N+3) + ABS( DM(J,R) )
      NS = NS + 01
 4035 NFT = NFT + NFP
      GOTO KB1000,(300,400)
 8000 IF( ONCE ) GOTO 8050
      ONCE = .TRUE.
      REFYN = .FALSE.
      EPSXW = SQRT( EPSX*EPSXW )
      EPSCW = SQRT( EPSC*EPSCW )
      GOTO 200
 8050 IF( REFYN ) GOTO 9000
      REFYN = .TRUE.
      EPSXW = EPSX
```

```
      FPSCW = EPSC
      GOTO 105
 9000 IF( NORYTE ) GOTO 9010
      WRITE(6,2)
      ASSIGN 9010 TO KBRYT
 9005 WRITE(6,1) IT,NFT,FM,X
      GOTO KBRYT,(250,9010)
 9010 RETURN
    1 FORMAT(11HOMNWD4A, ITI3,4H, NFI6,5H, FUN1PE12.4/17HOPARAMETER VECT
     ROR/(8E15.6))
    2 FORMAT(17HOSEARCH COMPLETED)
      END
    4   22   10
0.5 43.00 1.0 45.00 1.5 47.00 2.0 48.00 2.5 49.00 3.0 49.75 3.5 50.25 4.0 50.80
4.5 51.20 5.0 51.50 5.5 51.80 6.0 52.00 6.5 52.25 7.0 52.50 7.5 52.70 8.0 52.90
8.5 53.00 9.0 53.10 9.5 53.20 10.0 53.3 10.5 53.4 11.0 53.4
0.4100 0.4500
```

VITA

Charles Edward Willis, son of Mrs. Charlotte C. Willis and the late Noble S. Willis, was born in Shreveport, Louisiana on November 7, 1953. He graduated from C. E. Byrd High School in May 1971. He graduated from Louisiana State University in Baton Rouge in May, 1975, with a Bachelor of Science degree in General Studies, which included coursework from the United States Air Force Academy and LSU in Shreveport. Upon graduation, he was commissioned in the United States Army Reserve. He married Miss Diana Natalie Gray, also of Shreveport, on June 7, 1975. Their son, Michael, was born May 11, 1976. Charles Willis began graduate study in Nuclear Engineering at Louisiana State University in August, 1975. In addition to being a candidate for the degree of Master of Science in the Department of Nuclear Engineering, he is also a candidate for the Doctorate in Biophysical Sciences at the University of Houston, where he has studied since August, 1977. He is presently employed by Bristol Baylor Laboratories at Baylor College of Medicine in Houston, Texas.